International Journal of Computer Applications Technology and Research
Volume 12–Issue 03, 01-05, 2023, ISSN:-2319–8656
DOI:10.7753/IJCATR1203.1001

Image Super-Resolution Reconstruction Based on Residual Convolution and Double Attention Mechanism

Qinglin Huang
School of Communication Engineering
Chengdu University of Information Technology
Chengdu, China

Congcong He
School of Communication Engineering
Chengdu University of Information Technology
Chengdu, China

Jieyuan Luo
School of Communication Engineering
Chengdu University of Information Technology
Chengdu, China

Abstract: Currently, single-image super-resolution reconstruction based on deep learning has achieved good results. To address the problems that most networks will have long training time, weak image learning ability and not fully utilizing the high frequency information of images, an image super-resolution reconstruction method based on residual convolution and double attention mechanism is proposed. The model performs deep feature extraction of the image by cascading deep convolutional networks, introduces local residual blocks to solve the model degradation brought by too many network parameters, and embeds the dual attention mechanism module in the residual blocks for adaptive calibration to adjust the feature map weights of each channel and the spatial correlation between features, so as to obtain deep texture detail information and reconstruct the feature image by sub-pixel convolutional layers to up sampling to reconstruct the high-resolution image. In the test sets of Set5 and Set14, peak signal-to-noise ratio (PSNR) and structural similarity (SSIM) are used as evaluation indexes, while comparing SRCNN, FSRCNN and VDSR methods all reconstructed images with better results. The experimental results show that the method can effectively improve the utilization of high-frequency feature information and can increase the reconstruction capability of the images to a certain extent.

Keywords: Deep learning; super-resolution reconstruction; residual convolution; dual attention mechanism

1. INTRODUCTION

Image super-resolution reconstruction (SR) is a challenging and popular research topic in the field of computer vision and image processing, where image resolution is a set of performance parameters used to evaluate the richness of detail information contained in an image. However, in practice, most imaging devices are disturbed by various factors such as hardware and environment, which makes the image resolution not meet the needs of practical applications. Therefore, in order to improve the image resolution without changing the imaging device, researchers have started to try to reconstruct low-resolution (LR) images into high-resolution (HR) images by using image processing and machine learning algorithms. Due to the property that deep learning can adaptively learn the nonlinear mapping relationship between LR images and HR images, the SR algorithm for images based on deep learning is significantly better than the traditional methods, so it has also become the mainstream research method for image super-resolution reconstruction methods [1]. Meanwhile, SR techniques have been widely used and achieved significant results in practical scenarios such as analysis and recognition of medical images, face super-resolution, video surveillance and security, and remote sensing images. Image super-resolution is mainly divided into two categories, single image super-resolution (SISR) and multiple image super-resolution (MISR), which are discussed in this paper [2-3].

With the development of deep learning techniques, convolutional neural network-based approaches have achieved great success and made an important impact in the field of computer vision. In 2014, the pioneering introduction of convolutional neural networks into the field of image super-resolution by Dong [4] et al. proposed the super-resolution convolutional neural network (SRCNN) to learn the mapping relationship between high- and low-resolution images in an end-to-end manner, which greatly simplifies the workflow of super-resolution algorithms. The algorithm combines traditional sparse coding with deep learning as the basis, uses dual cubic interpolation to put a low-resolution image of the target size as the input, and uses a convolutional neural network containing three convolutional layers to fit the nonlinear mapping between high- and low-resolution images, completing the extraction and feature representation, nonlinear mapping, and image reconstruction process, realizing end-to-end image reconstruction, and its reconstruction The effect is significantly better than the traditional super-resolution algorithm, which opens the way for deep learning research in the field of image super-resolution. Later, in 2016, Dong et al [5] proposed a modified fast super-resolution convolutional neural network (FSRCNN) for SRCNN, using the original low-resolution image without processing as the input for training, and up-sampling and reconstructing the high-resolution image by the deconvolution layer at the end of the network. In the same year, Shi et al [6] proposed an efficient sub-pixel convolutional neural network (ESPCN), which achieves the up-sampling operation of LR images by pixel rearrangement, which greatly reduces the computational effort and improves the reconstruction efficiency compared to the inverse convolutional layers. Kim [7] et al also proposed a very deep super-resolution network (VDSR) in the same year by stacking 20 convolutional layers for image features for deep extraction and introduced a residual model to speed up the convergence of the network and improve the reconstruction results.

Based on the consideration of the training time of most networks, the performance of image reconstruction effect and the utilization of high-frequency image information perspectives, an image super-resolution reconstruction method based on residual convolution and double attention mechanism is proposed in the paper. The method takes the low-resolution image input model after double triple

International Journal of Computer Applications Technology and Research
Volume 12–Issue 03, 01-05, 2023, ISSN:-2319–8656
DOI:10.7753/IJCATR1203.1001

interpolation, and firstly uses the convolution layer with smaller convolution kernel to extract the shallow features of the input image; then extracts the deep features of the image by cascading deep convolutional network, introduces the local residual block to solve the problem of model degradation and gradient caused by too many parameters of the network, and adds the double attention mechanism module in the residual block to give the network feature weights Finally, a sub-pixel convolutional layer is used as the up sampling method at the end of the network to reconstruct a high-resolution image of the target size. The experimental results show that this method can effectively improve the utilization of high-frequency information, recover image details, and improve the image reconstruction effect.

2. RELATED JOBS

In order to enable the network to pay more attention to the ground high frequency information and ignore the irrelevant information in the network data, the attention mechanism has been reapplied in the field of computer vision. The attention mechanism is an information processing mechanism that originated from the study of human vision. In the human vision system, the received visual information is not processed all at once, but some of the key information is selected for processing, and resources are allocated rationally to solve the information overload problem, thus improving efficiency [8]. Since Hu et al. proposed the channel attention (CA) mechanism in SENet [9] in 2018, it has been widely used in deep learning, and although it increases the number of certain parameters, the performance has been well improved.

The Convolutional Block Attention Module [10] (CBAM) is a dual attention mechanism that combines the attention mechanisms of space and channel, which can achieve better results than the CA mechanism that focuses only on the channel. CBAM starts from two scopes, channel and space, and introduces both spatial CBAM starts from two scopes of action, channel and space, and introduces two analysis dimensions, spatial attention and channel attention, to achieve a sequential attention structure from channel to space. The spatial attention allows the neural network to focus more on the pixel regions in the image that play a decisive role in classification and ignore the irrelevant regions, while the channel attention is used to deal with the assignment relationship of feature map channels, and the simultaneous attention allocation to both dimensions enhances the effect of the attention mechanism on model performance. the structure of the CBAM module is shown in Figure 1.

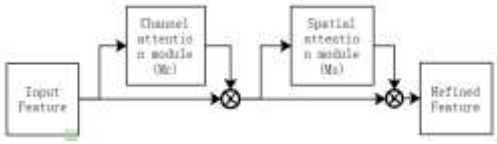

Figure 1. The structure of the CBAM module

Given an intermediate feature map F ∈ R(C × H × W) as input, CBAM sequentially derives a 1D channel attention map Mc ∈ R(C × 1 × 1) and a 2D spatial attention map Ms ∈ R(1 × H × W), and the whole attention process can be summarized in Equation as:

$$F' = M_c(F) \otimes F, F'' = M_s(F') \otimes F'$$

where ⊗ denotes element-by-element multiplication, during which the attention values are propagated accordingly and F^" is the final refined output.

In the channel attention module, each channel of the feature map is considered as a feature detector, and the channel attention focuses on "what" is meaningful in a given input image. The global maximum pooling and global average pooling are applied to the input feature maps, and the feature maps are compressed based on two dimensions to obtain two different dimensional feature descriptions, F^c_{avg} and F^c_{max}; the pooled feature maps share a multilayer perceptron network (MLP) and a hidden layer, and the hidden activation size is set to R(C/r×1×1) to reduce the parameter overhead, where r is the scaling rate; the two feature maps are combined using element-by-element summation to merge the output feature vectors, and the weights of each channel of the feature map are normalized by the sigmoid activation function, and the normalized weights are multiplied with the input feature map. the flowchart of the channel attention mechanism module in CBAM is shown in Figure 2.

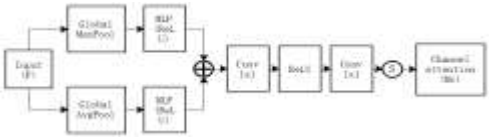

Figure 2. The channel attention mechanism module

The channel attention of channel attention is calculated by equation as follows:

$$M_c(F) = \sigma(W_1\left(W_0\left(F^c_{avg}\right)\right) + W_1\left(W_0(F^c_{max})\right))$$

where σ is the sigmoid activation function, $W_0 \in R(C/r \times C)$, and $W_1 \in R(C \times C/r)$, noting that the MLP weights W_0 and W_1 are shared for both inputs.

The spatial attention mechanism mainly processes the spatial domain of the output feature map of the channel attention mechanism, and uses the spatial attention module after the channel attention module to extract the spatial features between channels and generate the spatial attention map. When extracting the feature information, the spatial attention module shifts the focus of the network model from "what features are meaningful" to "where features are meaningful", thus further extracting the spatial feature information from the output features of the channel attention module. The spatial attention mechanism module in CBAM is shown in Figure 3.

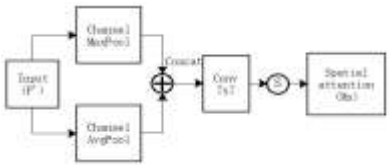

Figure 3. The spatial attention mechanism module

The feature map F^' output from the channel attention module is used as the input feature map of this module. First, the feature maps are subjected to maximum pooling and average pooling based on the channel dimension to obtain two H×W×1 2D maps: the average pooling feature F^s_{avg} and the maximum pooling feature F^s_{max} across channels, respectively; then the two output feature maps are stacked in the channel dimension are connected and convolved by a standard convolution layer, and the spatial features are filtered using a 7×7 convolution kernel to produce a 2D spatial attention map; finally, the final attention map is obtained by normalizing the

International Journal of Computer Applications Technology and Research
Volume 12–Issue 03, 01-05, 2023, ISSN:-2319–8656
DOI:10.7753/IJCATR1203.1001

weights with a sigmoid activation function. The spatial attention is calculated by equation as follows.

$$M_s(F) = \sigma(f^{7\times7}([F^s_{avg}, F^s_{max}]))$$

where σ is the sigmod activation function and $f^{7\times7}()$ is the 7×7 convolution operation.

3. METHODOLOGY OF THIS PAPER

3.1 Network Structure

Although increasing the network depth and number of layers can improve the image reconstruction, it also makes the network difficult to train and hard to converge. For image super-resolution reconstruction tasks, high-frequency features are more valuable for the reconstruction of high-resolution images. By introducing the attention mechanism, the model can focus on the extraction of high-frequency features among the many input information, which can improve the accuracy and efficiency of the model processing. Considering the image reconstruction performance, the training time of the network and the utilization rate of high-frequency feature information of the image, an image super-resolution reconstruction method based on residual convolution and double attention mechanism is proposed in the paper. The local residual block is introduced to solve the information overload and model degradation caused by too many network parameters, and then the dual attention mechanism module is embedded in the residual block to adaptively calibrate the network features and adjust the feature map weights on each channel and spatial domain to improve the model reconstruction effect, and its network structure model is shown in Figure 4.

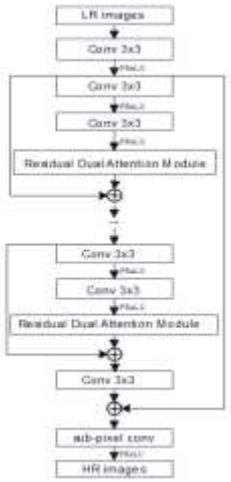

Figure 4. Network Structure Diagram

The method incorporates a residual double attention module, which takes the low-resolution image after double triple interpolation as the input of the model, first extracts the shallow feature information of the image using a convolutional layer, maps the image features nonlinearly into a high-dimensional vector, then learns the depth feature information of the image by cascading residual blocks, nests a residual double attention module in each local residual block to adaptively calibrate the generated image features to suppress redundant information, and finally up samples the features through a sub-pixel convolutional layer [11] to reconstruct the high-resolution image.

3.2 Residual Dual Attention Module

The residual double attention module adds a double attention mechanism module on the basis of the residual module to give different weights corresponding to the importance of different feature outputs and suppress the relatively redundant features, so as to extract the key features that are beneficial to image reconstruction.

In order to enhance the nonlinearity of the network, a convolutional layer with smaller convolutional kernel and PReLU activation function are added to the module to deepen the depth of the module to extract the depth features of the image, and its specific module structure framework is shown in Figure 5.

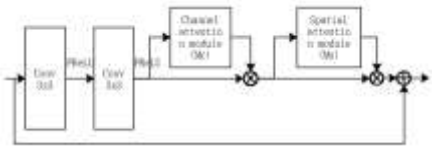

Figure 5. Residual double attention module structure diagram

Let the input of the module be x_0, then the output y of the module can be expressed as equation:

$$y = x_0 + M_s(M_c(x_l)\otimes x_l)\otimes(M_c(x_l)\otimes x_l)$$

where $M_c(\cdot)$ denotes the channel attention mechanism, $M_s(\cdot)$denotes the spatial attention mechanism, and $x_l$denotes the input of the residual dual attention module, obtained by the convolution operation.

3.3 Loss Function

The task of image super-resolution reconstruction is to obtain the reconstructed image through a series of learning by convolutional neural networks, so that the difference between the reconstructed image and the original high-resolution image is as small as possible.

The method in this section uses mean square error (MSE) as the loss function to optimize the parameter training model, which is shown in equation.

$$MSE = \frac{1}{H \cdot W}\sum_{i=1}^{H}\sum_{j=1}^{W}(x(i,j) \quad y(i,j))^2$$

Where, H and W denote the height and width of the image, respectively, and x(i,j) and y(i,j) denote the pixel points corresponding to the reconstructed image and the original image, respectively.

4. EXPERIMENTAL ANALYSIS

4.1 Data Set and Experimental Setup

The experiments use the publicly available image super-resolution dataset DIV2K, which contains 800 training images, 100 validation images, and 100 test images. The method in the paper uses 800 training images of this dataset as the training dataset. Set5 and Set14 benchmark datasets are used as the test datasets.

The LR images in the training set after double triple interpolation are randomly cropped into 96×96 size image blocks, and data enhancement is achieved by random rotation of 90°, 180°, 270° and horizontal flip. In the training phase, the network parameters were optimized using the Adam optimizer with parameters $\beta1$ and $\beta2$ set to 0.9 and 0.999, respectively, and ϵ set to 10^(-8). The learning rate was

initialized to 0.0001 and the learning rate was halved every 200 cycles. Each batch input was set to 64.

4.2 Evaluation Criteria

The evaluation criteria of single-frame image super-resolution methods are usually divided into subjective and objective evaluations. The subjective evaluation is performed by the human eye visually comparing the original image with the generated image. To verify the quality of the model, objective evaluation criteria such as peak signal-to-noise ratio (PSNR) and structure similarity (SSIM) are usually used to evaluate the reconstruction quality of the generated image for different models.

The peak signal-to-noise ratio measures the image reconstruction quality by calculating the error between the corresponding pixel points, which is calculated as follows:

$$PSNR = 10lg\frac{MAX^2}{MSE}$$

Where MAX indicates the maximum value of the image signal, i.e., the peak value, expressed as (2^n-1), and n is the number of image bits per pixel, generally 8. MSE is the mean square error between the original image and the generated image. the unit of PSNR is dB, and the larger the value, the smaller the image distortion.

Structure similarity measures the similarity of the image from three perspectives: brightness, contrast and structure. Assuming that x and y denote the original high-resolution image and the recovered high-resolution image, respectively, the calculation is shown below:

$$SSIM(x,y) - l(x,y) * c(x,y) * s(x,y)$$

$$l(x,y) = \frac{2\mu_x\mu_y + C_1}{\mu_x{}^2 + \mu_y{}^2 + C_1}$$

$$c(x,y) = \frac{2\sigma_x\sigma_y + C_2}{\sigma_x{}^2 + \sigma_y{}^2 + C_2}$$

$$s(x,y) = \frac{\sigma_{xy} + C_3}{\sigma_x\sigma_y + C_3}$$

where l(x,y) denotes brightness comparison, c(x,y) denotes contrast comparison, and s(x,y) denotes structure comparison; μ_x and μ_y denote the pixel mean of the two images, σ_x and σ_y denote the standard deviation of the two images, and σ_{xy} denotes the covariance of the pixel blocks in the two images; C_1, C_2, and C_3 are constants to avoid the systematic error when the denominator is 0. SSIM takes values in the range of [0, 1], and the closer the result is to 1, the smaller the distortion is; when the result is 1, it means that the input image and the output image are identical.

4.3 Analysis of Results

To verify the performance of the method in the paper, experimental comparisons and data analysis are performed for different models of single-image super-resolution reconstruction with different data sets and reconstruction magnifications.

The peak signal-to-noise ratio and structural similarity of the algorithms such as SRCNN, FSRCNN, VDSR and the method in the paper were compared at different reconstruction magnifications using the trained models for super-resolution reconstruction of low-resolution images at 2x, 3x and 4x, and the test results are shown in Table 1 and Table 2, respectively.

Table 1. Average PNSR of different algorithms at different reconstruction multiples

Datasets	Multiples	SRCNN	FSRCNN	VDSR	Ours
Set5	×2	36.66	36.87	37.33	37.49
	×3	32.37	33.05	33.56	33.78
	×4	30.07	30.46	31.19	31.24
Set14	×2	32.45	32.57	32.69	32.96
	×3	29.01	29.26	29.61	29.74
	×4	27.49	27.69	27.95	28.01

From the data in the table, it can be seen that the algorithm in the paper achieves better super-resolution reconstruction performance by improving both the PNSR average and SSIM average at different reconstruction multiples compared with other algorithms.

Table 2. Average SSIM of different algorithms at different reconstruction multiples

Datasets	Multiples	SRCNN	FSRCNN	VDSR	Ours
Set5	×2	0.9452	0.9521	0.9543	0.9623
	×3	0.8972	0.9036	0.9126	0.9147
	×4	0.8590	0.8557	0.8830	0.8894
Set14	×2	0.9031	0.9061	0.9181	0.9207
	×3	0.8169	0.8153	0.8317	0.8337
	×4	0.7534	0.7456	0.7674	0.7832

Specifically, in the Set5 data set, the PNSR improved by 0.16 dB, 0.22 dB, 0.05 dB, and SSIM improved by 0.0080, 0.0021, and 0.0064, respectively, compared with the VDSR method at magnifications of 2, 3, and 4; in the Set14 data set, the PNSR improved by 0.27 dB, 0.13 dB, 0.06 dB, and SSIM improved by 0.0026, 0.0020, and 0.01 dB, respectively, compared with the VDSR method at magnifications of 2, 3, and 4. In the Set14 data set, the PNSR is improved by 0.27 dB, 0.13 dB and 0.06 dB, and the SSIM is improved by 0.0026, 0.0020 and 0.0158, respectively, compared with the VDSR method. It can be seen that the reconstruction effect of the method in the paper is overall better than the other three methods.

5. CONCLUSIONS

In order to improve the image reconstruction accuracy and make full use of the image high-frequency information, an image super-resolution reconstruction algorithm based on residual convolution and double attention mechanism is proposed in the paper. Then, we learn the depth features of the image with the help of residual blocks, embed a residual double attention module in each residual block to adaptively calibrate the generated image features, fully utilize the high-frequency features and suppress the invalid information, and finally up sample the features through a sub-pixel convolution layer to reconstruct a high-resolution image of the target size. The experimental results show that compared with SRCNN, FSRCNN and VDSR methods, the method in the paper has a great improvement in both peak signal-to-noise ratio and

structural similarity. In the subsequent research work, the method can be tried to be applied to a specific field, such as medical imaging and satellite remote sensing. However, the image reconstruction effect of this network still needs to be improved, and the network design will be further optimized in the future to further improve the super-resolution reconstruction accuracy.

Captions should be Times New Roman 9-point bold. They should be numbered (e.g., “Table 1” or “Figure 2”), please note that the word for Table and Figure are spelled out. Figure’s captions should be centered beneath the image or picture, and Table captions should be centered above the table body

6. REFERENCES

[1] Xu Mengxi,Yang Yun. Super-resolution image video restoration methods and applications [M]. Beijing:People's Post and Telecommunications Publishing House,2020:1-3.

[2] Liu Y. X., Duan T. T.. Research on image super-resolution reconstruction technology based on deep learning[J]. Technology and Innovation,2018(23):40-43.

[3] YANG J，WANG Z，LIN Z，et al. Coupled dictionary training for image super — resolution[J].IEEE Transactions on Image Processing,2012, 21(8):3467 — 3478.

[4] DONG Chao，LOY C C，HE Kaiming, et al.Image super-resolution using deep convolutional networks［J］.IEEE Transactions on Pattern Analysis and Machine Intelligence,2016,38(2):295-307.

[5] DONG Chao，LOY C C，TANG Xiaoou．Accelerating the super-resolution convolutional neural network［C］//Computer Vision–ECCV 2016.Amsterdam，The Netherlands: Springer，2016:391-407.

[6] Shi W, Caballero J, Huszár F, et al. Real-time single image and video super-resolution using an efficient sub-pixel convolutional neural network[C]//2016 IEEE Conference on Computer Vision and Pattern Recognition (CVPR), June 27-30, 2016, Las Vegas, NV, USA. New York:IEEE,2016：1874-1883.

[7] KIM J，LEE J K，LEE K M，et al.Accurate image super-resolution using very deep convolutional networks［C］//Proceeding of the 2016 IEEE conference on computer vision and pattern recognition．Las Vegas，NV，USA:IEEE，2016:1646-1654.

[8] Corbetta M,Shulman G.L.Control of goal-directed and stimulus-driven attention in the brain[J].Nature Reviews Neuroscience.2002,(3)：3201-215.

[9] Hu J, Shen L, Sun G. Squeeze-and-excitation networks.Proceeding of 2018 IEEE/CVF Conference on Computer Vision and Pattern Recognition. Salt Lake City: IEEE, 2018:7132–7141.

[10] Woo S,Park J,Lee J Y,et al.CBAM: Convolutional Block Attention Module[J]. Springer,Cham,2018:32-49.

[11] Li Lan,Zhang Yun,Du Jia,Ma Shaobin. Research on super-resolution image reconstruction method based on improved residual sub-pixel convolutional neural network[J]. Journal of Changchun Normal University, 2020(39):23-29.

International Journal of Computer Applications Technology and Research
Volume 12–Issue 03, 06-08, 2023, ISSN:-2319–8656
DOI:10.7753/IJCATR1203.1002

UVA Image Registration Model Based on VGG and Multi-Branch Attention

Jieyuan Luo
School of Communication Engineering
Chengdu University of Information Technology
Chengdu, China

Penjing Dong
School of Communication Engineering
Chengdu University of Information Technology
Chengdu, China

Qinglin Huang
School of Communication Engineering
Chengdu University of Information Technology
Chengdu, China

Abstract:
For UVA images with different resolutions and large areas of weak texture, image feature extraction is insufficient and mis-matching is increased during image registration. To solve these problems, an unsupervised registration model based on VGG feature extraction and multi-branch attention is proposed. First of all, two feature extraction networks with shared weight parameters are used to extract the low and high level fusion features of the moving image and the reference image. The convolution neural network is used to extract the high-dimensional feature map of the image, and the key points are selected according to the conditions that meet both the channel maximum and the local maximum, and the corresponding 512-dimensional descriptor is extracted on the feature map, In the matching stage, add multi-branch attention based on residual block to filter out the wrong features. The algorithm is tested with multiple groups of images and compared with several image matching algorithms. The results show that the algorithm can extract the scale-invariant similar features of images, and has strong adaptability and robustness.

Keywords: deep learning; image matching; convolution neural network; unsupervised learning; multi-branch attention

1. INTRODUCTION

At present, image registration is one of the essential key technologies in the process of image mosaic. Image registration methods include gray-level based registration methods and feature-based registration methods [1]. Among them, gray-level based methods complete image registration through gray-level value calculation. This method is simple and intuitive, but the calculation amount is large and sensitive to the gray-level value of the image, and the illumination change of the image Scale change and rotation change will cause large matching error; The feature-based registration method obtains the registration results by extracting and matching the common features between images to calculate the transformation parameters. This method has good robustness and high efficiency. The illumination and inclination of different UAV images often differ greatly, so it is more appropriate to use feature-based registration method.

Feature-based image registration methods can be subdivided into traditional methods and learning-based methods The typical traditional method is the SIFT (Scale Invariant Feature Transform) algorithm proposed by D.G. Lower et al. [2] The algorithm performs registration by extracting scale, scale and rotation invariance features, which has stable performance but high complexity and is sensitive to mismatched data Although a series of optimization algorithms [3] have been generated for this algorithm, they all have certain scenario constraints and computational efficiency is not high.

In recent years, deep learning methods have shown excellent performance in the field of image [4]. Many researchers have used deep learning methods such as convolutional neural networks (CNN) to solve image registration problems [5] In order to solve the problem of lack of tag images in deep learning, some scholars explored unsupervised learning registration method VoxelMorph [6] method has achieved good results on brain data sets; VTN (Volume Tweening Network) adopts integrated affine transformation module and network block cascade mode, and has achieved success in medical image registration with large deformation; Literature [7] used unsupervised learning of photometric loss to estimate homography; Literature [8] added mask structure to learn the depth information of the image after feature extraction, so as to make more accurate homography estimation, and so on . In general, image registration based on depth learning is becoming the mainstream However, due to the large resolution and large area of weak texture areas of aerial images taken by UAVs, it is easy to cause feature mis-matching, thus reducing the registration accuracy. Therefore, at present, there are few studies on applying depth learning model to such image registration.

2. Design of feature extraction module

The feature extraction module design, as the first step of the registration model design in this paper, is mainly to use the high performance of deep learning to extract the advanced feature information of the image pair to be registered, so as to achieve robust and efficient feature alignment. In view of the excellent performance of VGG-16 network on ImageNet, the front part of VGG-16 network structure is used to extract features. However, VGG structure has no branch structure, In the shallow network part, the low-level contour features of the image are extracted, while in the deep network part, the high-level detail information is filtered. Simply stacking the network can not combine the low-level and high-level features. Therefore, using a simple VGG network structure can not effectively extract the features that are conducive to image registration. The ResNet structure can apply the output of the previous layer to the next layer, The low-level contour features and high-level semantic features can be fused, but the ResNet series network is deep and complex, and the image registration task requires a relatively simple model to ensure the operational efficiency. Therefore, this paper combines the

International Journal of Computer Applications Technology and Research
Volume 12–Issue 03, 06-08, 2023, ISSN:-2319–8656
DOI:10.7753/IJCATR1203.1002

ResNet idea with the VGG network structure. It can not only screen out the low and high level fusion features required for registration, but also ensure that the network structure is relatively simple. The specific network structure is shown in Figure1.

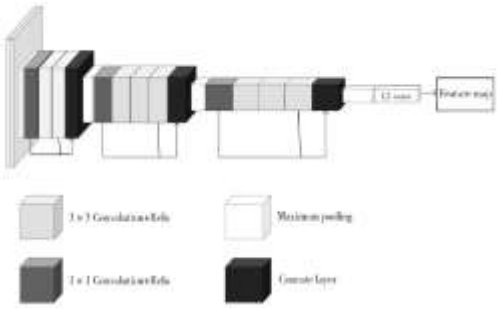

Figure. 1 Feature extraction network structure diagram

The image with the input resolution (H×W) size is first passed through two convolution kernel sizes of 3 and channel number 64 to obtain Conv1; The pooling operation of Conv1 makes the image resolution 1/2 of the original image to reduce the dimension. For pooling results (Pool1), use (1×1) convolution to increase the number of channels to 128 to obtain r1; Conv2 is obtained by convolution of r1 with two convolution kernel size of 3, step size of 1 and channel number of 128; R1 and Conv2 are added in the channel dimension, so that the output of the previous layer is applied to the next layer to achieve the effect of feature fusion. The subsequent network structure is so on, the number of channels of convolution is 256,512, the resolution is 1/4, 1/8 of the original image, each convolutional layer is followed by a modified linear unit (Relu), and (1×1) convolution is carried out after each pooling, the result is applied to the next layer, the network is cut to (pool4), and finally the feature map is L2 normalized.

3. Feature matching module design based on Multi-branch attention

The feature matching layer is used to calculate all similarity pairs between the local descriptors of the moving image feature map f_M and the reference image feature map f_F. Preliminary feature matching can be achieved by using the correlation layer [6], but due to the existence of a large area of weak texture areas (such as water, sky, etc.) in the UAV image, it is easy to cause wrong feature matching in the feature matching stage, so a multi-branch attention module is added to filter the wrong feature matching to enhance the robustness of the model outliers.

The initial matching partial correlation layer is input to two feature maps f_M and f_F, and output a three-dimensional correlation diagram $C_{FM} \in R^{H\times W\times(H\times W)}$, and define each element on the position (i, j, k) as a pair of corresponding positions The scalar product of a descriptor, the mathematical description of which is:

$$C_{FM}(i,\ j,\ k) = f_M(i,\ j)^T f_F(i_k, j_k)$$

$i\in\{1, \ldots, W\}$, $j\in\{1, \ldots, H\}$, $k\in\{1, \ldots, W \times H\}$. (i , j) and ($i_k$, j_k) refer to dense features at H×W;A single feature location in the diagram; $k=H(j_k-1)+ i_k$, (ik,jk), that is, each of length W ×H correlation Vector; C_{FM} (i,j,k) stands for f_M The neutral coordinate is the local of (i,j).Descriptor with f_F.

The degree of similarity between local descriptors in. The design idea of multi-branch attention module to filter out false matching is to take the correlation graph C_{FM} as input and output the weight matrix W with the same resolution as C_{FM}, in which the corresponding position weight value of the correct match is larger and the weight of the corresponding position of the wrong match is small. After this, the original is related The C_{FM} figure is weighted by the weight matrix W, and the value at the correct match is increased and the value at the false match is decreased. On this basis, an attention network composed of two parallel branches is designed, and two weight plots W1 and W2 are generated respectively. In Multi-branch module, each branch consists of two parts, encoding and decoding, using the residual element as the basic unit, and the basic structure of the residual element is shown in Figure 2.

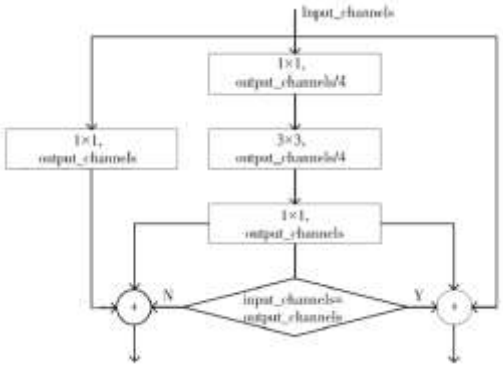

Figure.2 Residual unit structure information graph

4. Experimental results and analysis

4.1 Experimental parameter settings

The overall network is designed using the TensorFlow framework, and UAV-123[9] is used to form 2k registration image pairs, including buildings, roads, cars, sailboats and other categories. Divide all pairs of images to be registered into three parts, namely training set, verification set and test set, with a ratio of 0.75:0.05:0.2. With the help of NVIDIA TITAN X GPU server training network, the initial learning rate selected in training is 0.000 1, attenuation is 10% every 10 rounds, and the batch size is set to 4, for a total of 50 rounds of training. After several experiments, the weight λ of perceived loss in the loss function is finally set to 10, and the neural network is trained until convergence using Adam optimizer.

4.2 Mean Absolute Error MAE

Mean Absolute Error MAE (Mean Absolute Error) represents the average absolute error of a pixel position, which is a general form of error average. When doing model evaluation, it has better robustness to outliers. The smaller the value of MAE, the more similar the two images, that is, the better the registration effect x_i, y_i Indicates the registration result image and the reference image, respectively the pixel value at the i position; N represents the total number of pixels.

$$MAE = \frac{\sum_{i=1}^{N} |y_i - x_i|}{N}$$

4.3 Objective indicators evaluation analysis

Table 1. Statistics evaluation indicators different methods on the test set

method	MAE	Time(CPU)/s
SIFT	161.3254	1.09
ORB	196.4541	0.37
UBHE	178.5633	0.53
CAU-DHE	170.4625	1.99
R-VGG	**140.0882**	**0.88**

It can be seen from Table 1 that the proposed method achieves the best results in MAE indicators, followed by SIFT algorithm and lowest indicators of ORB algorithm, which is consistent with the results of subjective observation. In addition, the indicators of all methods in the table are at low values, mainly due to the large difference between the pairs of images to be registered, the overlapping range of the reference image and the moving image is small, and the registration result image has a large area of black edges. The overall evaluation index of the proposed method is high and the calculation time is short, which proves that the proposed method is non-existent Effectiveness on human-machine image registration tasks.

5. Conclusion

In this paper, an image registration model for UAV based on unsupervised learning is proposed. Firstly, making full use of the high performance of deep learning, the R-VGG feature extraction module is designed to screen out the low- and high-level fusion features with robust characteristics. Secondly, the feature matching module adds Multi-branch attention (MBA) constraints are introduced to filter out false matches, thereby improving registration accuracy. In addition, the composite loss function weighted by content loss and perceived loss is used to improve network performance, and the analysis of visual perception and objective indicators is verified Effectiveness and stability of the method in the field of UAV aerial image registration. In future work, the analysis of drone images will be studied The depth information is improved to make full use of the image information to improve the registration accuracy.

6. REFERENCES

[1] LONG Yongzhi. Research on infrared and visible image registration and fusion algorithms[D] Chengdu : University of Electronic Science and Technology of China,2020.

[2] Lowe D G . Distinctive Image Features from Scale-Invariant Keypoints[J]. International Journal of Computer Vision, 2004, 60(2):91-110.

[3] Qy A , Dn A , Yj A , et al. Universal SAR and optical image registration via a novel SIFT framework based on nonlinear diffusion and a polar spatial-frequency descriptor[J]. ISPRS Journal of Photogrammetry and Remote Sensing, 2021, 171:1-17.

[4] Bay H , Tuytelaars T , Gool L V . SURF: Speeded up robust features[C]// Proceedings of the 9th European conference on Computer Vision - Volume Part I. Springer-Verlag, 2006.Forman, G. 2003. An extensive empirical study of feature selection metrics for text classification. J. Mach. Learn. Res. 3 (Mar. 2003), 1289-1305.

[5] Ye F , Su Y , Hui X , et al. Remote Sensing Image Registration Using Convolutional Neural Network Features[J]. IEEE Geoscience & Remote Sensing Letters, 2018, PP(2):1-5.

[6] Rocco I , Sivic J . Convolutional neural network architecture for geometric matching[J]. IEEE Computer Society, 2017.

[7] Nguyen T , Chen S W , Shivakumar S S , et al. Unsupervised Deep Homography: A Fast and Robust Homography Estimation Model[C]// International Conference on Robotics and Automation. IEEE, 2018.

[8] Zhang J , Wang C , Liu S , et al. Content-Aware Unsupervised Deep Homography Estimation:, 10.48550/arXiv.1909.05983[P]. 2019.

[9] Leibe B , Matas J , Sebe N , et al. [Lecture Notes in Computer Science] Computer Vision – ECCV 2016 Volume 9905 || A Benchmark and Simulator for UAV Tracking[J]. 2016, 10.1007/978-3-319-46448-0(Chapter 27):445-461.

International Journal of Computer Applications Technology and Research
Volume 12–Issue 03, 09-13, 2023, ISSN:-2319–8656
DOI:10.7753/IJCATR1203.1003

KVM Terminal Software Design Based on RK3399 Processor

Xiaoqiang Xin
School of Communication Engineering
Chengdu University of Information Technology
Chengdu, China

Fengbo Wang
School of Communication Engineering
Chengdu University of Information Technology
Chengdu, China

Qinglin Huang
School of Communication Engineering
Chengdu University of Information Technology
Chengdu, China

Abstract: KVM denotes the initials of the keyboard, monitor and mouse of a computer. digital KVM systems are composed of two parts, one is the device terminal and the other is the software adapted to this device terminal. KVM systems are emerging remote centralized management technologies for multiple devices in multiple locations based on IP networks in recent years [1,2]. digital KVM systems mainly use IP networks to control remote computers to control remote computers mainly through IP networks [3]. Therefore, KVM systems are widely used in computer management and remote control of computers. In practical applications, the compression efficiency of images is relatively low and the delay of mouse movements is relatively large. To address these two shortcomings, this paper designs a software based on the RK3399 processor, which on the one hand performs fast image acquisition and high-quality encoding, and on the other hand realizes input control of the target computer through the mouse and keyboard control chip UI012.

Keywords: Digital KVM; Capture Video;Mouse and Keyboard Control; Video Codec

1. INTRODUCTION

With the rapid technological development of society's information industry, digital network systems based on embedded technology are constantly emerging [4]. With computers and networks distributed in all corners of our cities and servers of large multinational companies all over the world, digital KVM systems make it possible for network administrators not to go back and forth between servers in order to complete the maintenance and management of servers, but to access and centrally manage up to thousands of computers with just one set of I/O devices [5]. Instead, they can remotely access and centrally manage up to thousands of computers through a single set of I/O devices [5]. This can create tremendous benefits for centralized information management in enterprise server rooms or data centers [6], not only reducing energy consumption and saving space in server rooms, but also avoiding the clutter that can be caused by too many keyboards, monitors, and mice, greatly simplifying workflow and improving enterprise productivity. Among the various data center server management solutions and remote control solutions, KVM systems are a better choice because managers can manage multiple servers from a single terminal and break through distance limitations. Even if the computers are distributed in different locations, maintenance personnel do not need to travel around for maintenance and management work, but can access and centrally manage multiple computers remotely with just one set of I/O devices [7]. Traditional KVM systems are affected by the video codec technology, and the quality of the received audio and video is very poor, which is an important reason for the extremely poor user experience. Moreover, due to the limitation of network bandwidth, the problems of data transmission rate and transmission delay are also very prominent, and a series of problems reduce the efficiency of data management. In such a context, this paper uses RK3399, which supports H.265 video encoding, as the core controller to design and implement a KVM terminal software based on the characteristics of KVM terminal devices, aiming to reduce the video transmission bandwidth and overall time delay, improve the video quality, and also support mouse and keyboard control, which has good practical application value.

2. KEY TECHNOLOGIES

In our daily learning life, all kinds of audio and video can be seen everywhere, whether it is the elderly or children, whether it is on the bus or in the restaurant, people are holding their cell phones to use the network to brush a wonderful video. Video has gradually become an important way for us to know and perceive the world. Behind the wonderful video is a very serious problem, which is brought by the storage and transmission of the video. For example, a 1-hour 1080P, 30FPS lossless video requires about 660G of storage space, which obviously exceeds the storage capacity and transmission capacity of our existing media, so it is necessary for us to perform some lossy compression - that is, video codec. The goal is to represent the same video with fewer bits, thus reducing the size of this video and achieving the goal of taking up less space and being easier to transmit.

In 2013, ITU-T and ISO/IEC jointly developed a new generation of video coding standard, which is called High Efficiency Video Coding HEVC in the ISO standard, hereinafter referred to as H.265 [8]. In modern multimedia applications, the obtained video information is compressed efficiently with the help of video coding technology in order to achieve real-time playback, or storage on hard disk [9].

H.265 is an improvement on H.264, the technique of efficient prediction in the structure is retained and the framework used is still the hybrid coding framework. In order to optimize the compression performance of H.265, numerous coding tools such as flexible CTU quadtree image division, inter-frame prediction asymmetric motion division and multi-directional intra-frame prediction patterns are then used. Its newly adopted coding techniques are as follows.

(1) image chunking technology. H.264 standard uses macroblock to divide a frame image, the maximum size of macroblock is 16×16. H.265 uses three concepts of coding unit CU (Coding Unit), prediction unit PU (Prediction Unit) and transform unit TU (Transform Unit) to describe the whole coding process. Among them, CU is the basic unit of H.265 coding, and the size of CU can range from 64×64 to 8×8, which can effectively segment images of various resolutions.

(2) Predictive coding technology. H.265 still uses time and space correlation to perform intra-frame or inter-frame coding to eliminate redundant information, but thanks to the use of multi-angle prediction, advanced displacement vector prediction technology, high-precision motion compensation technology and other technologies, the prediction accuracy and coding efficiency are greatly improved.

(3) Transformation and quantization. H.265 reduces the correlation between image blocks by transforming the frequency domain and compresses the prediction residual information to achieve further compression. Both intra-frame prediction and inter-frame prediction, the obtained prediction residuals are transformed by the transform matrix to achieve the concentration of signal energy. The quantization and inverse quantization processes are integrated into the transform matrix operations, and the size of the quantization step (Qstep) depends on the quantization parameter (Qp). When the quantization step is larger, the quantization error is larger and the image quality suffers a more significant degradation, but the compression effect is better. Conversely, the decrease of quantization step size reduces the quantization error and the loss of image quality, but the compression effect is poorer.

(4) The in-loop filter filters the reconstructed image obtained after inverse transform and inverse quantization to remove the block boundary effect and reduce the distortion of the reconstructed image to the original image in the coding process. The loop filtering process of H.265 adds adaptive sampling point compensation after the deblocking filter, and compared with H.264, H.265 increases the minimum block of the deblocking filter from 4×4 to 8×8 to reduce the number of filtering times, and for each 8×8 For each 8×8 grid, the first judgment is whether it is the boundary of TU or PU, if it is not the boundary, no filtering is needed, if it is the boundary, the corresponding boundary intensity is calculated, and the boundary intensity value is 0, 1 or 2. For the luminance component, the boundary with intensity 1 or 2 will be filtered; for the chrominance component, only the boundary with intensity 2 will be filtered. For the luminance boundary with intensity 1 or 2, and the chrominance boundary with intensity 2, it is also necessary for the quantization parameters to meet certain conditions before filtering.

The advantage of H.265 is that it adopts advanced coding and technology, and the compression rate is doubled compared with H.264. The disadvantage is that the complexity of coding computation is increased several times, especially the computation of CTU division method selection, intra-frame prediction and inter-frame prediction mode in pattern decision is greatly increased. Therefore, H.265 video coding puts higher requirements on the hardware implementation platform.

3. DESIGN SOLUTIONS

3.1 Overall software framework

The software design of this paper revolves around the structure of the RK3399 processor, relying on its rich interfaces, running the Linux real-time operating system on its ARM Cortex-A53 and Cortex-A72 [10], managing the entire software system, including the driver support for each device and the various requirements of the business, as follows: configuring the TC358743XBG through I2C working mode through I2C; audio and video acquisition and encoding through MPP; debugging service content through UARTO port and network port connected to the host; controlling UI012 through UART1 port to complete the keyboard and mouse control of the host. The overall framework of the system is shown in Figure 1.

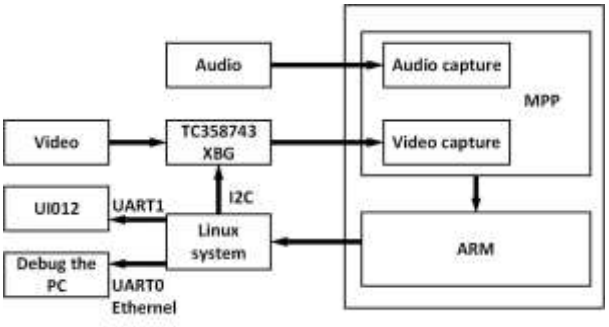

Figure 1. Overall system framework

3.2 Video module design

Rockchip Micro provides a media processing software platform MPP, which shields the application software from the complex underlying chip-related processing, and directly provides multimedia processing interface MPI interface to complete the corresponding module functions. Developers directly through the combination of calls MPI to achieve different system functions, which framework greatly reduces the development cycle, cost and development difficulties, but also makes the system maintenance becomes more convenient.

Before using the MPP development platform for software development, the initialization of the MPP system needs to be completed. After the application completes the MPP service, it also needs to de-initialize the MPP system to release the system resources. the initialization of MPP includes the initial processing of video cache pool, binding system interfaces, etc. MPP provides MPI including video input, video processing, video output, video processing subsystem, video coding, video detection and analysis, area management, audio and video graphics subsystem. The rich multimedia processing interfaces cover all aspects of audio and video multimedia processing for users to develop specific functions.

The video module is designed to perform a series of tasks related to video. The purpose of this module is to implement multi-resolution video acquisition for the KVM market, which can be used to adapt to various resolutions in the KVM market; to perform corresponding processing such as scaling, frame rate control or video encoding quality selection according to user requirements; to feed the acquired video data to the H.265 encoder for encoding and compression of the data according to the MPP programming framework. The captured video data is encoded and compressed according to the MPP programming framework and sent to the H.265 encoder to obtain a high compression rate video stream for

International Journal of Computer Applications Technology and Research
Volume 12–Issue 03, 09-13, 2023, ISSN:-2319–8656
DOI:10.7753/IJCATR1203.1003

network transmission. The video processing flow is designed in accordance with the design purpose of this module.

In order to perform adaptive capture of the current actual video resolution, the TC358743XBG decoder chip needs to be accessed via the I2C interface to get the actual resolution information of the current video, and then the multimedia module is designed and connected to the VI module according to the MPP programming framework, and the video channel and cache pool are initialized according to the current resolution. After initialization, the video image is captured, and it can be cropped, color space conversion and other processing, and output multiple image data of different resolutions; the VPSS module receives the image sent from VI, and can scale the image, frame rate control and other processing, and realize the same source output multiple image data of different resolutions for encoding; the VENC module receives the image data captured by VI and output after processing by VPSS, and supports multi-channel real-time encoding, and each encoding independent.

Video input (VI) unit to achieve the function: through I2C to obtain the current video resolution, and according to the resolution information to complete the initialization work, VI and VPSS unit binding, will be outside the processor video data received through the ITU-R BT1120 interface, directly to the VPSS. In this process, VI can crop, color space conversion and other processing of the received original video image data, and realize the original video image input all the way, and output all the way video image function. The overall design of the video processing flow is shown in Figure 2.

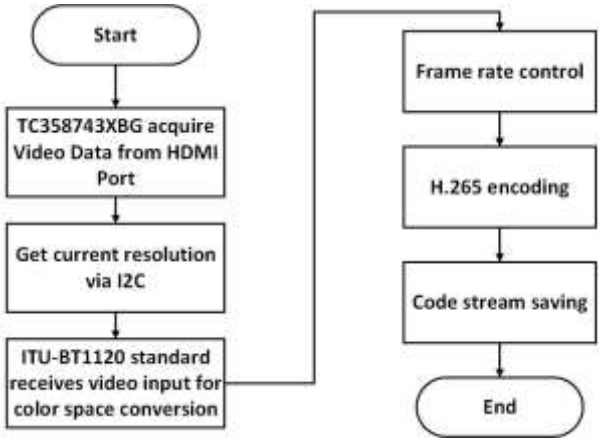

Figure 2. Video processing flow design flowchart

The video processing (VPSS) unit implements the functions:Uniform pre-processing of a pair of input images, such as scaling, frame rate control, etc. The frame rate is controlled in the VPSS by channel CHANNEL, which binds the physical channel and takes the physical channel output as its own input, and when the image data of the physical channel passes through CHANNEL, it can choose to discard some of the data to achieve When the image data of the physical channel passes through CHANNEL, it can choose to discard some data to achieve frame rate control, and it can crop the data in the channel to achieve the effect of cropping the image.

In the online mode of the RK3399, the VPSS supports sending images to the encoding unit for encoding according to the line unit, sending while capturing, which can reduce the delay time generated during the process of processing the complete frame image by the VPSS and then sending it to the encoding unit.

Video encoding (VENC) unit functions: This unit supports multiple video encoding in real time, and each encoding is independent of each other, and the encoding protocol and encoding profile can be different. A typical encoding process includes the reception of the input image, the encoding of the image and the output of the code stream.

The coding specifications supported by RK3399 processor include H.264 coding algorithm supporting BP, MP and HP coding levels, JPEG coding algorithm, MOTION JPEG coding algorithm, and most importantly, H.265 coding algorithm supporting MP coding level, which makes the efficiency of video compression reach the first line level and is the basis for the design of this paper to achieve high quality video transmission with low latency and bandwidth. The basis of compressed video transmission under low latency and bandwidth conditions.

The VENC unit consists of the receiving channel subunit and the encoding channel subunit, and the flow chart of encoded data in VENC is shown in Figure 3. If the input image is larger than the encoding channel size, VENC will reduce the source image to the size of the encoding channel and then encode the image; if the input image is smaller than the encoding channel size, VENC will discard the original image because VENC does not support enlarging the input image for encoding; if the input image is comparable to the encoding channel size VENC accepts the source image directly and encodes it.

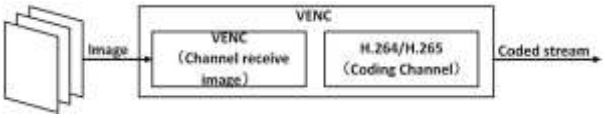

Figure 3. Data flow diagram of VENC

3.3 Web Media Data Interaction Design

The TCP/IP (Transmission Control Protocol/Internet Protocol) protocol is the result of protocol research and development work carried out on the packet-switched network ARPANET (Advanced Research Project Net). Today TCP/IP protocol is widely used by developers and has become the industry standard for communication on the Internet. The four-layer TCP/IP model is used more often in the development process, which mainly includes network layer, transport layer, application layer, and data link layer, and each layer is responsible for a different function.

The process of establishing the server and client structure in this paper is as follows, and the schematic diagram is shown in Figure 4, where the client actively connects to the server to communicate and interact with data.

International Journal of Computer Applications Technology and Research
Volume 12–Issue 03, 09-13, 2023, ISSN:-2319–8656
DOI:10.7753/IJCATR1203.1003

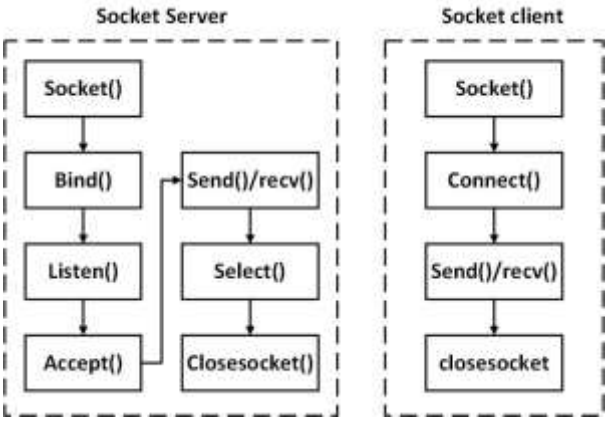

Figure 4. Schematic diagram of the server client

The data sending interaction unit requires the RK3399 system side to send the encoded audio and video data over the TCP network, and after the data reaches the client, a series of processing such as decoding the audio and video data is performed.

In this paper, a thread is created for the data sending interaction unit, and the thread completes a series of operations to obtain video frame data, the process of which is shown in Figure 5.

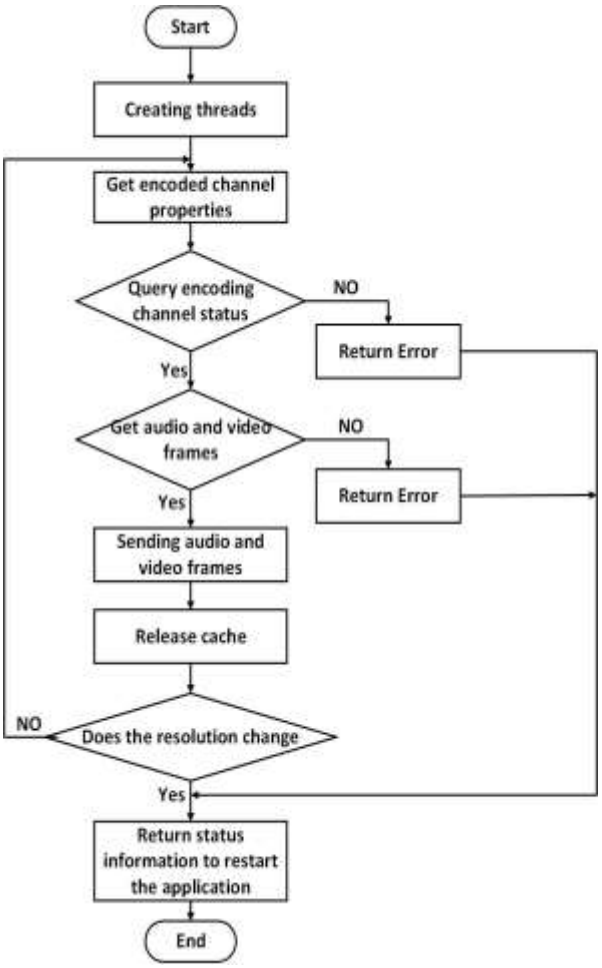

Figure 5. Flow chart of sending data interaction

The data reception interaction unit requires the RK3399 system side to receive the keyboard and mouse data from the client via TCP network and encode the data according to the data interaction format of the UI012 chip.

When a packet is received in the thread, the packet is parsed and if a control signal is received for the keyboard and mouse, the corresponding keyboard and mouse control interaction is executed. In this paper, a thread is created for the data reception interaction unit, in which the socket interface is used to complete the reception of keyboard and mouse signals and control commands sent from the client, and the encoder parameters are adjusted according to the control commands through MPI in this thread, and the flow is shown in Figure 6.

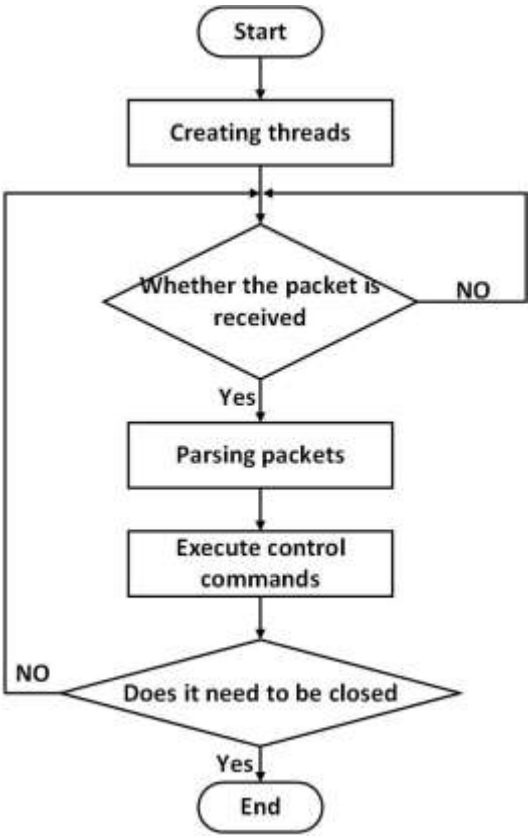

Figure 6. Receiving data interaction flow chart

3.4 Keyboard and mouse interaction design

The keyboard and mouse signal data is received by the remote client through the data reception interaction unit, and after parsing and unpacking, the actual control signal is obtained, and then the RK3399 processor controls the UART1 serial port to output the corresponding data according to the interaction protocol of UI012 to achieve the actual effect of controlling the controlled machine by UI012.

The UART1 pin of RK3399 is a multiplexed pin, and the default initialization is not enabled, so you need to set the pin multiplexing in core.c file, The code of the intercepted fragment is shown in Figure 7 below.

International Journal of Computer Applications Technology and Research
Volume 12–Issue 03, 09-13, 2023, ISSN:-2319–8656
DOI:10.7753/IJCATR1203.1003

```
#define MUXCTRL_REG_BASE 0x200F0000
#define UART1_RXD_REG
IO_ADDRESS( MUXCTRL_REG_BASE + 0x7c )
#define UART1_TXD_REG
IO_ADDRESS( MUXCTRL_REG_BASE + 0x84 )

writel ( 1 , UART1_RXD_REG ) ;
writel ( 1 , UART1_TXD_REG ) ;
```

Figure 7 Pin reuse fragment code

When the UART1 multiplexing configuration is completed, you can directly open the UART1 device and write the data received from the client by the data reception interaction unit and encapsulated according to the UI012 data protocol.

4. EXPERIMENTAL TESTING

4.1 Video delay test

Place Tables/Figures/Images in text as close to the reference Once the data transmission interaction and video encoding module is designed, the encoded video stream can be sent directly to the remote client for decoding and playback through the data transmission interface. The test method is to use the laptop as the video input source, and use the HDMI interface to copy the video output all the way to 108OP60 to the KVM device, which encodes the video stream at 1920×1080 resolution, 30fps frame rate, and 2Mbps bit rate, and sends the encoded video stream to the client of the master. At the same time a stopwatch timer is run on the display desktop of the laptop, and the laptop (i.e., the controlled machine) is placed together with the monitor of the master PC.

Operations such as Word browsing and video viewing are performed on the controlled PC to increase the complexity of the video image. Under normal operation of the KVM system, a photo is taken of the controlled PC and the local PC screen to calculate the time difference between the two stopwatch software displays. The time difference value is the delay time between the video capture source and the remote client interface display.The video latency test results are shown in Table 1, and l0 latency test results were recorded for statistical analysis. The minimum video latency is 80ms, the maximum is 101ms, and the average latency is 89ms, which is the leading level of KVM terminal equipment in terms of latency and can bring users a good experience.

Table 1. Video delay test results

Number of times	Extension time
1	92ms
2	84ms
3	80ms
4	97ms
5	87ms
6	101ms
7	83ms
8	93ms
Average value	89ms

4.2 Keyboard and mouse delay test

When the keypad and mouse delay test, the master PC prints the current system time when it sends out the control keyboard and mouse signals, and runs an auxiliary software for testing the keypad and mouse delay on the controlled PC server. When the controlled PC receives the keyboard signal or mouse signal, it sends UDP packets to the master PC. After receiving the UDP packet, the master PC prints the current system time, then the difference between the two system printing times is the keyboard and mouse signal delay time.Keystroke delay test results are shown in Table 2.

Table 2. Keystroke delay test results

Number of times	Extension time
1	15ms
2	17ms
3	15ms
4	15ms
5	14ms
6	15ms
7	14ms
8	15ms
Average value	15ms

5. CONCLUSIONS

This paper designs and implements KVM terminal software based on the RK3399 processor in order to achieve low latency, high quality KVM video encoding transmission and keyboard and mouse control with low bandwidth. Under the MPP framework of the RK3399, the audio and video capture and encoding modules are designed, and each module in the MPP framework is connected together according to the multimedia processing interface MPI to complete the overall audio and video capture and encoding work. Then the control of the mouse and keyboard is completed.

6. REFERENCES

[1] Huang YF. IP network multimedia communication technology [M]. Beijing: People's Post and Telecommunications Publishing House, 2003.Ding, W. and Marchionini, G. 1997 A Study on Video Browsing Strategies. Technical Report. University of Maryland at College Park.

[2] Wang Da. Computer network remote control [M]. Beijing: Tsinghua University Press, 2003.Tavel, P. 2007 Modeling and Simulation Design. AK Peters Ltd.

[3] Bovberg J. KVM Over IP [J]. Windows It Pro, 2011,15(2):1322-1323.

[4] Zhang P. Software design of embedded network multi-channel audio and video server[D]. Jilin University, 2007.

[5] Thomas C L, Anderson R L, Gilgen R L, et al. Network based KVM SWIening systen. uo,US7555567 [P]. 2009.

[6] Hao Liu J. Design and implementation of a virtualized server management system [D]. Xi'an University of Electronic Science and Technology, 2011.

[7] Thomas C L. Anderson R L,Gilgen R L, et al. Network based KVM switching system: Us,US7555567[P]. 2009.

[8] Jaja E, Omar Z,Rahman A H A, et al. Efficient Motion Estimation Algorithms for HEVC/H.265 Video Coding [M].Berlin: Springer Berlin Heidelberg, 2015: 287-294.

[9] He Junfeng. Implementation and application of motion detection technology in digital surveillance [J. China Security, 2004,(4):47-49.

International Journal of Computer Applications Technology and Research
Volume 12–Issue 03, 14-17, 2023, ISSN:-2319–8656
DOI:10.7753/IJCATR1203.1004

A Two-stream Convolutional Neural Network-based Pornography Recognition Method

Congcong He
School of Communication Engineering
Chengdu University of Information Technology
Chengdu, China

Qinglin Huang
School of Communication Engineering
Chengdu University of Information Technology
Chengdu, China

Jieyuan Luo
School of Communication Engineering
Chengdu University of Information Technology
Chengdu, China

Abstract: The main approach taken to identify pornographic video content is achieved by performing pornography detection on the video content. By extracting features from video key frames and using some common neural network models to recognize the extracted key frame images, a certain accuracy rate can be obtained. However, another key information of video recognition, action information, is ignored, which leads to misclassification of some indistinguishable videos such as sumo wrestling and boxing. A dual-stream convolutional neural network-based pornographic video recognition method is proposed to address this problem. The experimental results show that the dual-stream convolutional neural network effectively improves the recognition rate of indistinguishable pornographic videos.

Keywords: Video Identification, Two-stream convolutional neural network, Keyframe styling

1. INTRODUCTION

With the rapid development of the short video and live streaming industry, the audience of short video and live streaming is becoming more and more widespread. Many primary and secondary school students like to watch live or short video, video content safety issues are very serious. At present, many Internet companies still use human supervision for video supervision. In this period of short video screens everywhere, human supervision consumes a lot of human, material and financial resources. At the same time long time human supervision is also a great threat to the psychological health of the regulator This paper proposes the use of dual-stream convolutional neural network model to improve the recognition efficiency and reduce the misjudgment rate of difficult-to-identify videos.

2. DEVELOPMENT OF NEURAL NETWORK

In 1996, D. A. Fprsyth and M. Fleck successfully implemented a nude recognition system by studying the color and texture characteristics of skin tones. m.-H. Yang and N. Ahuja et al. used the distribution of skin pixels in color space for modeling and used the model for detecting skin tone acorns. m. J. Jones and J. M. Rehg et al. The histogram of color distribution was derived from RGB color space, and then the histogram of color distribution of normal images was compared with the histogram of color of pornographic images, and convolutional neural network was used to classify normal images from pornographic images, and finally, pornography identification was achieved.[1]

The above methods, the effect of pornographic image identification based on the detection of skin color depends only on skin color pixels. These methods are too single in judging the labeling and not highly reliable.In 2012, the AlexNet convolutional neural network model was introduced and its designer Alex Krizhevsky won the ImageNet large-scale vision challenge using the AlexNet convolutional neural network model. the shockingly high recognition rate of AlexNet has led many scholars to join the research of convolutional neural networks. For video recognition, Karen Simonyan et al. used dual-stream convolutional neural networks for two dimensions of temporal and spatial information to study the characteristics of video that are different from images. Based on many studies on image recognition and video recognition, this paper proposes a method to recognize pornographic videos using Two-Stream CNN model. Since the key frame image only contains the spatial information of the image, the action information of the video is completely lost, which cannot achieve the role of video recognition, and the final result will not be able to recognize some indistinguishable pornographic videos well, causing a large rate of misjudgment. Adding video action information to the model, optical stream can express the change information of adjacent images, and the pornography recognition method based on Two-Stream CNN has good reliability[2].

3. CONVOLUTIONAL NEURAL NETWORK

3.1 Convolutional neural network model

Yann LeCun, a tenured professor at New York University, proposed the convolutional neural network in order to recognize handwritten letters. In the convolutional neural network has developed rapidly for several years, but its structural principle is roughly the same as that originally proposed by Yann leCun, consisting of a convolutional layer, a downsampling layer, and a classification layer[3]. As shown in Figure 1.

International Journal of Computer Applications Technology and Research
Volume 12–Issue 03, 14-17, 2023, ISSN:-2319–8656
DOI:10.7753/IJCATR1203.1004

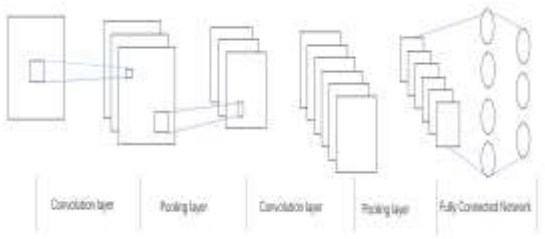

Figure 1. CNN typical struture.

CNN is to learn the features of the image by convolutional operation, the convolutional layer receives the output data of the data downsampling layer and multiple convolutional kernels for convolution, the formula of convolutional operation is.

$$Y_{i,j}^{l} = f(\sum_{i \in m_h} \sum_{i \in n_w} x_{i,j}^{l} G_{i,j}^{l} + b^{l})$$

In the above equation, $Y_{i,j}^{l}$, denotes the value of the (i,j) point output from the Lth layer, $x_{i,j}^{l}$ denotes the input value of the (i,j) point in the Ist layer, G denotes the convolution kernel, b denotes the bias term, m_h, n_w denotes the window size of the local perceptual field in the Lth layer.[4]

In the structure of CNN, multiple feature maps are output after one convolution. Downsampling the feature maps makes the network robust to image rotation, translation, and scale transformation, and reduces the computational effort of network training.[5] Commonly used downsampling methods are mean sampling and maximum sampling. The mean sampling averages the feature values in the sampling window as the sampling result, and the mean sampling formula is:

$$Y_{i,j} = \max_{0 \le h \le H-1, 0 \le w \le W-1} (x_{i*H+h, j*W+w})$$

In the above equation, $Y_{i,j}$ is used as the output value of the convolutional neural network downsampling, X_(1*H+h,j*w+w) is used as the input value of the convolutional neural network, and H,W denotes the length and width of the sampling window. The maximum downsampling method is to take the maximum value within the sampling window as the sampling result, and the calculation formula is.

$$Y_{i,j} = \max_{0 \le h \le H-1, 0 \le w \le W-1} (x_{i*H+h, j*W+w})$$

3.2 Two-stream network model

Each video contains both temporal and spatial information. The change of background from each image frame to the next represents the temporal information of the video. The background of the behavior in the video represents the spatial information of the video. For extracting the number of key frames, passing each of these frame images through a neural network does this very poorly. the Two-stream network design compensates for these deficiencies. Both spatial and temporal streams are placed on the Two-stream network model. The video extracted keyframe images and optical flow images are trained on the Two-stream network model, and the extracted spatial and temporal information is fused using the mean fusion method for the recognition results.

The extracted keyframe images are fed into the Two-stream network as spatial information. The keyframe images are sufficient for the relatively easy to distinguish pornographic videos. The extracted optical flow images are fed into the Two-stream network as motion information[6].

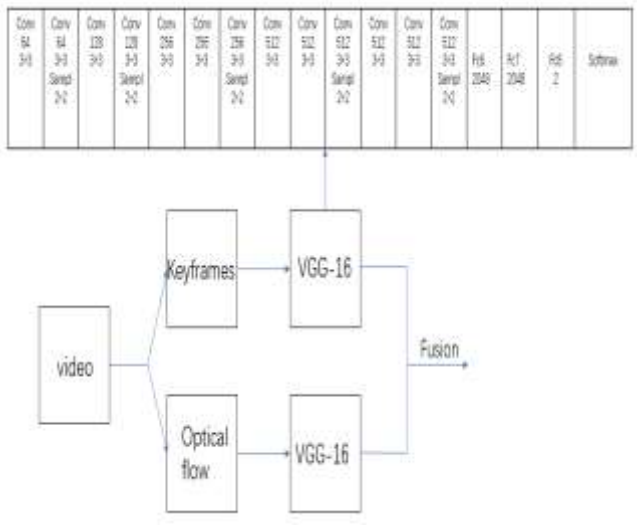

Figure 2. Two-Stream Model Architecture.

3.3 Video Segmentation

Firstly, the video should be segmented, and then the segmented video should be extracted with key frames and optical flow images. In this paper, we mainly refer to the method of video segmentation with unsupervised clustering proposed by Jin Hong et al. Firstly, the video is divided into n classes using clustering method, and the video frames in each class have similarity, and the frames in different classes are not similar or have low similarity. For the class with fewer frames, i.e., the class is not representative, it is directly merged with the neighboring frames[7].

The images stored in the computer are in RGB space, and since HSV color space has better color characteristics than RGB color space, it is necessary to map the colors to HSV space[8]. The preprocessing steps are as follows:

1. Map the RGB images distributed in 0~255 directly to the HSV color space of 0~255.

2. partition the HSV colors, divide the H component into 12 equal blocks, and the S and V components into 5 equal blocks each. 3. map the original colors in the range of 0~255 to the range of 12×5×5.

4. Build the color space of HSV, set the image size as M×N, and count the percentages of H, S, and V components respectively.

The calculation formula is shown in 3.1:

$$H(i) = \frac{H\_follow(i)}{M * N}$$

International Journal of Computer Applications Technology and Research
Volume 12–Issue 03, 14-17, 2023, ISSN:-2319–8656
DOI:10.7753/IJCATR1203.1004

$$S(j) = \frac{S\_follow(j)}{M * N}$$

$$V(k) = \frac{V\_follow(k)}{M * N}$$

To calculate the similarity of two images, we need to calculate the similarity of the three color histograms H,S,V, respectively, by the minimum value corresponding to the same index of the histogram of the two images is accumulated. The formula is as follows:

$$S_h(f, Shot) = \sum_{i=1}^{12} \min\left(H(i), Shot\_H(i)\right)$$

$$S_s(f, Shot) = \sum_{i=1}^{5} \min\left(S(i), Shot\_S(j)\right)$$

$$S_v(f, Shot) = \sum_{i=1}^{5} \min\left(V(k), Shot\_V(k)\right)$$

Since the human eye is more sensitive to the H component than to the S component, and the S component is greater than the V component, for each.

The weights are set for each component, 0.5 for H, 0.3 for S, and 0.2 for V.

The video segmentation and key extraction algorithm using clustering is described as follows:

Maintain a center of mass for each class.

1.For each frame, use Equation 3.2 to calculate the similarity of the cluster cores, if the similarity is less than the set valve value, then it will be placed in a new class, otherwise it will be added to the previous class.

2.Merge some of the clusters that are too small.

3.According to the clustering results Class1,... , Class, perform video segmentation.

4.Calculate the first and largest image in each cluster and use it as a key frame.

3.4 Extraction of optical flow diagrams

Optical flow is a technique that is widely used in computer vision and computer graphics. The concept was first introduced by Gibson in 1950. Optical flow describes pixel motion information, such as the direction of motion as well as the speed of motion. The change of pixels in the image sequence in the time domain and the correlation between adjacent frames are used to find the correspondence that exists between the previous frame and the current frame. In general, the motion information in a video is mainly generated by the motion of the foreground target, the motion of the camera, or the joint motion of both, and is described by optical flow. Optical flow algorithms can be applied to many fields, such as video processing, robot vision, virtual reality, etc. In visual perception, when the human eye observes a moving object, the moving object leaves a continuous image on the retina, just like the flow of light; therefore, the motion information in the video is called optical flow[7].

Optical flow is further divided into sparse optical flow and dense optical flow. Sparse optical flow is a type of image alignment method that specifically targets sparse points on an image, that is, given a number of points on a reference map, these points are generally corner points, and find their counterparts in the current image. Dense optical flow is an image alignment method that matches point by point for an image. In this paper, we mainly use dense optical flow to extract action information from video. The dense optical flow obtains the motion information in the video by performing a complete calculation of the offsets of all points on the image. It can be seen that the computation of dense optical flow is much larger than that of sparse optical flow, so the effect of its alignment is significantly better than that of sparse optical flow alignment[8].

his paper uses the Lucas-K anade optical flow algorithm, which is a common optical flow algorithm in Opencv. It has three assumptions: firstly, the luminance is constant. Secondly, the image motion varies little with time. Finally, spatially consistent[9].

The constraint equation of the image is :

$$I(x, y, z, t) = I(x + \Delta x, y + \Delta y, z + \Delta z, t + \Delta t)$$

4. ANALYSIS OF EXPERIMENTAL RESULTS

4.1 Data pre-processing

This paper uses the NPDI dataset, which is a public pornography dataset containing a total of 800 videos, including 400 pornographic videos and 400 non-pornographic videos, with a total duration of 77 hours. The videos are divided into 200 videos that are easily distinguishable and 200 videos that are not easily distinguishable. The easily distinguishable videos are mainly about eating and playing games. The content of the videos that are not easily distinguishable is mainly swimming, wrestling, etc.
All the videos in the NPDI dataset were keyframed, and on average, multiple keyframes were extracted from each video, and a total of 16727 keyframes were extracted from all 77 hours of video frames. The entire dataset is described in Table.[10]

Table 1. Dataset

Category	Number of Videos	Duration/h	Frames Per Video
Pron	400	57	15.6
Non-Porn(easy)	200	11.5	33.8
Non-Porn(difficulty)	200	8.5	17.5
All Videos	800	77	20.6

4.2 Experiment content

NPDI consists of 16727 keyframe images extracted from 800 videos, of which 10340 are non-pornographic images and 6387 are pornographic images. The non-pornographic images are further divided into 6785 easy-to-distinguish images and 3555 hard-to-distinguish images. In the training, 80% of the pre-processed images are used as the training set, and the top, bottom, left, right and middle images are extracted and then flipped horizontally by mirroring, and 10 training images are generated for each image.

The training of optical flow convolutional network extracts dense optical flow images from 16727 segmented videos in the NPDI dataset. In this paper, the stacking unit is 10, and the dimension of the stacked optical flow image is (224,224,20), where 20 can be regarded as the number of channels of the image. A total of 151,893 optical flow stacking data are obtained after stacking all extracted optical flow images, and the label of each optical flow stacking data is consistent with the classification label of the corresponding video[11].

In order to evaluate the detection effect of Two-stream model, 50 pornographic videos and 50 non-pornographic videos were randomly selected from the NPDI dataset to test the VGG16 model and Two-stream model, and the accuracy, recall and F1 were calculated for each model. The higher the classification effectiveness of the models. The test results are shown in the table below. Comparing the data in the table, we can conclude that the VGG-16 model has a higher accuracy and recall rate than the Two-stream model, and is more accurate in detecting pornographic videos.

Table 2. Experiment results

Model	Accuracy(%)	Reall(%)	F1(%)
VGG-16	93.3	93.1	93.2
Two-Strean	95.2	95.0	95.1

To address the problem that traditional recognition of keyframe images leads to a high false positive rate for indistinguishable videos such as swimming, the Two-Stream model was tested using the same test data set for both models. The test data included 10 boxing videos, 10 swimming videos, and 10 breastfeeding videos. The test results indicated that the M-Two-Stream model improved the classification of videos such as boxing from 50% to 80% compared to the VGG-16 model, the 30% accuracy for the swimming category to 80%, and the 10% accuracy for the lactation videos, showing through experiments that the Two-Stream model reduced the misclassification rate for difficult video detection.

5. CONCLUSION

In this paper, a two-stream convolutional neural network based pornographic recognition method (Two-Stream CNN) is proposed. The method introduces motion information in the video, video segmentation, key frame extraction, feature extraction, and feature combination. The experiments show that the Two-Stream model has higher accuracy in detecting pornographic videos compared with the VGG-16 model, and reduces the misclassification rate of hard-to-distinguish videos such as breastfeeding, wrestling, swimming, and sumo wrestling.

6. REFERENCES

[1] D.A.Forsyth, 1996.M.Fleck.Finding naked people[C]. In Proc.European Conference on Computer Vision.

[2] M-H. Yang，N.Ahujia.1999. Gaussian mixture model for human skin color and its application in image and video. database[J]. SPIE Storage and Retrieval for Image and Video Database.

[3] M.J.Jones, JM. Rehg.2002.Statistical color models with application to skin detection[J]. International Journal of Computer Vision.

[4] Srisaan C.A classification of internet pornographic images[J]. International of Electronic Commerce Studies.

[5] Basilio J AM, Torres G A,Perez G S, et al.2011. Explicit content image detection[J]. Signal & Image Processing,

[6] Karavarsamis S, Atarmos N,Blekas K, et al.2013 Detecting pornographic images by localizing skin ROIs[J].International Journal of Digital Crime & Forensics.

[7] Krizhevsky A, Sutskever I, Hinton G E.2012. Imagenet classsificaton with deep convolution neural networks[C].Advances in Neural Information Processing Systems. Lake Tahoe:NIPS.

[8] Simonyan K,Zisserman A.2014. Very deep convolutional networks for large-scale image recognition [J].Computer Science.

[9] Szegedy C, Liu W, Jia Y, et al.2015. Going deeper with convolutions[C]. Proc of TEEE Conf on Computer Visionand Pattern Recognition. IEEE.

[10] He kaiming, Zhang Xiangyu, Ren Shaoqing, et al.2015 Deep residual learning for image recognition[J]. ComputerScience.

[11] Mohamed N. 2015.Moustafa.Applying deep learning to classify pornographic images and videos[C]. Pacific-rimSymp on Image and Video Technology.

International Journal of Computer Applications Technology and Research
Volume 12–Issue 03, 18-21, 2023, ISSN:-2319–8656
DOI:10.7753/IJCATR1203.1005

Design of a High Precision RC Oscillator

Fengbo Wang
School of Communication Engineering
Chengdu University of Information Technology
Chengdu, China

Xiaoqiang Xin
School of Communication Engineering
Chengdu University of Information Technology
Chengdu, China

Bo Gou
School of Communication Engineering
Chengdu University of Information Technology
Chengdu, China

Abstract: This paper introduces a high-precision RC oscillator circuit that is less affected by temperature and supply voltage. The circuit mainly consists of a bandgap reference voltage source, a low-voltage linear regulator, a low-pass filter, and a digital trim circuit, which reduces the circuit's sensitivity to temperature variations and achieves high stability of the oscillator frequency over a wide temperature range. Because of the current digital trimming technique, the circuit's ability to cope with the effects of frequency instability caused by process deviations is further enhanced.The simulation results show that the output center frequency accuracy is maintained within ±0.5% under the supply voltage range of 2.5V~5.5V, temperature range of -40℃~125℃, and different process corners. The RC oscillator has a high precision output frequency and can be used as a clock signal for a number of highly integrated and high precision applications.
Keywords: High-precision; RC Oscillator;Temperature Sensitivity; Digital Trimming

1. INTRODUCTION

As a clock signal circuit, oscillator is an important part of many electronic systems. With the rapid development of integrated circuits, oscillators will play an extremely important role in digital and digital-analog hybrid integrated circuits. Therefore, a highly stable and high-precision integratable oscillator is needed.

An oscillator is an oscillator that generates a periodic output signal by self-excited oscillation of the circuit alone without an applied input signal. Generally, the more common ones are RC oscillators, ring oscillators and crystal oscillators.RC oscillator has adjustable frequency, can be integrated, small size, low price, etc. However, the output frequency of RC oscillator is related to the power supply voltage and temperature fluctuations[1,2].Crystal oscillators are minimally affected by supply voltage and temperature fluctuations, but their large size and inability to be integrated affects their range of use [3].

This paper introduces a high-precision RC oscillator circuit whose circuit's internal current source circuit uses a high-order temperature-compensated design scheme to obtain a current source circuit with temperature-independent operation over a wide temperature range, and the circuit is virtually unaffected by temperature. In addition, a current digital trim circuit is used to improve the stability of the oscillator frequency for the deviation that the process will bring.

2. RC OSCILLATOR STRUCTURE

In The core components of RC oscillator are: current source circuit, LDO circuit, comparator, RS latch, digital trimmer circuit, integer inverter and other modules. the schematic diagram of RC oscillator, as shown in Figure 1..

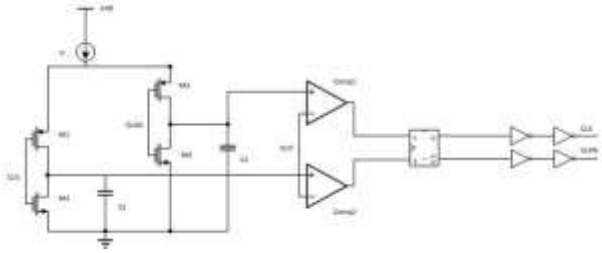

Figure 1. RC Oscillator

The operation principle of RC oscillator is as follows: assume that after the circuit is powered on, the output of RS latch in the initial state is Q=0, and the output of integer inverter is CLK=0 and CLKN=1. At this time, switch tube M1 is on, M2 is off, charging current Ic charges capacitor C1, and the voltage across the capacitor rises continuously, at the same time, switch tube M3 is off, M4 is on, and capacitor C2 is discharged to ground until 0V. When the voltage across capacitor C1 rises to Vref, the output of comparator Comp2 jumps to 1. At this time, the output of RS latch is Q=1, the output of integer inverter CLK=1, CLKN=0. Switching tube M3 is on, M4 is off, capacitor C2 is charged by current source current I_c, and at the same time, the voltage across capacitor C1 is put to 0V. When the voltage at both ends of capacitor C2 is charged to Vref, the output of comparator Comp1 jumps to 1, the output of RC latch changes again to Q=0, the output of integer inverter CLK=0, CLKN=1, the circuit returns to the initial state, the capacitor completes a charge/discharge cycle, the circuit forms an oscillation cycle, and so on and so forth, so that the RC oscillator at a certain frequency continuously.

According to the previous analysis and the charging and discharging characteristics of the capacitor, it is known that the capacitor completes charging time t1 and discharging time t2 as follows

$$t_1 = \frac{C \times \Delta U}{I_c} \quad (1)$$

$$t_2 = \frac{C \times \Delta U}{I_c} \quad (2)$$

International Journal of Computer Applications Technology and Research
Volume 12–Issue 03, 18-21, 2023, ISSN:-2319–8656
DOI:10.7753/IJCATR1203.1005

C is the capacitance of the capacitor and ΔU is the difference in voltage across the capacitor. When the charge/discharge current Ic is a fixed value, the period T=t1+t2 for a complete capacitor charge/discharge.

Therefore, the output frequency of the RC oscillator is obtained as

$$f = \frac{I_c}{2C \times \Delta U} = \frac{I_c}{2C \times V_{ref}} \quad (3)$$

In equation (3), Ic is the charging current, i.e., as the charging current of capacitors C1 and C2, V_ref is the bandgap reference voltage value, and C is the capacitor value. When the capacitors C1 and C2 are charged until they are equal to the bandgap reference voltage value Vref, the charging current I_c stops charging the capacitors, and then the capacitors start discharging to ground until the voltage across the capacitors is 0. After the charging current charges the other capacitor, the charging and discharging time of the two capacitors is one oscillation cycle.

3. CIRCUIT STRUCTURE DESIGN

3.1 Bandgap Reference Voltage Sources

The voltage reference circuit is a current-type low-voltage bandgap reference, which is based on the principle that the current with positive temperature coefficient and the current with negative temperature coefficient can be summed up in a certain ratio to make I_D4 with zero temperature coefficient. As shown in Figure 2.

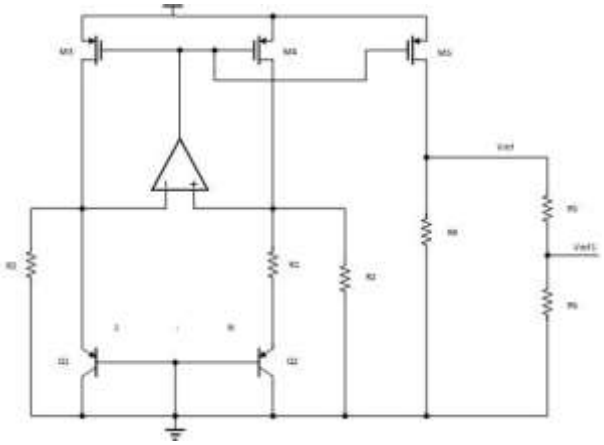

Figure 2. Voltage Reference Circuit

Vref and Vref1 are both reference voltages with zero temperature coefficient of order 1.

3.2 LDO Regulators

LDO regulator is low dropout linear regulator. It is widely used for its simple structure, low dropout voltage, and output voltage is less affected by the change of supply voltage. As shown in Figure 3, it mainly consists of error amplifier, power tube, feedback resistor, etc. Since the error amplifier, power tube Mp, and resistor R1 form a negative feedback structure, the feedback voltage will gradually approach the reference voltage Vref until the voltage values of both are equal. Therefore, the output voltage can be seen as minimally influenced by the supply voltage [4]. By analysis, the output voltage expression can be obtained as

$$V_{OUT} = V_{ref}\left(1 + \frac{R_1}{R_2}\right) \quad (4)$$

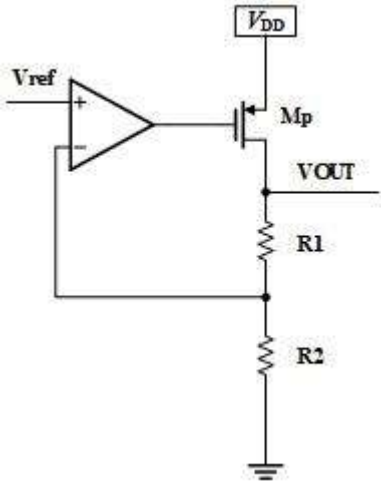

Figure 3. Video Low Dropout Linear Regulators

The From the above analysis, it can be seen that when the LDO output voltage VOUT becomes larger, after the feedback resistor divides the voltage, the negative input of the error op-amp will also become larger, at this time the error op-amp output becomes larger, so that the power tube VGS becomes smaller, the current flowing through the power tube is reduced, which in turn reduces the value of the output voltage VOUT, and vice versa.

Therefore, the LDO circuit can obtain a stable output voltage, which is almost constant by the supply voltage and temperature, and use this voltage value as the supply voltage for the core module of the RC oscillator.

3.3 Low-pass filter

The RC oscillator circuit system in this paper contains both analog and digital circuits. The core circuit of the oscillator is mainly a digital circuit, while its supply voltage is powered by the output voltage VOUT of the analog circuit LDO, and in addition, the voltage reference and current source circuits are also analog circuits. However, when high and low potential transitions occur in the digital circuit, a certain amount of jitter occurs on the power supply, which is directly transferred to the output of the LDO, and thus affects the performance of the analog circuit. The analog circuit can be isolated from the digital circuit, as shown in Figure 4.

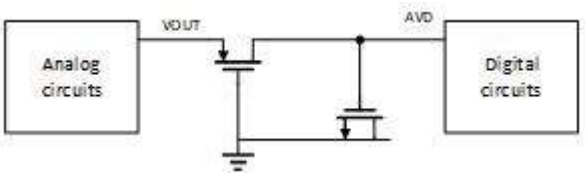

Figure 4. Schematic diagram of the isolation of analog circuits from digital circuitst

The analog circuit is isolated from the digital circuit by using a PMOS tube operating in the linear region and an NMOS capacitor to form an RC low-pass filter. The simulation results show that this approach can effectively improve the power supply jitter phenomenon and optimize the performance of the analog circuit when jitter noise is generated in the power supply of the digital circuit.

International Journal of Computer Applications Technology and Research
Volume 12–Issue 03, 18-21, 2023, ISSN:-2319–8656
DOI:10.7753/IJCATR1203.1005

3.4 Digital trimming circuit

In fact, the entire circuit design, and then the final simulation verification process, the RC oscillator circuit is functional without considering the digital trim module. However, there is a process drift, which affects the output frequency of the RC oscillator, and this error value is large, which affects the normal use.Therefore,digital trimming of the circuit's charging current, resistor and capacitor arrays is required [5-7].

The digital trim circuit is composed of MOS tubes only and occupies a small area. The 8-bit modulation signal is used to control the on/off of PMOS switch. The initial trim data is 01111111, and each bit controls one switch. When the output signal frequency decreases, more switches are opened, for example, 01111000, the charging current Ic increases, and the output frequency increases. The higher the number of trim bits, the higher the accuracy of the oscillator. As shown in Figure 5.

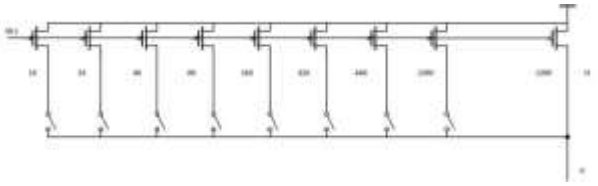

Figure 5 Current digital trimming circuit

4. SIMULATION RESULTS AND ANALYSIS

In this paper, the circuit is simulated and analyzed using CSMC 0.18 um CMOS process using Cadence Spectre circuit simulation tool. The simulation conditions are: tt process corner, supply voltage 2.5V~5.5V, and temperature -40℃~125℃. In addition, the results are simulated for ss and ff process corners after trimming.

The accuracy of the LDO output voltage can be measured by the linear adjustment rate, the smaller the linear adjustment rate, the higher the accuracy of the LDO output voltage. This output voltage provides the supply voltage for the RC oscillator. The simulation results show that the output voltage is around 2V with an error of no more than 0.5% under the supply voltage of 2.5V~5.5V. As shown in Figure 6.

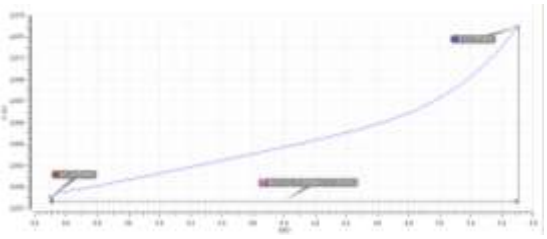

Figure 6 LDO Simulation Diagram

The output of the RC oscillator at tt process corner, at a temperature of 27 degrees Celsius, is shown in Figure 7.

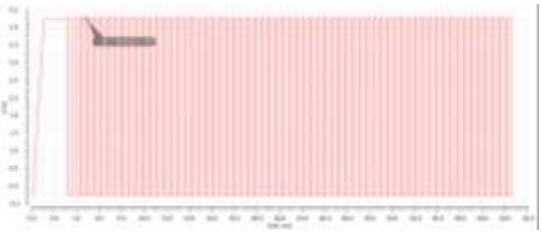

Figure7 RC oscillator output signal

The maximum value, minimum value, error and trimmed results of the output frequency of the RC oscillator at three different process corner at temperatures of -40°C to 125°C and supply voltages of 2.5V to 5.5V. As shown in Table 1.

Table 1. Output frequency of RC oscillator at different process corner

Process corner	Maximum /MHz	Minimum /MHz	Error /%	Trimmed results
tt	2.008	1.9916	±0.42	01111111
ss	2.0058	1.9942	±0.29	11110111
ff	2.0062	1.9939	±0.31	00010101

The simulation results of the high-precision RC oscillator designed in this paper are compared with the design performance indexes of domestic and foreign references. As shown in Table 2.

Table 2. Comparison of the oscillator results in this paper with those in the literature

	Process /um	Frequency /MHz	Error /%	Supply Voltage/V	Temp /℃
This work	0.18	2	±0.42	2.5~5.5	-40~125
[8]	0.18	2.3	±0.51	1.3~2.0	-40~125
[9]	0.18	1.6	±0.15	1.2~1.52	0~90

5. CONCLUSION

In this paper, a high-precision RC oscillator is implemented based on CSMC 0.18 um CMOS process by using a high-order temperature compensated current source and current digital trimming technique. The simulation results show that the output center frequency of the oscillator is maintained within ±0.5% at the supply voltage of 2.5V~5.5V and the temperature of -40℃~125℃; the output center frequency is also maintained within ±0.5% at different process corners (TT,SS,FF) after adding current digital trimming. The circuit can be integrated into a digital-to-analog hybrid system as an on-chip clock, for example, as an internal clock for an ADC, or as a separate clock chip.

5. REFERENCES

[1] Yu S, Chen Y, Guo W, et al. A digital-trim con trolled on-chip RC oscillator[C]// Circuits and Systems,IEEE Midwest Symposium. 2001:882-885.

[2] Lasanen K, Raisanen-Ruotsalainen E, KostamovaaraJ. A 1-V, self-adjusting, 5-MHz CMOS RC-oscillator[C]// Circuits and Systems, IEEE International Sympo sium.2002:377-380.

[3] Vittoz E,Degrauwe M G R,Bitz S.High-performance crystal oscillator circuits: theory and application[J].IEEE Journal of Solid-State Circuits,1988,23(3): 774-783..

[4] A. Asteriadis, T. Laopoulos, S. Siskos and M. Bafleur, "A low quiescent-current, low supply-voltage linear regulator," Proceedings of the 21st IEEE Instrumentation and Measurement Technology Conference (IEEE Cat. No.04CH37510), Como, Italy, 2004, pp. 1536-1541.

[5] L. Jiang, W. Xu and Z. Xu, "Two high accuracy CMOS RC oscillators with different trimming approach," 2010 10th IEEE International Conference on Solid-State and Integrated Circuit Technology, Shanghai, China, 2010, pp. 376-378.

[6] M.Dukic, A. Galimberti, M. Demicheli and E. Bonizzoni, "A 11.3-ppm/°C, Two Temperature Points Trimmed Current Generator for Precise RC Oscillators," 2019 26th IEEE International Conference on Electronics, Circuits and Systems (ICECS), Genoa, Italy, 2019, pp. 254-257.

[7] A. Olmos, "A temperature compensated fully trimmable on-chip IC oscillator," 16th Symposium on Integrated Circuits and Systems Design, 2003. SBCCI 2003. Proceedings., Sao Paulo, Brazil, 2003, pp. 181-186.

[8] Y. Ji, J. Liao, S. Arjmandpour, A. Novello, J. -Y. Sim and T. Jang, "A Second-Order Temperature-Compensated On-Chip R-RC Oscillator Achieving 7.93ppm/°C and 3.3pJ/Hz in -40°C to 125°C Temperature Range," 2022 IEEE International Solid-State Circuits Conference (ISSCC), 2022, pp. 1-3.

[9] W. Zhou, W. L. Goh and Y. Gao, "A 1.6MHz Swing-Boosted Relaxation Oscillator with ±0.15%/V 23.4ppm/°C Frequency Inaccuracy using Voltage-to-Delay Feedback," 2019 IEEE International Symposium on Circuits and Systems (ISCAS), 2019, pp. 1-4.

International Journal of Computer Applications Technology and Research
Volume 12–Issue 03, 22-25, 2023, ISSN:-2319–8656
DOI:10.7753/IJCATR1203.1006

Design of a Wide Input Voltage Low Quiescent Current LDO

Tianfu Li
School of Communication Engineering
Chengdu University of Information Technology
Chengdu, China

Fengbo Wang
School of Communication Engineering
Chengdu University of Information Technology
Chengdu, China

Bo Gou
School of Communication Engineering
Chengdu University of Information Technology
Chengdu, China

Abstract: A low-dropout linear regulator (LDO) with wide input voltage range, wide output voltage range and low quiescent current power consumption is proposed, which is applied to the switching power supply chip to power the internal module of the switching power supply chip. The low-dropout linear regulator is based on a P-type PowerFET design consisting of an error amplifier, a Bandgap reference. The circuit was designed and implemented by SMIC 0.18um BCD process, simulated and verified using Spectre software. The simulation results show that the linear regulation is 0.04mV/V in the input voltage range of 3.5-30V, and the load regulation is 1mV/mA in the output load current range of 10uA to 10mA, and the quiescent current is only 10uA.

Keywords: LDO; wide input voltage range; low quiescent current; low-dropout linear regulator; BCD process; wide output voltage range

1. INTRODUCTION

Low-dropout linear regulator (LDO) is a voltage converter with simple structure, low cost and small output voltage ripple, which is widely used in portable wearable devices, high-end medical testing instruments, industrial robot arms and low-power LED lighting fixtures[1]-[3]. The traditional pure CMOS process LDO can support the input voltage range is generally below 5V, which cannot meet the complex input voltage scenarios of modern electronic devices, and mobile electronic devices put forward more stringent requirements for battery life, and the smaller the LDO quiescent current index, the better. For wide input voltage LDO, the design challenge lies in the isolation of high and low voltages to prevent damage to the LDO internal MOSFET during operation. When the LDO supplies power to the internal module of the DC-DC switching power supply in the chip, the power consumption of the oscillator circuit fluctuates by the order of MHz, resulting in a large overshoot of the output voltage. At low quiescent current, there is more reliance on the transient response enhancement structure to reduce overshoot to stabilize the output voltage. Therefore, ensuring a wide input range and low quiescent current, proper function and stable output of the LDO are the keys to designing high-performance wide input and output LDO.

At present, the main research hotpots of LDO focus on low quiescent current, fast transient response, and high power supply rejection ratio for different application scenarios. Literature[4] proposes an error amplifier with dynamic adaptive bias function and a new FVF (flipped voltage follower) structure LDO, designed for 0.8V low voltage application scenarios, the normal operation quiescent current is only 16nA. Literature[5] proposes a multi-loop compensated high-performance LDO, in which the bias current of the difference amplifier and output buffer changes with the load current, and the dynamic current generated by monitoring the output voltage and the voltage of the EA output node is generated to charge and discharge each node of the loop to improve the output transient response of the LDO. Literature[6] proposes a high-efficiency LDO with multiple small gain stages that provide loop gain without introducing low-frequency poles within the closed-loop bandwidth. Therefore, the response speed of the LDO is improved while maintaining the accuracy of the output voltage. Literature [13] proposes a feed-forward ripple cancellation technique to achieve high power supply rejection ratio of wide-range LDO. It achieves a power supply rejection ratio of less than -56dB at 10MHz at 25mA load current.

In this paper, an LDO circuit supporting a wide input and output voltage range is proposed to achieve high and low voltage isolation using the BCD process with very low quiescent current power consumption, this LDO is suitable for powering internal modules of DC-DC switching power supplies. At the same time, it has good power supply rejection ratio performance under the input range voltage, which is enough to effectively reduce the interference of the power supply voltage.

2. THE STRUCTURE AND PRINCIPLE OF LDO

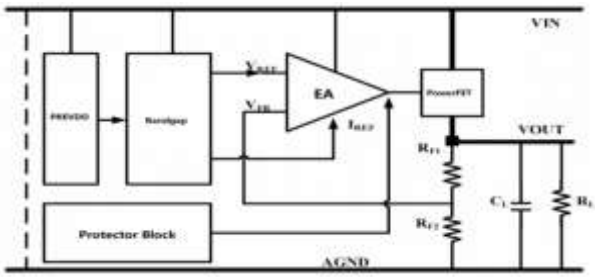

Figure 1. block of LDO

As DC voltage source, the basic principle of a low-dropout linear regulator is to sample the output voltage through an error amplifier and adjust the PowerFET gate control voltage in real time to keep the output voltage stable[7]. The block diagram is shown in Figure 1 and consists of an error amplifier, a PowerFET, a feedback resistor string, a Pre-Buck circuit, a Bandgap reference, and protection module. The Pre-Buck circuit provides a start-up signal and bias current to limit the speed at which voltage and current settle during power-up and avoid circuit instability[8]. A reference reference superimposes

currents or voltages with positive and negative temperature coefficients to produce a zero temperature coefficient current or voltage. The abnormal protection module can effectively avoid the damage of the chip due to over voltage, over temperature and other conditions. Power tubes are used to supply current to the load and are available in N-type and P-type PowerFET, both of which have advantages and disadvantages.

3. CIRCUIT STRUCTURE DESIGN

3.1 LDO Core Circuit

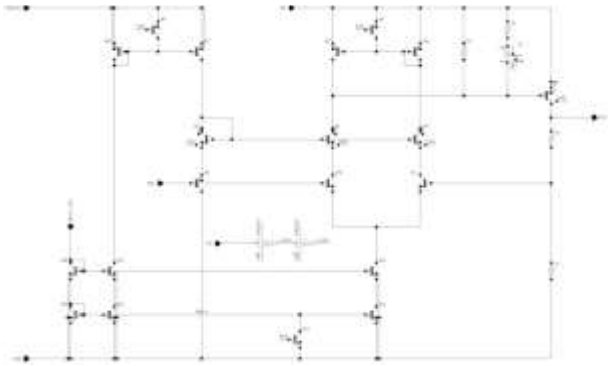

Figure 2. LDO Core Circuit

The core circuit structure of the LDO module proposed in this paper is shown in Figure 2. The circuit includes a bias current mirror composed of M29, M30, M33, M34, M35 MOSFET, error amplifiers composed of M10, M11, M3, M3a MOSFET, and power pass transistors M0. The bias circuit provides the error amplifier with a bias current that guarantees proper operation of the LDO, and the bias current of the error amplifier is set to 6uA for low quiescent current. M2, M77 MOSFET is N-type drain extend MOSFET, source leakage energy high voltage resistance, their role is to isolate high voltage and low voltage, avoid 5V low voltage pipe damage, M6 pipe function is to raise M2, M77 tube bias voltage. The LDO internal error amplifier is a single-stage structure with a high impedance point that introduces a lower frequency pole with a frequency of:

$$P_s = \frac{1}{R_4 \cdot C_{GD,MO}} \quad (1)$$

As can be seen from the above equation, the pole frequency can be set by resistor R4, and C_{GD} and M0 are the power tube gate leakage parasitic capacitance. The pole P_s is the secondary point, the main pole of the LDO is set by an external capacitor, and the main pole frequency is:

$$P_n = \frac{1}{R_{OUT} \cdot C_L} \quad (2)$$

When the load current is larger, the smaller the R_{OUT} resistance, the higher the frequency of the main pole, at which time the frequency of the main pole and the secondary point is closer, which will affect the frequency stability. The stability of the LDO at the output of the main pole decreases as the load current increases.

3.2 Pre-Buck Circuit

Pre-Buck circuit powers the bias circuit and Bandgap references. Since a reference voltage and bias current are required for proper operation of the LDO, a simple power supply circuit is also required before the LDO starts. The Pre-Buck circuit proposed in this article is shown in Figure 3.

Figure 3. Pre-Buck Circuit

The circuit consists of a Zener diode and an N-type drain extend MOSFET, which is a source follower structure, and capacitors C1 and C2 are filter capacitors to reduce output capacitance disturbance. The breakdown voltage of the Zener diode serves as the gate reference voltage of the source follower, and the output voltage of the PREVDD port can be expressed as:

$$V_{PREVDD} = V_{BV,ZDIO} - V_{TH,NDE} \quad (3)$$

Among them, $V_{BV,ZDIO}$ are the Zener diode breakdown voltage, and $V_{TH,NDE}$ are the threshold voltages of N-type drain extend MOSFET. Since the current flowing through the N-type drain extend MOSFET is small, the threshold voltage of the N-type drain extend MOSFET is used to approximate the PREVDD port output voltage.

3.3 Bandgap Reference Circuit

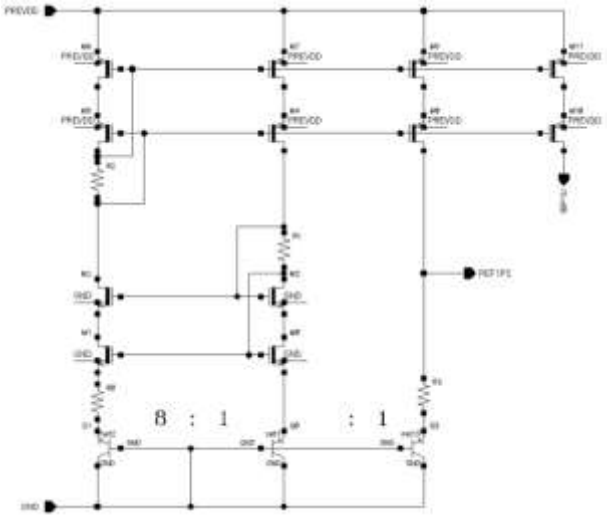

Figure 4. Bandgap Reference Circuit

The Bandgap reference circuit proposed in this paper is shown in Figure 4, Q0-Q1 and M0-M7 form a positive feedback loop with a gain of less than 1, so that the source voltage of M0 and M1 is equal and the emitter currents at both ends of PNP type transistors Q0 and Q1 are also equal, and the emitter currents at both ends are:

International Journal of Computer Applications Technology and Research
Volume 12–Issue 03, 22-25, 2023, ISSN:-2319–8656
DOI:10.7753/IJCATR1203.1006

$$\Delta V_{BE} = V_{BE,Q0} - V_{BE,Q1} \quad (4)$$

$$I_E = \frac{\Delta V_{BE}}{R_0} \quad (5)$$

where $V_{BE,Q0}$, $V_{BE,Q1}$ is the base-emitter voltage of Q0 and Q1, the current is copied from the 1:1 current mirror to the Q2 branch, then the reference voltage is:

$$V_{REF} = R_3 \cdot \frac{\Delta V_{BE}}{R_0} + V_{BE,Q2} \quad (6)$$

The base-emitter voltage of triode is negative temperature coefficient and the voltage is positive temperature coefficient, so zero temperature coefficient reference voltage can be obtained by setting the appropriate proportional relationship between resistors R0 and R3.

4. Simulation results and analysis

The LDO in this paper is designed using the device library of SMIC 0.18um BCD process, which supports 3.5-30V input voltage range, output voltage range 3V-5V, and max load current range 0~10mA.

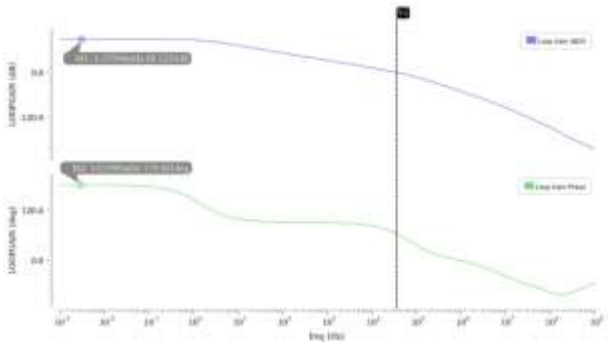

Figure 5. LDO AC Analysis

At the maximum load current, the main pole frequency is highest. At this point, the frequency of the main pole is closest to the secondary pole, and the overall loop stability of the LDO under this condition is the worst case. At 10mA load, the amplitude-frequency characteristic curve is shown in Figure 5. It can be seen that the low-frequency loop has a gain of 88dB and a phase margin of 64°, and the loop remains stable in the worst-case scenario.

Figure 6 and Figure 7 are the simulation results of linear regulation and load regulation, respectively. It can be seen that the input voltage rises from 5V to 30V, the output voltage hardly changes, and the linear regulation rate is excellent. The output load current rises from 10uA to 10mA, the output voltage changes at 1mV/mA, and load regulation is also excellent.

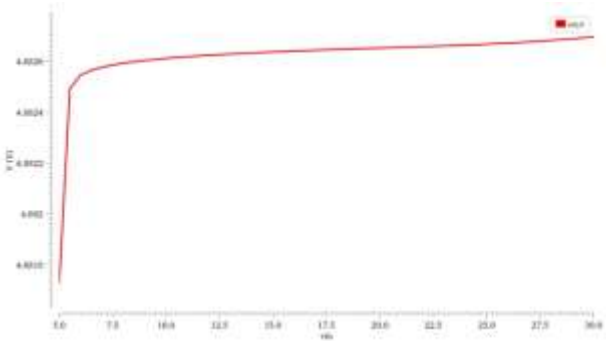

Figure 6. Line Regulation Analysis

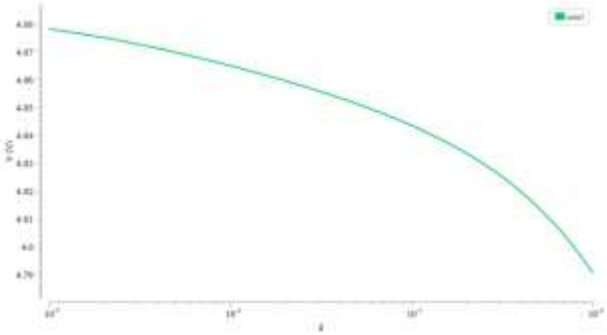

Figure 7. Load Regulation Analysis

A comparison of LDO parameters in this paper with other literature is shown in Table 1. It can be seen that this article has certain advantages in terms of input voltage range, output voltage range, and quiescent power consumption.

Table 1. Comparison of LDO parameters

parameters	[9]	[10]	[11]	This work
Process/nm	250	350	65	180
Input voltage Range/V	3.9-20	1.4-3.3	1.3	3.5-30
Output voltage Range/V	2.5	1.2	1.1	2-5
Max load current/mA	800	50	50	10
quiescent current/uA	800	200	50~190	10

5. CONCLUSIONS

In this paper, a wide input and output voltage range, low quiescent current LDO applied to switching power supply chips, input voltage range of 3.5-30V. linear regulation performance and load regulation performance are good. In the full load current range of 10uA-10mA, LDO can keep the loop stable. Quiescent current consumption is only 10uA.

6. REFERENCES

[1] Akhamal H, Chakir M, Qjidaa H. A 90nm CMOS LDO regulator with high load regulation using a gain boost-up technique[C]// 2016 5th International Conference on Multimedia Computing and Systems (ICMCS). IEEE, 2016.

[2] Yang X, Lu T, Zhang J, et al. A Low-Quiescent Current Low-Dropout Regulator with Wide Input Range. 2014.

[3] Li Z, He L, Chen C. A novel low-dropout regulator with large load current and high stability[C]// 2014 IEEE Workshop on Advanced Research and Technology in Industry Applications (WARTIA). IEEE, 2014.

[4] Adorni N, Stanzione S, Boni A. A 10-mA LDO With 16-nA IQ and Operating From 800-mV Supply[J]. IEEE Journal of Solid-State Circuits, 2020, 55(2):404-413.

[5] Duong Q H, Nguyen H H, Kong J W, et al. Multiple-Loop Design Technique for High-Performance Low-Dropout Regulator[J]. IEEE Journal of Solid-State Circuits, 2017, 52(10):2533-2549

[6] HO M. A Low-Power Fast-Transient 90-nm Low-Dropout Regulator With Multiple Small-Gain Stages[J]. IEEE Journal of Solid-State Circuits,2010,45(11).

[7] Al-Shyoukh M, Lee H, Perez R. A Transient-Enhanced Low-Quiescent Current Low-Dropout Regulator With Buffer Impedance Attenuation[J]. IEEE Journal of Solid-State Circuits, 2007, 42(8):1732-1742.

[8] Hazucha P, Karnik T, Bloechel B, et al. An area-efficient, integrated, linear regulator with ultra-fast load regulation[C]// 2004 Symposium on VLSI Circuits. Digest of Technical Papers (IEEE Cat. No.04CH37525). IEEE, 2004.

[9] Yin J, Huang S, Duan Q, et al. An 800 mA load current LDO with wide input voltage range[C]// 2017 International Conference on Circuits, Devices and Systems (ICCDS). IEEE, 2017.

[10] Blakiewicz G. Output-capacitorless low-dropout regulator using a cascoded flipped voltage follower[J]. IET Circuits, Devices & Systems, 2011, 5(5):418-423.

[11] Huang M, Feng H, Lu Y. A Fully Integrated FVF-Based Low-Dropout Regulator With Wide Load Capacitance and Current Ranges[J]. IEEE Transactions on Power Electronics, 2019, 34(12):11880-11888.

International Journal of Computer Applications Technology and Research
Volume 12–Issue 03, 26-29, 2023, ISSN:-2319–8656
DOI:10.7753/IJCATR1203.1007

Design of a 12 bit SAR ADC with Self-Calibration

Yu Guan
School of Communication Engineering
Chengdu University of Information Technology
Chengdu, China

Pan Luo
School of Communication Engineering
Chengdu University of Information Technology
Chengdu, China

Bo Gou
School of Communication Engineering
Chengdu University of Information Technology
Chengdu, China

Abstract: Successive approximation analog-to-digital converter (SAR-ADC) are widely used in intelligent sensing fields due to it's low power consumption, medium and high precision and such characteristics. Traditional binary SAR ADC have non-ideal factors such as DAC capacitor array mismatch and comparator offset, which severely limit it's performance. Therefore, a self-calibration method for non-ideal factors is proposed in this work, and theoretical derivation and simulation analysis are carried out. A 12-bit non-binary SAR ADC with self-calibration is designed based on the TSMC 40nm CMOS process, which reduces the capacitance area, improves the conversion accuracy, and eliminates most of the errors caused by non-ideal factors. Simulation results show that the ADC's SNDR is 72.01dB, and INL within +1.2/-1LSB, meets most of the market requirements.

Keywords: SAR ADC; non-binary; self-calibration; capacitor array mismatch; comparator offset; intelligent sensing

1. INTRODUCTION

In recent years, with the rapid development of SoC in various fields, higher requirements have been put forward for the performance of CMOS analog-to-digital converters (ADCs) [1-3]. At present, the common ADC structures on the market include Flash ADC, Pipeline ADC, SAR ADC, and Sigma-Delta $\Sigma - \Delta$ ADC, and it can be seen from Table 1 that different structures bring different electrical characteristics. SAR ADC has the characteristics of medium conversion speed and accuracy, low power consumption and small area, and is widely used in various consumer products.

Table 1. Several common ADC electrical characteristics

Structure	Resolution	Speed	Power
Flash	<8 bit	fast	high
Pipeline	10~14bit	fast	medium
SAR	8~16bit	medium	low
Sigma-Delta	16~31bit	slow	medium

The digital-to-analog converters (DAC) in traditional SAR ADC are typically implemented with binary weighted capacitor arrays, but as the resolution increases, the capacitor array size increases proportionally, resulting in significant area and wasted power consumption. Therefore, segmented capacitive arrays are typically used in SAR ADCs above 10 bit to reduce capacitance area [2]. In the SAR ADC, due to the device mismatch caused by process deviation, the error generated at ADC quantization seriously limits it's performance. The error mainly include nonlinear errors caused by capacitor mismatch; comparator offset error due to mismatch between the MOS tubes.

In this paper, a 12-bit SAR ADC with self-calibration using a segmented non-binary capacitor array architecture is designed. Technology of capacitor calibration and offset cancellation correction are implemented in it, which can reduce errors caused by capacitor mismatch and comparator offset, improve the conversion accuracy of SAR ADC. Simulation using Cadence to build circuits shows that the ADC achieves the desired specifications.

2. CIRCUIT IMPLEMENT

2.1 ADC Circuit Structure

The proposed ADC structure is shown in Figure 2.1. It includes a pre-stage AFE, a main capacitor array DAC, a Bootstrap switch , a comparator, a sub-DAC for comparator offset calibration, and a SAR control logic controller. The proposed SAR ADC uses a nonbinary split capacitive array DAC consisting of a 6-bit binary weighted capacitor array and a 9-bit non-binary redundant capacitor array.

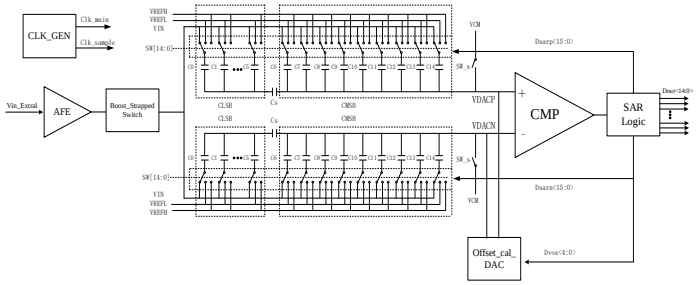

Figure. 2.1 Proposed Non-binary SAR ADC structure

The working process of this design is divided into two phases, the power-on self-calibration phase and the analog-to-digital conversion stage.The mismatch and offset are calibrated at the beginning of power up, and obtain the best capacitor weights [4]. After calibration, the final weights are updated in registers, and in normal conversion mode, the ADC conversion result is combined with the corresponding weight to convert 15-bit data to a 12-bit binary output. Compared with the traditional split binary SAR ADC, it only needs 196 unit capacitors, which greatly reduces the capacitor array size and reduces the power consumption of the capacitor array.

3.1.1 Sturcture of Non-binary Capacitor Array

The proposed weight of the non-binary capacitor array is shown in Figure 2.2. According to the sub-radix-2 (sub-binary) DAC capacitor array theory proposed by LIU W et al.

[5], it can be seen from Figure 2.2 that the weight values of the high-bit capacitors are less than the sum of the weight values of other low-bit capacitors, satisfying the sub-binary relationship, and the redundancy value of each capacitor is > 31LSB, about 3mV, which has good redundancy characteristics, so the high-bit comparison error can be corrected.

	C0	C1	C2	C3	C4	C5	C6	C7	C8	C9	C10	C11	C12	C13	C14
Weight	1	2	4	8	16	32	33	66	99	165	264	363	594	924	1518
Sum	2	4	8	16	32	64	97	163	262	427	691	1054	1648	2572	4090
Redundancy	0	0	0	0	0	0	31	31	64	97	163	328	460	724	1054

Figure. 2.2 Non-binary capacitor array weight

2.2 Self-Calibration

2.2.1 Comparator offset cancellation

This design adopts digital front-end calibration scheme[6], before the SAR ADC power on, the SAR ADC calibrates the comparator offset firstly. After the calibration done, the capacitor mismatch calibration process is entered, and generates a flag signal when it done. Then the normal conversion starts when the sample clock comes, after convertion the 15bit output datas will be calculated according to the corresponding weight and aquire the final 12bit results. The details of self-calibration process is as follows.

Because comparator offset consumes redundancy of the capacitor array, this design calibrates the comparator offset firstly, after power up done [7]. In order to avoid errors caused by mismatch of main DAC, a comparator offset calibration sub-DAC is built, and the unit capacitance is taken by 1fF to reduce the size of the calibration capacitor. As shown in Figure 2.3, where Vip and Vin are connected to the positive and negative terminals of the comparator, respectively. At the beginning of the offset calibration, Vip and Vin are connected to the common-mode voltage Vcm. At the same time, the comparator input is disconnected from the main capacitor array, the capacitor lower plate is connected to ground, and the both capacitor arrays store the same charge. After that, the common mode is disconnected, and due to the presence of the comparator offset, an offset voltage Vos is superimposed on the Vip and Vin voltages, and the traditional dichotomy is used to complete the quantization of the comparator offset[8]. The quantization results are sent to the digital part, which obtains the multiple offset calibration codes by triggering the offset calibration multiple times, averaging them into registers, and passing them into the ADC in subsequent processes through the registers for offset elimination.

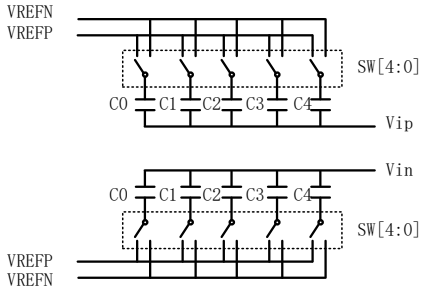

Figure. 2.3 Sub-DAC Capacitor Arrary

2.2.2 Capacitor array self-calibration process

The capacitor mismatch in low bit segment is small, so a binary capacitor array is used instead of calibrated. In the capacitance array self-calibration process, the upper 9-bit capacitor is calibrated. The 7th bit is calibrated firstly, in the sampling stage, the upper and lower plates of all capacitors are connected to Vcm, in the quantization stage, the lower plate of the high 8-bit capacitance is still connected to Vcm, the 7th bit is forced to Vref, the rest of the capacitance is normalized, and the quantization result Dout1 is obtained. Then the 7th bit capacitor is forcibly connected to Vss, and the remaining capacitors are normalized to obtain the quantization result Dout2. The two results are subtracted to get the 7th bit mismatch value, which is processed by a numerical algorithm, and the capacitance weight value of this bit is updated and recorded in the register. After the 7th bit capacitor calibration is completed, the 8~15th bit capacitor is calibrated in the same way, and in the normal conversion process, the output of each code is multiplied by the corresponding weight to obtain the 12bit digital output. The ADC output code processing principle is shown in Figure 2.4.

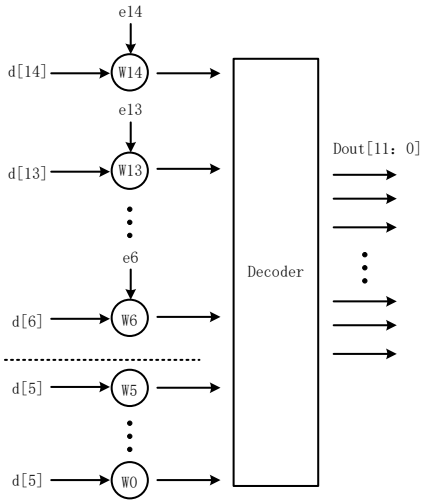

Figure. 2.4 Output principle of capacitor array calibration result

2.3 Convertion Process

After the power-up self-calibration is complete, the ADC begins normal analog-to-digital conversion work, which is divided into sampling and conversion stage. The proposed ADC uses synchronous timing logic, as shown in Figure 2.5. The clk_main is an external input master clock with a frequency of 20Mhz. clk_sample is an internal 1Mhz sample clock, generated by CLK_GEN circuit. clk_cmp is the comparator clock, according to the first-order RC network full response equation[9], as shown in Equation(1.1).

$$u(t) = u(\infty)\left(1 - e^{-\frac{t}{RC}}\right) \tag{1.1}$$

Even if the switch resistor R=20Ω, the capacitance C=5pF, the time constant is 100ps, and the half comparator clock cycle is much greater than 4RC, the DAC is guaranteed to fully settle. The sampled signal is converted analog-to-digital through 15 comparator clocks.

International Journal of Computer Applications Technology and Research
Volume 12–Issue 03, 26-29, 2023, ISSN:-2319–8656
DOI:10.7753/IJCATR1203.1007

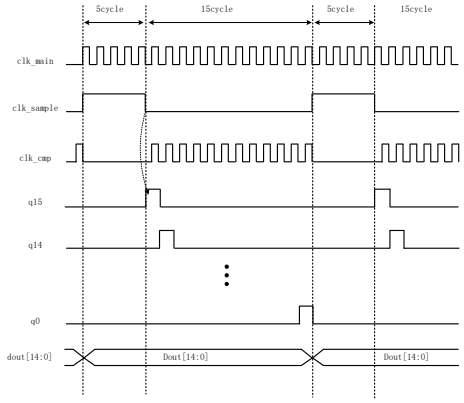

Figure. 2.5 Timing of this SAR ADC

2.3.1 Sampling

In order to reduce the influence of substrate noise on signal sampling, the lower plate sampling scheme is adopted in this design. When the clk_sample is high, the sampling stage is entered, and the SW_s switch is closed, and the capacitor C_{MSB} the upper plate of the high-bit segment are connected to the common-mode voltage V_{CM}. The positive capacitor array of the comparator C_{DACP}, the lower plate is connected to the input signal Vin, and the negative capacitor array C_{DACN} the lower plate of the comparator is connected to the reference low voltage V_{REFL}. At this time, the total amount of charge stored in the C_{DACP} and C_{DACN} capacitor arrays are:

$$Q_{DACP}=(V_{cm}-V_{in})\cdot C_{MSB,tot}+(V_{cm}-V_{in})\cdot C_{eq,L} \quad (1.2)$$

$$Q_{DACN}=(V_{cm}-V_{REFL})\cdot C_{MSB,tot}+(V_{cm}-V_{REFL})\cdot C_{eq,L} \quad (1.3)$$

$$C_{eq,L}=\frac{C_{LSB,tot}\cdot C_S}{C_{LSB,tot}+C_S} \quad (1.4)$$

where C_MSB,tot is the sum of all high-segment capacitances, and C_LSB,tot is the sum of the low-segment capacitance.

2.3.2 Convertion

After sampling, the clk_sample is pulled low, the upper plate of the capacitor array is disconnected from the common-mode voltage VCM, the comparator is working controled by clk_cmp, and the ADC enters the conversion process. During the conversion process, the capacitor array switch SW [14:0] is controlled by SAR logic outputs Dsarp [14:0] and Dsarn [14:0], so that the V_{DACP} voltage and the V_{DACN} voltage are approached successively to complete the 15-bit data conversion. In the MSB conversion process, the lower plate of the highest capacitance at the V_{DACP} end is first connected to V_{REFH}, and the lower plate of the remaining capacitance is connected to V_{REFL}. All capacitors at the V_{DACN} terminal are permanently connected to the V_{REFL} plate at all data conversion stages.

At this time, the charge stored in the V_{DACP} and V_{DACN} terminal capacitor arrays are:

$$Q_{DACP}=(V_{DACP}-V_{REFH})\cdot C_{MSB}+(V_{DACP}-V_{REFL})\cdot C_{M,R}+(V_{DACP}-V_{REFL})\cdot C_{eq,L} \quad (1.5)$$

$$Q_{DACN}=(V_{DACN}-V_{REFL})\cdot C_{MSB,tot}+(V_{cm}-V_{REFLO})\cdot C_{eq,L} \quad (1.6)$$

where $C_{M,R}=C_{MSB,tot}-C_{MSB}$, because there is no discharge path between the sampling and conversion stage, thus the V_{DACN} and V_{DACP} voltages are changed, and the two voltages are compared by the comparator to obtain the highest output, and the state of the switch SW [14:0] is controlled according to the output. And the next highest comparison is made when the next comparison clock comes.

3. SIMULATION RESULTES

According to the above structure, a 1Msps sampling speed 12bit SAR ADC is designed and realized based on the TSMC40nm process, and the circuit is simulated using the Cadence ADE, under the simulation conditions of IO voltage of 1.8V and external input clock of 40MHz.After 15 cycles of data conversion, the 15-bit data output is obtained to the digital part for weighting processing, and finally the 12-bit binary data output is obtained, and the voltage at both ends of the V_{DACP} and V_{DACN} is approached successively as shown in Figure 3.1.

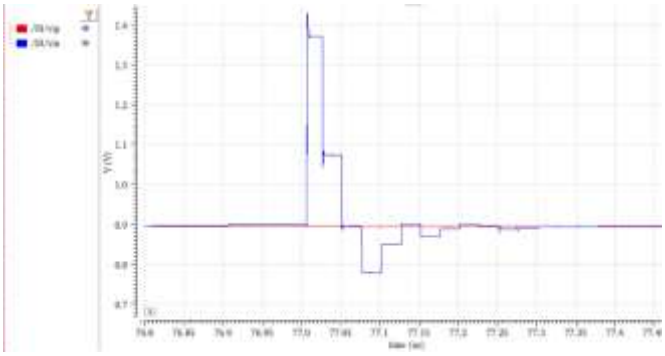

Figure. 3.1 Successive approximation simulation

Build a simulation circuit to simulate the dynamic performance of the ADC, under the simulation conditions of an input frequency of 414.06KHz and a sampling frequency of 1MHz, 4096 points are sampled, and 12-bit binary parallel data is obtained after conversion, and a fast Fourier transform is performed on the results, and the simulation results are shown in Figure 3.2.

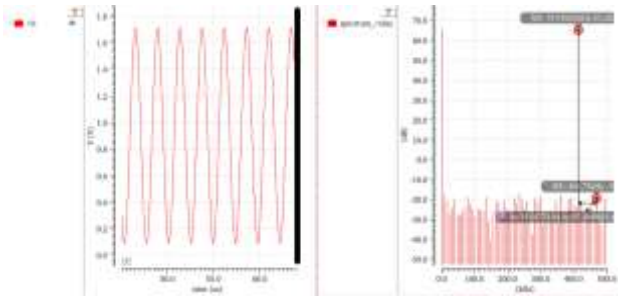

Figure. 3.2 Output wave FFT simulation result

The performance parameters of the 12-bit SAR ADC designed in this article are shown in Table 2.

Table 2. ADC Performance Summary

Parameter	Conditions	Result
ENOB	Fin=414.0625KHz Rin=10 KΩ VREF=1.8~3.3V	11.54bit
SNDR		72.01dB
THD		-83.24dB
SFDR		85.06dB

4. CONCLUSION

Based on the TSMC 40nm CMOS process, this paper designs a 12-bit SAR-ADC with self-calibration, optimizes the SAR-ADC structure, adopts a non-binary split capacitor array structure, reduces the capacitance area, and leaves sufficient redundant bits for calibration. In addition, a non-ideal factor calibration method is proposed to calibrate non-ideal factors such as comparator offset and capacitor array mismatch in the ADC, and at the same time, the non-ideal factors can be quantified and presented in the form of code, which can help designers accurately judge process errors and adjust the circuit. The simulation result shows the ENOB of this ADC reaches 11.54bit, the SNR is 72.01dB. The measured results show that the effective number of the ADC after calibration reaches 11.2bit, while compared with the ADC without calibration, the ENOB is 1~2bit higher, which has a high cost performance in the current consumer electronics field.

5. REFERENCES

[1] Y. Chen et al., "Split capacitor DAC mismatch calibration in successive approximation ADC," 2009 IEEE Custom Integrated Circuits Conference, 2009, pp. 279-282, doi: 10.1109/CICC.2009.5280859.

[2] A. H. Chang, H. -S. Lee and D. Boning, "A 12b 50MS/s 2.1mW SAR ADC with redundancy and digital background calibration," 2013 Proceedings of the ESSCIRC (ESSCIRC), Bucharest, Romania, 2013, pp. 109-112.

[3] P. Xiaomin and W. Peiyuan, "Design and modeling of a 12-bit SAR ADC IP with non-lumped capacitor array," *2010 2nd International Conference on Future Computer and Communication*, Wuhan, China, 2010, pp. V3-392-V3-395.

[4] Z. Lan, L. Dong, X. Jing and L. Geng, "A 12-Bit 100MS/s SAR ADC with Digital Error Correction and High-Speed LMS-Based Background Calibration," 2021 IEEE International Symposium on Circuits and Systems (ISCAS),2021,pp.1-5.

[5] W. Liu, P. Huang and Y. Chiu, "A 12-bit, 45-MS/s, 3-mW Redundant Successive-Approximation-Register Analog-to-Digital Converter With Digital Calibration," in IEEE Journal of Solid-State Circuits, vol. 46, no. 11, pp. 2661-2672.

[6] P. X. -L. Huang *et al.*, "A self-testing and calibration method for embedded successive approximation register ADC," *16th Asia and South Pacific Design Automation Conference (ASP-DAC 2011)*, Yokohama, Japan, 2011, pp. 713-718.

[7] J. Shen et al., "A 16-bit 16MS/s SAR ADC with on-chip calibration in 55nm CMOS," 2017 Symposium on VLSI Circuits, 2017, pp. C282-C283.

[8] S. Haenzsche, S. Henker and R. Schüffny, "Modelling of capacitor mismatch and non-linearity effects ini charge redistribution SAR ADCs," *Proceedings of the 17th International Conference Mixed Design of Integrated Circuits and Systems - MIXDES 2010*, Wroclaw, Poland, 2010, pp. 300-305.

[9] W. -Y. Pang, C. -S. Wang, Y. -K. Chang, N. -K. Chou and C. -K. Wang, "A 10-bit 500-KS/s low power SAR ADC with splitting comparator for bio-medical applications," 2009 IEEE Asian Solid-State Circuits Conference, Taipei, Taiwan, 2009, pp. 149-152.

International Journal of Computer Applications Technology and Research
Volume 12–Issue 03, 30-31, 2023, ISSN:-2319–8656
DOI:10.7753/IJCATR1203.1008

Technological View on Smart Waste Management

Dr. K. Karunambiga
Department of CSE
Karpagam Institute of Technology
Coimbatore, India

Dr. M. Sathiya
Department of IT
Karpagam Institute of Technology
Coimbatore, India

Abstract: The sustainable development goal of society, need of healthy environment and due to growing population quantity of solid waste increases rapidly drives the smart waste management. Since it is unhealthy for humans who involve in manual waste management those field works need automation. The Artificial Intelligence provides the way to achieve the automation to collect and process the solid waste with the help of Internet of Things, Cloud Computing and Intelligent Transport System. We explored the technological development towards the implementation of smart waste management to support further development in this domain.

Keywords: Artificial Intelligence, IoT, Cloud Computing, Smart Bin, Waste Management

1. INTRODUCTION

The solid waste management is an unhealthy task, the involvement of human in that domain directly affects their physical condition. Apart for that, the expansion of human strength plays a vital role in generation of solid waste in the environment. To deal with this problem, the research towards the Smart Waste Management(SWM) attracts more concern. In waste management, the technological support involved are Internet of Things [5,9], Artificial Intelligence [1,4,10], Intelligent Transport System [11] and Cloud Computing as depicted in the figure 1.

2. INTERNET OF THINGS AND CLOUD COMPUTING FOR SWM

The smart bin design using the Internet of Things to sense the condition of dustbins using sensors such as ultrasonic, load and so on [9]. In [11] the framework for smart waste management in Indonesia is depicted using IoT and ICT with the policy designed to face the challenges in the implementing waste management. The technology, economy, social, governance, and environmental are the five dimensions followed for the framework to achieve the sustainable development goals of smart waste management.

The information gathered from the different smart bin were transferred to cloud to store and process. IoT transmits the smart bin data using the internet to the cloud computing device. The LoRa was frequently used protocol in IoT to transfer the data for long range in SWM [8].

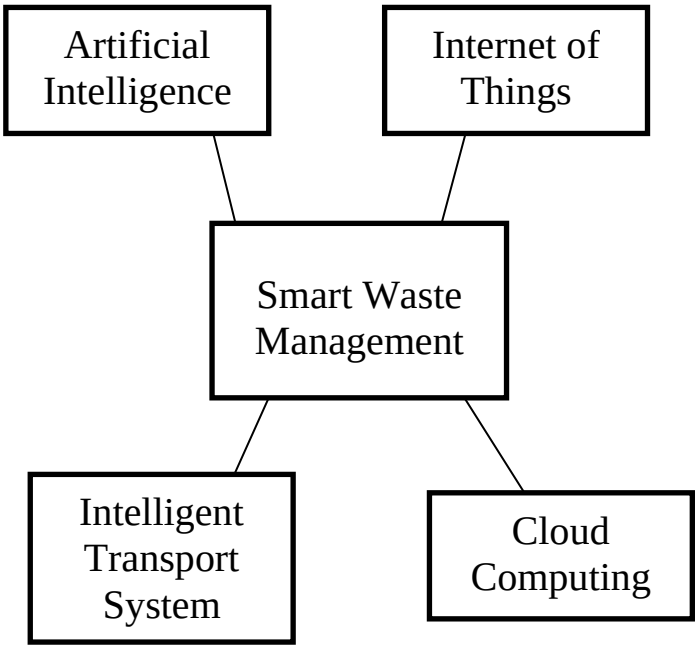

Figure 1: Components of Smart Waste Management

3. ARTIFICIAL INTELLIGENCE IN SWM AND INTELLIGENT TRANSPORT SYSTEM

The CNN based predictive models was proposed in [2] for smart waste management. The CNN was used to categorized the waste to take decision of disposal or recycling, which was stored in the cloud. Optimized route selection for the transport system helps to collect the solid waste in order to minimise the transport cost and maximise garbage collection [6]. Generally, the waste were collected periodically or when the bin was full [10]. Those decisions were taken based on the intelligent system implemented for SWM. The controller with GSM convey the information through SMS to the central system to enable intelligent transport system[3].

4. DISCUSSION

Internet of Things combined with smart bin helps in collecting the bin status. It also transfers the data using low energy conversing data transfer protocol to the cloud for further process. The machine learning and deep learning algorithms applied on the cloud data helps to design the prediction model. The prediction using artificial intelligence forecasts the garbage which give better performance.

5. REFERENCES

[1] Khan, Feroz, and Yousaf Ali. "A facilitating framework for a developing country to adopt smart waste management in the context of circular economy." Environmental Science and Pollution Research 29.18 (2022): 26336-26351.

[2] Jude, A. Belin, et al. "RETRACTED ARTICLE: An Artificial Intelligence Based Predictive Approach for Smart Waste Management." Wireless Personal Communications 127.Suppl 1 (2022): 15-16.

[3] Yadav, Honey, Umang Soni, and Girish Kumar. "Analysing challenges to smart waste management for a sustainable circular economy in developing countries: a fuzzy DEMATEL study." Smart and Sustainable Built Environment 12.2 (2023): 361-384.

[4] Reddy, Anuradha, et al. "Smart Waste Management Systems by Using Automated Machine Learning Techniques." Journal of Artificial Intelligence, Machine Learning and Neural Network (JAIMLNN) ISSN: 2799-1172 2.04 (2022): 16-25.

[5] Anjum, Mohd, Sana Shahab, and Mohammad Sarosh Umar. "Smart waste management paradigm in perspective of IoT and forecasting models." International Journal of Environment and Waste Management 29.1 (2022): 34-79.

[6] Zhang, Abraham, et al. "Barriers to smart waste management for a circular economy in China." Journal of Cleaner Production 240 (2019): 118198.

[7] Pardini, Kellow, et al. "A smart waste management solution geared towards citizens." Sensors 20.8 (2020): 2380.

[8] Sheng, Teoh Ji, et al. "An internet of things based smart waste management system using LoRa and tensorflow deep learning model." IEEE Access 8 (2020): 148793-148811.

[9] Ali, Tariq, et al. "IoT-based smart waste bin monitoring and municipal solid waste management system for smart cities." Arabian Journal for Science and Engineering 45 (2020): 10185-10198.

[10] Sallang, Nicholas Chieng Anak, et al. "A CNN-based smart waste management system using tensorFlow lite and LoRa-GPS shield in Internet of things environment." IEEE Access 9 (2021): 153560-153574.

[11] Fatimah, Yun Arifatul, et al. "Industry 4.0 based sustainable circular economy approach for smart waste management system to achieve sustainable development goals: A case study of Indonesia." Journal of Cleaner Production 269 (2020): 122263.

International Journal of Computer Applications Technology and Research
Volume 12–Issue 03, 32-39, 2023, ISSN:-2319–8656
DOI:10.7753/IJCATR1203.1009

Huffman Algorithm Valuation Using Residue Number System

Lawal T. Dauda
Department of Computer Science
Federal Polytechnic Offa
Kwara State, Nigeria

Eseyin Joseph B
ICT Directorate
University of Jos
Jos, Nigeria

Azeez O. Isiaka
Department of Statistics
Federal Polytechnic Offa
Kwara State Nigeria

Abstract: The Huffman algorithm is a widely used method for lossless data compression, which assigns variable-length codes to characters based on their frequency of occurrence in the input data. However, the traditional implementation of Huffman coding using binary arithmetic can be computationally intensive, particularly for large data sets. In recent years, the Residue Number System (RNS) has emerged as a promising alternative to binary arithmetic for certain types of computations, due to its potential for parallel processing and reduced hardware complexity. This paper evaluates the use of RNS as a basis for implementing the Huffman algorithm, comparing its performance with the traditional binary approach. The results demonstrate that RNS-based Huffman coding can achieve comparable or superior compression ratios, while reducing the computational requirements and potentially enabling faster compression and decompression. The study also highlights the importance of choosing appropriate RNS moduli and operands to optimize performance. Overall, the evaluation suggests that RNS can be a viable and efficient alternative to binary arithmetic for implementing the Huffman algorithm, particularly in applications with high computational demands or limited hardware resources. However, further research is needed to explore the potential benefits and limitations of RNS in other areas of data compression and signal processing.

Keywords: Residue Number System, lossless compression, compression ratio, decompression, moduli set, binary value, bit coding

1.0 INTRODUCTION

Data management and processing must include data compression since it reduces the size of data files, allowing for more effective storage and quicker transfer. Compression in computer science is based on the philosophy that some data can be represented more efficiently by using fewer bits than their original representation without losing significant information. This can help reduce storage requirements and transmission times, making it an important tool in managing large amounts of data. There are numerous data compression algorithms that each have benefits and drawbacks. This widely used data compression algorithm—Huffman coding will be the subject of this paper. These methods were chosen as a decent illustration of the numerous kinds of algorithms available and because they are among the most used data compression algorithms.

By reducing the amount of data files, compression methods improve the efficiency of storage and transmission. There are several compression methods available, and each has advantages and disadvantages. Arithmetic coding, Shannon-Fano coding, and Huffman coding are three popular compression techniques.

Huffman Coding: Based on the frequency with which characters appear in the input data, Huffman Coding assigns characters' variable length codes. The technique employs a binary tree to represent the code words, with the weight of the tree's nodes based on the frequency of each character. The shortest code words are given to the characters with the lowest frequency, while the longest code words are given to the characters with the highest frequency. Because the shortest code words may represent the most characters, there is a higher compression ratio as a result. Huffman coding is one of the most frequently used coding algorithms for lossless data compression, claim creators J. Ziv and A. Lempel [1].

2.0 REVIEW OF RELATED LITERATURE

Data files can be made smaller and more efficiently stored and sent by using compression methods. Numerous compression techniques have been created throughout the years, but Huffman coding, Shannon-Fano coding, and arithmetic coding are the three that are still in use today.

Huffman Coding Since its invention in the 1950s, Huffman coding has been extensively utilized for lossless data compression. Recent studies have concentrated on increasing the compression ratio of the technique by representing the code words in more complex data structures, such as Fibonacci heaps and B-trees. Researchers have also looked into Huffman coding as a method for compressing images, and they discovered that the process can offer high compression. For instance, a new picture compression technique based on Huffman coding and the Discrete Cosine Transform (DCT) was proposed by Y. Lee et al. in a recent work [1]. High compression ratios were attained using the suggested technique while still keeping the integrity of the reconstructed image.

In recent years, a great deal of study has been done on arithmetic coding, leading to numerous developments in both lossless and lossy data compression. Using arithmetic coding and the DCT, J. Kim et al. recently proposed a new lossy image compression technique [3]. The suggested technique produced large compression ratios with good image reconstructed quality. A new lossless data compression method based on arithmetic coding and a context-based coding scheme was proposed by X. Zhang et al. in another paper [4].

3.0 METHODOLOGY

The algorithms were implemented in Python and the implementation was based on the standard algorithms as described in literature. The algorithms were evaluated based on their compression ratios and computational time. The compression ratio was calculated as the ratio of the size of the compressed file to the size of the original file. The computational time was calculated as the time taken to compress the file. The algorithms were tested on a range of text files of different sizes to provide a representative evaluation of the algorithms.

3.1 Framework for an enhanced Huffman Algorithm and Shannon-Fano Algorithm

To build enhanced Lossless data compression algorithms namely enhanced Huffman algorithm hereafter referred to RNS-Huffman the data were obtained from which the unique character and their frequencies of occurrence were extracted. The next stage is to extract the ASCII value of each symbol making up the message along with their frequency.

The next stage is to get the residue value with respect to the given moduli set. This is followed by employing RNS arithmetic in Huffman computations. This is shown in Figure 1.

Figure 1: Framework for RNS Lossless Compression Algorithms Design

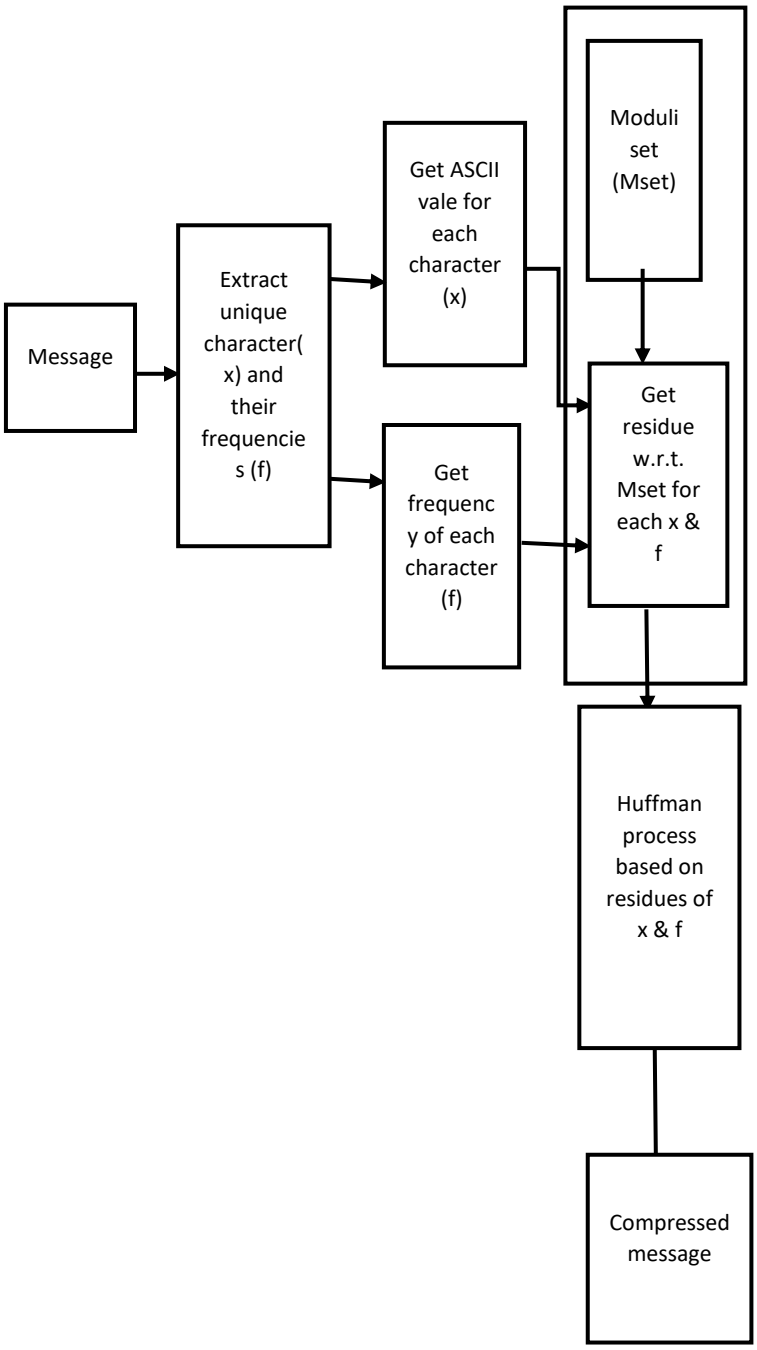

International Journal of Computer Applications Technology and Research
Volume 12–Issue 03, 32-39, 2023, ISSN:-2319–8656
DOI:10.7753/IJCATR1203.1009

3.2 Algorithm 1: RNS-Huffman Algorithm

Input: the message to be compressed
Output: the compressed message

1) *Extract each character*
2) *for a given list of symbols,*
3) *develop a frequency table;*
4) *sort the table according to the frequency, in ascending order*
5) *obtain the ASCII value of each character;*
6) *obtain the traditional moduli set;*
7) *get residue of each character's ASCII value with respect to moduli set*
8) *get residue with respect to moduli set for each frequency;*
9) *perform Huffman compression process based on residues of characters and frequencies.*
10) *obtain a compressed information*

4.0 EXPERIMENTAL RESULTS

RNS-based Computation using Traditional Moduli set;

The traditional moduli set is $(2^n + 1, 2^n, 2^n - 1)$ was used. Using the value of n to be equal to 2, the moduli set is (5, 4, 3). For ASCII value of a character, its equivalent residue value is calculated with respect to the moduli set. For example, given the message

"FFFAAABBEBBCCCCCDDDEEEBBFFFFBBDDB CBBBFFF"

to be store or transmitted. The length of the message is 40. Without compression, the message will be stored or transmitted using the ASCII code. In the ASCII code, each alphabet is 8 bits.

Table 1: Characters and their Frequencies

Character	A	B	C	D	E	F
Frequency	3	12	6	5	4	10

Table 2: Message Distribution

Character	Frequency	ASCII code	Binary bit Value	No of Bits	Freq* No of bits
A	3	65	01000001	8	24
B	12	66	01000010	8	96
C	6	67	01000011	8	48
D	5	68	01000100	8	40
E	4	69	01000101	8	32
F	10	70	01000110	8	80
Total	40		48		320

The space required to store or send this message is 320 (i.e., 40 * 8) bits.

4.1 Huffman Technique

The Huffman technique of storing or sending this message is accomplished by first tabulating the characters along with their frequencies.

Table 3: Characters and their Frequencies in the message

Character	Frequency
A	3
B	12
C	6
D	5
E	4
F	10
Total	40

The next step is to arrange the characters horizontally in ascending order of their frequencies after which two smallest ones are merged and the sum is recorded. This action will be repeated until all the alphabet are exhausted as shown in Figure 2 below.

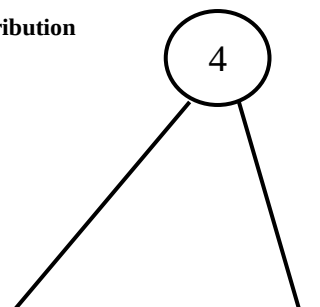

International Journal of Computer Applications Technology and Research
Volume 12–Issue 03, 32-39, 2023, ISSN:-2319–8656
DOI:10.7753/IJCATR1203.1009

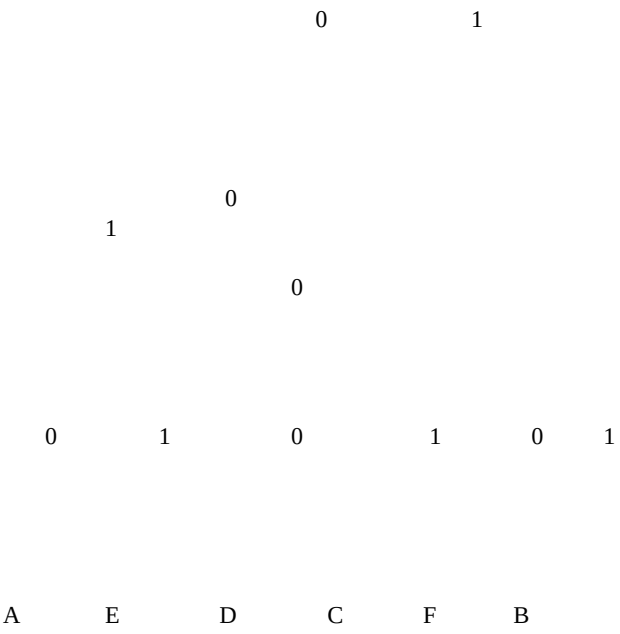

Figure 2: Huffman Data Compression Tree Sourse: (Umarani, Sriram & Kumar, 2017)

On the left of each alphabet, mark them as 0s and on the right mark them as 1s. For each alphabet, follow the path from the root. The codes are as indicated in the Table 4 below.

Table 4: Message bits representation

Character	Frequency	codes	No of bits
A	3	000	3*3 =9
B	12	11	12*2 =24
C	6	011	6*3 = 18
D	5	010	5*3 = 15
E	4	001	4*3 = 12
F	10	10	10*2 =20
Total	40	16 bits	98 bits

The total size of the message is 98bits. But along this message, the chart or table must also be stored or sent, so that the decoding can be done. Thus, the table or the chart must be preserved. In addition, the ASCII code of the alphabet must also be stored or sent. The number of alphabets is 6. Therefore 6*8 will give 48 bits. The total number of the codes is 16 bits. To preserve the tree, the number of bits require is 64 bits i.e., 48 + 16. The message is 98 bits and the tree is 64 bits given a total of 162 bits. The message size has been reduced from 320 bits to 162 bits i.e. it has been reduced by about 50% by Huffman technique.

4.2 RNS-Huffman ASCII Value Computation

Table 5: Conversion of ASCII code value to its RNS equivalent

Character	ASCII Code	Binary Code	RNS with Moduli set			Bits Space
			3	4	5	
A	65	8	2	1	0	4
B	66	8	0	2	1	4
C	67	8	1	3	2	5
D	68	8	2	0	3	5
E	69	8	0	1	4	5
F	70	8	1	2	0	4
Total		48				27

Table 6: RNS-Huffman Computation

Character	freq	RNS with moduli set			Hufman code	RNS with moduli set			Freq* Huffman code	RNS with moduli set			Bits Space
		3	4	5		3	4	5		3	4	5	
A	3	0	1	2	111=3	0	1	2	3*3=9	0	0	4	5
B	12	0	0	2	00=2	2	2	2	12*2=24	0	0	4	5
C	6	0	2	1	101=3	0	1	2	6*3=18	0	2	2	5
D	5	2	1	0	100=3	0	1	2	5*3=15	0	1	0	3
E	4	1	0	1	110=3	0	1	2	4*3=12	0	0	2	4
F	10	1	2	0	01=2	2	2	2	10*2=20	2	0	0	4
Total	40				16 bits				98 bits				26 bits

Table 7: Total Huffman and RNS-Huffman bits

	Huffman codes	RNS-Huffman Codes
Message	98 bits	27 bits
ASCII binary codes	48 bits	26 bits
Total bits on tree	16 bits	16 bits
Total	162 bits	69 bits

4.3 Performance Metrics

The performance metrics used for evaluating the algorithms are Compression Ratio (CR)

4.3.1 Compression Ratio

Data compression ratio is the compression power of an algorithm. It is a measurement of the relative reduction in size of data representation produced by a data compression algorithm. It is usually expressed as a division of uncompressed size by a compressed size.

It is the ratio of total number of bits required to store uncompressed data and total number of bits required to store compressed data. It is termed a bit per bit (bpb) which defined the number of bits required to store the compress data. This was calculated by finding the ratio between the compressed and original file as:

$$CR = \frac{\text{Number of bits in uncompressed data}}{\text{Number of bits in compressed data}}$$

4.3.2 Evaluation of RNS-Huffman

Twenty-five different file documents of different sizes were compressed using Huffman coding and RNS-Huffman algorithms. The results were evaluated and analyzed using Compression Ratio (CR).

4.3.3 RESULT OF EVALUATION

Sizes of Output in bits of Huffman,

The output of the twenty-five (25) text file document of different sizes from Huffman coding, compression algorithms is given in the Table 4.

Table 8: Compressed File Size (bits)

Text File	Original File size (bits)	Huffman Compressed File size (bit)
1	2552	1843
2	5152	3343
3	7392	4579
4	9904	5950
5	12440	7331
6	15056	8791
7	17576	10157
8	20352	11801
9	24680	15068
10	27280	16625
11	29616	18096
12	31880	19491
13	35416	21612
14	37968	22997
15	40600	24563
16	43224	26042
17	45968	27627
18	48576	29075
19	51352	30644
20	53968	32103
21	56592	33567
22	59160	35232
23	61808	36903
24	64552	38417
25	67080	39894
Average	**34806**	**20871**

From table 8 The average file size of 20871 for Huffman coding from the average original file size of 34806 were obtained. The variation in sizes from Table is given in Figure 4.1 below. This show that of Arithmetic coding performs better than Huffman which is also better than Shannon-Fano coding in term of compression size. Figures 4.1 and 4.2 show the result of sizes of output.

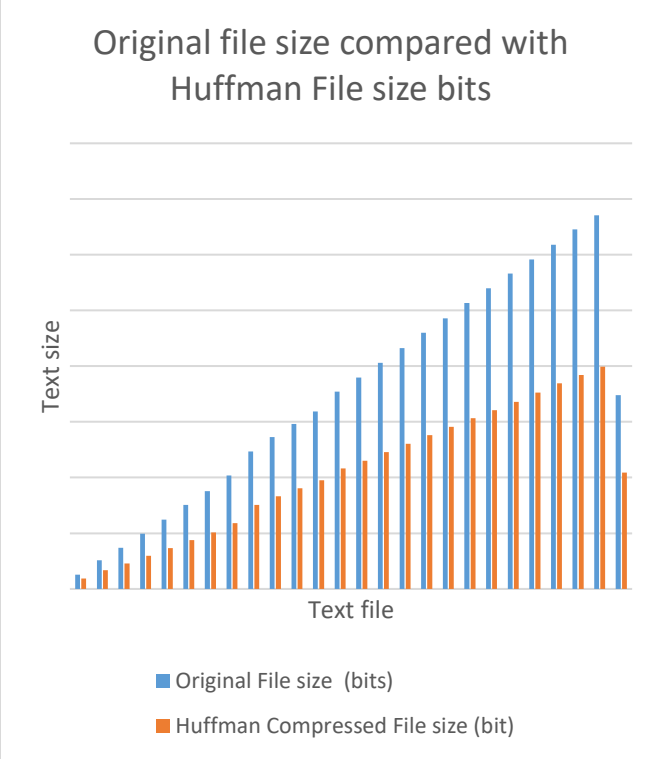

Figure 3 Huffman algorithm file size with bit size

4.3 Compression Ratio

The compression ratio was computed for Huffman coding for the twenty-five differently sized file documents. The results are shown in table 4.2 below.

Table 9: The Compression Ratio of Huffman, algorithms

Text File	Original File size (bits)	Huffman Algorithm
1	2552	1.384698861
2	5152	1.541130721
3	7392	1.614326272
4	9904	1.664537815
5	12440	1.69690356
6	15056	1.712660676
7	17576	1.730432214
8	20352	1.72459961
9	24680	1.63790815
10	27280	1.640902256
11	29616	1.636604775
12	31880	1.6356267
13	35416	1.63871923
14	37968	1.650997956
15	40600	1.652892562
16	43224	1.659780355
17	45968	1.663879538
18	48576	1.670713672
19	51352	1.675760345
20	53968	1.681088995
21	56592	1.68594155
22	59160	1.679155313
23	61808	1.674877381
24	64552	1.680297785
25	67080	1.681455858
Average	**34805.76**	**1.652635686**

4.3.4 Evaluation of RNS-Huffman Algorithms

In this stage, performance of RNS-Huffman coding is done. The same twenty-five text files of different sizes were compressed using these algorithms. Their CR were computed and used to compare their performances.

4.3.5 Compressed File sizes

The sizes of the output from RNS-Huffman Algorithm when fed with the file documents as inputs are shown in Table 7.

Table 10: Compressed file sizes of RNS-Huffman

Text File	Original Size (bits)	RNS-Huffman (bits)
1	2552	515
2	5152	610
3	7392	650
4	9904	696
5	12440	738
6	15056	755
7	17576	798
8	20352	855
9	24680	1114
10	27280	1128
11	29616	1136
12	31880	1155
13	35416	1186
14	37968	1174
15	40600	1180
16	43224	1172
17	45968	1175
18	48576	1180
19	51352	1187
20	53968	1201
21	56592	1208
22	59160	1191
23	61808	1196
24	64552	1198
25	67080	1190
Average	**34805**	**1023**

From table 10, compressed output of RNS-Huffman coding is 1023 bits, original uncompressed document is 34805 bits long.

4.3.6 Compression Ratio of RNS-Huffman Algorithms

Compression ratios for RNS-Huffman are presented in Table 8.

Table 11: Compression Ratio of RNS-Huffman algorithms

Text File	Original Size (bits)	RNS-Huffman
1	2552	4.955339806
2	5152	8.445901639
3	7392	11.37230769
4	9904	14.22988506
5	12440	16.85636856
6	15056	19.94172185
7	17576	22.02506266
8	20352	23.80350877
9	24680	22.15439856
10	27280	24.18439716
11	29616	26.07042254
12	31880	27.6017316
13	35416	29.86172007
14	37968	32.3407155
15	40600	34.40677966

16	43224	36.88054608
17	45968	39.12170213
18	48576	41.16610169
19	51352	43.26200505
20	53968	44.93588676
21	56592	46.84768212
22	59160	49.67254408
23	61808	51.67892977
24	64552	53.88313856
25	67080	56.3697479
Average	**34805.76**	**31.28274181**

The average compression ratio for RNS-Huffman algorithms are **31.28274181** and the average text size of **34805.76.**

4.3.7 Comparative Analysis of RNS-Huffman algorithm in relation to seven other recent algorithms

Comparing the proposed work with the existing state of the art algorithms. The table 4.15 below presents the results of text files of existing state of the art algorithms with the proposed RNS-Huffman algorithms.

Table 12: Recent works in compression algorithms

S/N	Author(s)	Original Size	Compress Size	CR	Compression Algorithm
1	Alhassan et al., 2015	30.33333	21.33333	1.421875	LZW
2	Alhassan et al, 2015	30.33333	18	1.685185	LZW-RNS
3	Athira and Ravisankar 2020	5.8864	2.803	2.803	Delta Encoding
4	Ibrahim & Gbolagade (2019)		6200.333		
5	Ibrahim & Gbolagade (2019a) Huffman CRT		6041.333	3.695	
6	Ibrahim & Gbolagade (2019)b LPZ-CRT		6200.333		
7	Satrial et al. (2020) AD 6200.333 APTIVE		0.93045		
	Proposed Approach 1	34805.76	1023.52	31.28274 181	RNS-Huffman
	Proposed Approach 2	34805.76	1420.76	22.31	RNS-Huffman

In the Table 12 above, Hasan et.al. (2013) obtained CR of 4.416, for Huffman based LZW and 2.587 for LZW based Huffman. Salunaz et.al. (2014) in Huffman with RLE 0.842556. Alhassan et. al. (2014) obtained 1.69 for LZW-RNS and Amandeep & Er.Meenakshi, (2014) obtained 2.08 in Dynamic bit reduction and Huffman algorithms. Gupta et.al. (2017) obtained 3.825 from DEFLATE, 5.88 from LZMA, 5.975 from BZIP2 and 7.088 for PPMONSTR. These are far lower than CR of proposed RNS-Huffman which is 22.31. This shows that the proposed RNS-Huffman

perform better than all the recent state of the art works in term of CR.

5.0 CONCLUSION

Both Huffman algorithm and RNS Huffman compression algorithm are lossless data compression techniques that can achieve high compression ratios.

Huffman algorithm is a general-purpose compression algorithm that works by assigning variable-length codes to each symbol in the input data based on their frequency of occurrence. It can achieve good compression ratios for text and other data with non-uniform frequency distributions.

RNS Huffman compression algorithm is a variant of Huffman algorithm that works by converting the input data into a residue number system (RNS) representation, which can be encoded using Huffman coding. This approach can be more efficient than standard Huffman coding for data with a large number of small values or a small range of values.

In general, the choice of which algorithm to use will depend on the characteristics of the input data. Both algorithms can achieve high compression ratios, but RNS Huffman may be more effective for certain types of data. Ultimately, the best way to determine which algorithm is most suitable for a particular application is to test them both on representative input data and compare their compression ratios.

REFERENCES

[1] Y. Lee, W. Lee, and S. Kim, “Image Compression Method Based on Huffman Coding and Discrete Cosine Transform,” Journal of Digital Imaging, vol. 32, no. 3, pp. 470–477, 2019.

[2] S. S. Al-Sarhan, O. A. Basalamah, and A. H. Al-Makhadmeh, “Shannon-Fano Coding for Data Compression in Wireless Sensor Networks,” Journal of Communications, vol. 14, no. 2, pp. 73–79, 2019.

[3] J. Kim, Y. Lee, and S. Kim, “Lossy Image Compression Method Based on Arithmetic Coding and Discrete Cosine Transform,” Journal of Visual Communication and Image Representation, vol. 71, pp. 101–109, 2019.

[4] Lawal, T. D., Olatunbosun L. O. and Gbolagade K A. (2021): An Improve Shannon Fano Data Compressio Algorithm using Residue Number System. Communications on Applied Electronics (CAE) – ISSN: 2394714 Foundation of Computer Science FCS, New York, USA Volume 7– No. 35, April 2021 – www.caeaccess.org 19

International Journal of Computer Applications Technology and Research
Volume 12–Issue 03, 40-45, 2023, ISSN:-2319–8656
DOI:10.7753/IJCATR1203.1010

Learning Media Development: Covid-19 Supplement Book-Based Science Literacy

Amalia Syah Putri
Biology Education
Postgraduate
Universitas Negeri Medan
Medan, West Sumatera
Indonesia

Hasruddin
Biology Education
Postgraduate, Leacture
Universitas Negeri Medan
Medan, West Sumatera
Indonesia

Tri Harsono
Biology Education
Postgraduate, Leacture
Universitas Negeri Medan
Medan, West Sumatera
Indonesia

Abstract: The purpose of this study was to determine the feasibility of the Covid-19 Supplement book on virus material and the effectiveness of the Covid-19 Introduction Supplement book in improving student learning outcomes. The development research method (Development & Research) produces products, so this research is oriented towards product development which has the process of describing it as well as possible and then its feasibility will be validated. In this study uses the ADDIE research model which includes the analysis, design, development, implementation, and evaluation stages. The subjects in this study were three expert validators (materials experts, linguists, and design experts), then teachers and class X students at SMA Negeri 1 Hutabayuraja. The results of this development research show that the Covid-19 Supplementary book on virus material was deemed appropriate by material experts, linguists, and graphic design experts, and the application of the Covid-19 Supplementary book on virus material can effectively improve student learning outcomes with student classical mastery of 75, 6%.

Keywords: instructional Media; supplement book; covid-19; scientific literacy; improve learning outcomes

1. INTRODUCTION

Viruses have become the most discussed topic in the last two years. This is because at the end of 2019, in Wuhan City, Hubei, China, a new type of disease was reported, which is currently known as Covid-19. This name was inaugurated by the World Health Organization (WHO) on 11 February 2020. COVID-19 is COVI for coronavirus, D for disease, and 19 to symbolize the year the virus was first detected [1].

The science that studies viruses or what is called virology is a branch of biology. Viruses are living things that are transitional between living things and inanimate things. Viruses are declared transitional living things because they have the characteristics of living things and inanimate objects. Viruses have genetic material which is the main characteristic of living things, but besides that viruses do not have protoplasm and can be crystallized which is characteristic of inanimate objects, and can only live if in the host's body. However, viruses are included in the scientific field of biology because they can reproduce and their presence has a major effect on the living things they infect.

The world of education is a place to prepare a new generation that is ready to compete in the future. So ideally matters related to educational interests need to be given specific attention and updated according to the latest knowledge. With the discovery of new knowledge about viruses that are included in the scientific field of Biology, information related to these discoveries also needs to be updated.

The learning process does not always run smoothly without obstacles, one of the problems in the learning process is that some students are not able to understand the learning material. Students only focus on memorization without being followed by a deep understanding. In short, learning difficulties are caused by students' lack of literacy skills. Literacy is defined as a reasoning ability related to the ability to analyze, synthesize, and evaluate information that can be grown by integrating it into lessons [2].

Scientific literacy over the last few decades has been considered an important problem in the world of national and international education. Scientific literacy is considered important because understanding science is fundamental to one's readiness to live in modern society [3]. Textbooks that can support learning are books that emphasize scientific knowledge whose scope corresponds to the scientific literacy category in a balanced way. Books based on scientific literacy cover four categories, namely, science as a body of knowledge; science as a way of investigation (science as a way of investigation); science as a way of thinking (science as a way of thinking); and the interaction of science with technology and society (science and its interaction with technology and society).

21st Century Biology Learning must adapt to changing times. The 21st century demands the field of education to be able to prepare students who have the skills to be able to face the information age which is faced with global economic competition. The skills that every student must have in the 21st century learning are critical thinking skills, knowledge, and literacy skills both personally and professionally. Individuals who have scientific literacy skills will be able to complete using scientific concepts obtained with the help of technology according to their level. Scientific literacy skills are an independent ability to find solutions to problems according to actual procedures and facts [4]

Problems in the learning process certainly have an impact on student learning outcomes that have not been completed [5]. The achievement of student learning outcomes in viral material still has not reached the Minimum Completeness Criteria (KKM) specified, namely ≥ 76. Researchers conducted pre-research observations at SMAN 1 Hutabayuraja to obtain data on student learning outcomes as

seen from assignment assessments and daily test assessments on the subject matter virus in class X MIA SMAN 1 Hutabayaraja as many as 94 students. Student learning outcomes that complete less than 50% for assignment scores and daily tests. The data reflects that student learning outcomes have not been achieved optimally.

Supplementary books are supporting books for the main textbooks which contain additional material not included in the textbooks. The function of the supplement book is to support students to get more information. Books that become reading are part of an unlimited self-development effort. The ability and willingness to seek information through books can become knowledge for readers.

1.1 Supplement Book

Supplement books are enrichment books or complementary books. This supplement book is used to complement the main textbook [6]. Supplementary books are books that enrich and improve mastery of science and technology, and skills, and shape the personality of students, educators, education administrators, and other communities. This type of book is not only for students but also for other parties or the general public, (Center for Bookkeeping, 2008). Several supplement books that have been developed can increase reader motivation through the good responses shown.

Supplementary books in learning are designed to increase reading interest, written for readers who are used to learning, can explain instructional objectives arranged based on flexible, systematic, and structured learning patterns based on student needs and the final competencies to be achieved, focus on providing opportunities for students to practicing, giving summaries, communicative writing style, providing feedback, accommodating student learning difficulties, explaining how to study teaching materials and written by experts in related fields [7].

The supplement book includes learning resources that may be used by users to make learning behavior occur. Supplementary books are practical learning resources because of their flexible use, low maintenance, and easy availability. The use of supplementary books is not limited by the time, place, or age of the user, but there are still provisions for their preparation and use. This makes the supplement book can be used as a learning resource.

Four aspects of Supplementary Book Writing Techniques, namely: (1) Aspects of Book Content. Designing supplementary books must adhere to three main principles namely, consistency with educational goals, adaptation to scientific developments, and development: of reasoning skills. (2). Aspects of Presentation In presenting supplementary material four main principles need to be considered, namely inductive and systematic logical systems, Presentation of Material, Stimulating the development of creativity (3) Aspects of Language When writing guides (both knowledge, skills and personality). You must comply with the standard rules of language use. Textbook language rules must be followed by the author. Without the careful application of language rules, readers often lose their written communication. Authors should use correct, harmonious, and rhythmic sentences, words, and terms. (4) Additional Graphical Aspects Graphical aspects that must be considered relate to the layout of attractive graphic elements to explain the contents of the book. It should also be noted that the typography used must be highly readable [8].

1.2 Corona Virus

Director General of the World Health Organization (WHO) Tedros Adhanon Ghebreyesus on 11 February 2020 stated that they had chosen the name of the disease caused by the coronavirus which is very dangerous and very threatening to the world. The name given is COVID-19 which is an acronym for Corona Virus Disease and 19 refers to 2019 when this virus was first detected.

The Covid-19 pandemic is an event where a disease spreads across the globe, killing more than 1,800 people within 50 days of its emergence. This disease is caused by a new type of coronavirus that has never been detected before. Initially called (2019-nCov) by the Centers for Disease Control and Prevention, the number 2019 indicates the year, the letter n indicates novel which means new, and CoV indicates coronavirus.

This disease was first detected in Wuhan, which is a business center in China, namely a trader at the Huanan Market. The first confirmed case of the Sars CoV-2 virus allegedly appeared on November 17, 2019. However, this case was still unknown at that time. This patient is then referred to as the “Zero Patient”. The search for the "Zero Patient" was then carried out by health authorities in China to find out traces of the spread.

The coronavirus that causes the Covid-19 infection has spike proteins on the surface. The spikes are used by viruses to attach to the surface of body cells and cause pain. The coronavirus vaccine works by recognizing the spike coronavirus and destroying it so it can't attach to body cells. If the vaccine used works optimally, it will be effective in protecting you from Covid-19 infection, and if the infection persists, it will reduce the risk of serious illness or death.

Several vaccines must be given in several doses, with intervals of weeks or months. This is sometimes necessary to encourage the body to produce stronger, longer-lasting antibodies and to allow immune cells to remember the disease. In this way, it is hoped that the body's defense system will be able to fight against incoming pathogens in the future, including fight the virus that causes COVID-19.

1.3 Science Literacy

Literacy is defined as a reasoning ability related to the ability to analyze, synthesize, and evaluate information that can be grown by integrating it into lessons [9]. The benefits of literacy include various aspects of development, namely cognitive, social, language, and emotions. Literacy is related to learning and decision-making skills, as well as adaptation to the environment. One of the characteristics of today's society and in the future is the enormous amount of information, a life that is increasingly digitized, and types of work that require high levels of reasoning - all of which require literacy. Literacy achievement indicators cover many aspects of reading comprehension, evaluating ability, ability to conclude and link information with other information or results of observatioand ns, reflections, which are expressed by exposure to information, and so on. There are quseveralr of tested scales and continuums that schools can use to assess those that are integrated with various disciplines.

Scientific literacy is formed from 2 words, namely literacy, and science. Literacy comes from the word Literacy which

means literacy/illiteracy eradication movement [10]. While the term science comes from the English language Science which means knowledge. The first person to use the term scientific literacy was Paul de Hurd in 1958 [11], who stated that scientific literacy means understanding science and applying it to society's needs. Pudjiadi [12] says that: "science is a group of knowledge about objects and natural phenomena obtained from the thoughts and research of scientists who are carried out with the skills of experimenting using scientific methods". Scientific literacy according to the National Science Education Standards (1995) is: Scientific literacy is knowledge and understanding of scientific concepts and processes required for personal decision-making, participation in civic and cultural affairs, and economic productivity. It also includes specific types of abilities. The National Research Council (NRC, 1996) [13] in the National Education Standards (NSES) explains that scientific literacy is knowledge and understanding of scientific concepts and processes needed to make personal decisions, participate in society and economic productivity, and other types of special abilities.

Scientific literacy is defined by PISA (OECD, 2003) as the ability to use scientific knowledge, identify questions, and draw conclusions based on evidence, to understand and make decisions regarding nature and changes made to nature through human activities. This definition of scientific literacy views scientific literacy as multidimensional, not only an understanding of scientific knowledge but more than that. According to the National Science Teacher Association INSTA (1997) [16], individuals who are scientifically literate are people who use science concepts, process skills, and values in making everyday decisions when they relate to other people or their environment, and understand the interrelationships between science, technology, and society. , including social and economic development.

Scientific literacy has four categories. The category of scientific literacy can be stated to have a balanced proportion if it fulfills a ratio of 2:1:1:1 in the following order of categories: (1). Science as the body of Knowledge; (2). Science as a path of inquiry; (3) Science as a way of thinking; checkers (4). The interaction of science with technology and society.

Based on these problems, the researcher is interested in developing a supplement book that is a source of learning to support Virus material. The book will later contain information about the SARS-CoV-2 virus that causes the Covid-19 outbreak. The products resulting from this research are expected to be learning resources that can improve learning outcomes.

2. METHOD

This research is a type of research and development (R & D). Development research (Development & Research) is a model in research that is used to produce certain products as well as test the feasibility of the media and the effectiveness of a product. In this research what will be developed is the Covid-19 supplement book learning media to improve student learning outcomes.

The subjects in this study were three expert validators (materials experts, linguists, and design experts), then teachers and class X students at SMA Negeri 1 Hutabayuraja, where the number of students in class X MIA was 94 people. As a trial sample, a large group of 20 students was taken, a medium group of 8 students and a small group of 3 people were taken as a total sample of 1 sample class with varying abilities, gender, and levels of intelligence. The object of this research is the Covid-19 supplement book to improve student learning outcomes.

The development model that will be planned in this study uses the ADDIE research model which includes the analysis, design, development, implementation, and evaluation stages.

Valid products will be applied to learning to see the level of effectiveness in improving student learning outcomes. In addition to being feasible and effective, the media developed must also have practical value, by what is needed when learning takes place, teachers who play a role in learning know what students need, and vice versa the responses given by students must be by what needed, the conditions for the media to be feasible to develop must pay attention to feasibility and effectiveness.

Data analysis techniques in this study include quantitative and qualitative analysis. Quantitative analysis was used to analyze the questionnaire score data, while qualitative analysis was used to describe the results of the quantitative analysis as well as suggestions and product improvements. Quantitative data obtained from the questionnaire were then converted to qualitative data with a scale of 5 (Likert scale) as described in Table 1 below:

Table 1. Likert Scale

Criteria	Score
Very good	5
Good	4
Enough	3
Not enough	2
Very less	1

The feasibility test uses a validator questionnaire percentage score of material experts, linguists, and design experts, namely:

$$P = \frac{f}{N} \times 100\%$$

Information:
P: Score Percentage
f: Total score obtained
N: Total maximum score

Table 2. Classification of eligibility for the Covid-19 Supplementary Book

Achievement Level	Validity Classification	Eligible Classification
84% < P ≤ 100%	Very Valid	Very worth it
68% < P ≤ 84%	Valid	Worthy
52 % < P ≤ 68%	Fairly valid	Pretty decent
36% < P ≤ 52 %	Invalid	Less Eligible

20% < P ≤ 36 %	Not Valid	Not feasible

To calculate the mastery of classical student learning is as follows:

$$PKK = \frac{\sum students\ who\ complete\ learning}{\sum all\ student} \times 100\ \%$$ [17]

According to the Ministry of Education and Culture "a class is said to have completed learning if in the class there are 85% who have achieved 70% mastery of learning.

After the individual and classical student learning completeness is analyzed, the pre-test and post-test scores are calculated by N-Gain to assess the increase and effectiveness of books before and after the use of scientific literacy-based supplementary books. The N-Gain formula is as follows:

$$N\text{-}Gain = \frac{Spost\ Spretest}{SMaks\ Spretest}$$ [18]

N-Gain is a good indicator to show the level of effectiveness of the treatment from the acquisition of post-test – pre-test scores. The N-Gain category is grouped in Table 3 below:

Table 3. Criteria for the N-Gain value

Coefficient Intervals	Criteria
0,7 < gs ≤ 1,0	High
0,3 < gs ≤ 0,7	Medium
0,0 < gs ≤ 0,3	Low

3. RESULTS AND DISCUSSION

3.1 Results

The designed book is a book based on scientific literacy which can be explained in detail in the following table:

Table 4. Scientific Literacy-Based Covid-19 Book Design for Class X High School Students

No	Science Literacy Component	Book Design
1	Science as a body of knowledge	The Science component as a body of knowledge encompasses concepts, principles, laws, and theories. So the book has designed materials consisting of: - History of Covid-19 - Characteristics of the Covid-19 virus - Transmission of Covid-19 - Clinical symptoms of being infected with Covid-19 - Prevention of transmission of Covid-19 - Covid-19 vaccine
2	Science as a way to investigate	Science as a way to investigate consists of: (1). Answering questions about the use of ingredients; (2) Answer questions through the use of tables, charts, etc.; (3) Perform Calculations; (4) Giving reasons for an answer; (5) Conducting experiments or other activities.
3	Science as a way of thinking	Science as a way of thinking consists of (1) Describing the experiments carried out by scientists; (2) Showing the historical development of an idea; (3) Emphasizing the empirical nature and objectivity of science; (4) Providing an overview of the use of assumptions; (5) Shows that science is obtained through inductive and deductive reasoning, (6) Provides a causal relationship; (7) Discuss the evidence, and (8) Show the scientific method and problem-solving.
4	The interaction of science with technology and society	The interaction of science, environment, technology, and society (interaction of science, technology, and society) consists of: (1) Explaining the benefits of science and technology for society, (2). Demonstrates the negative influence of science and technology on society; (3) Discusses social issues related to science and technology; and (4) Discusses careers and jobs in science and technology.

Table 5. Expert Validation

No	Expert Validation	Presents	Classification
1	Material Expert Validation	81,5 %	Very Valid and Feasible
2	Expert Validation of the Book Science Literacy Assessment Material	76%	Valid and Feasible
3	Language Expert Validation	72,5 %	Valid and Feasible
4	Design Expert Validation	84 %	Very Valid and Feasible

Product effectiveness is seen from the pretest and posttest values by looking for the N-Gain value. The average pretest and posttest values used to find the N-Gain value are described in Table 5 below:

Table 5. Average Pretest and Posttest Scores of Students

No	Trials	Average value	Percentage Average
1	Small Group	17	71
2	Medium Group	42	78
3	Total	59	149
4	Average	34	75,6

No	Trials	Average value	Percentage Average
	Standard Deviation	12,5	3,5

The effectiveness of learning resources developed in the form of supplementary books can be calculated using the N-Gain formula. The N-Gain category for assessing the effectiveness of the book is as follows:

0,70 < gs ≤ 1,00 = High
0,30 < gs ≤ 0,70 = Medium
0,00 < gs ≤ 0,30 = Low

The average pretest and posttest were obtained then converted into the formula to calculate the following N-Gain value:

$$g = \frac{75{,}6-34}{100\%-34} = 0{,}63$$

Calculation of the N-Gain value obtained a score of 0.63 which is included in the category of moderate effectiveness. With this ADDIE research phase that the researchers have gone through, it was found that the product being developed, namely: the Scientific Literacy-Based Covid-19 Supplement Book for class X SMA/MA, has met the elements of feasibility and effectiveness.

3.2 Discussion

The final product of this research and development is a scientific literacy-based Covid-19 supplement book for class X SMA/MA students. Based on the data validation results and product trials on students, it can be stated that this book product has the following advantages:

1. The developed scientific literacy-based Covid-19 supplement book received the title of "very decent" in all assessment indicators. So that the book is suitable for use as additional teaching materials in schools.
2. The developed scientific literacy-based Covid-19 supplement book can be used independently by students. 3. Not only acting as teaching materials, but the Covid-19 supplement book based on scientific literacy also trains analytical skills.
3. Scientific literacy-based Covid-19 supplement books developed on aspects of science as a way of thinking and science as problem-solving provide space for students to express ideas, thoughts, and hypotheses. They can convey the results of the analysis in the given room.
4. In the scientific aspect the body of the Covid-19 supplement book based on scientific literacy displays facts and a history of discoveries so that students get an accurate source of information.
5. A scientific literacy-based Covid-19 supplement book that was developed on aspects of science as a process of developing student creativity by searching for data directly in the neighborhood.
6. In the aspect of the interaction of science with technology, and society, the developed scientific literacy-based Covid-19 supplement book inspires students to be open to technology and utilize technology as a positive learning resource.

Scientific literacy-based Covid-19 supplement books also have drawbacks as teaching materials because the sources of information used are still very limited so further improvements are needed so that books can be more effectively used as teaching materials.

Supplementary books are textbooks that can be used as additional teaching materials in Biology subjects. Supplementary books can enrich and increase mastery of knowledge, and skills, and shape the personality of students, educators, education managers, and other communities. Books play an important role in the learning and learning process [19]. Learning and textbooks are two things that complement each other. Books are media in education that contain information about learning materials that are formulated from the basic competencies contained in the curriculum. Supplementary books are used by students in the learning process. Therefore books must not only make their readers smart but also be able to arouse curiosity that is much better than before as a result of increased scientific literacy [20]. Teaching materials in supplementary books must be more applicable to increase interest in reading for students because they do not just get concepts but are useful in their lives [21].

Based on the assessment by the expert validation team, the results were obtained: the criteria are valid and feasible to be tested with revisions, meanwhile, for the assessment of the scientific literacy component a score of 51 is obtained with a percentage of 70% with valid criteria and is feasible to be tested with revisions. After the revision was carried out, an assessment was carried out at the second meeting with an increase in the score increase to 73 with a presentation of 90%, in very valid criteria and very feasible to try out, then the assessment of the book science literacy component got a score of 59 with a percentage of 82%, in the valid criteria and worth trying. The material expert validator said that the book developed was by the validation indicators so that it was suitable for use and testing to become a supplementary book supporting learning.

According to Lepiyanti [22] Development products that are declared good by the validator must still go through the refinement stage according to expert advice. Referring to the regulation of the Minister of National Education of the Republic of Indonesia Number 2 of 2008 explaining that books that are suitable to be used as teaching materials must include quality criteria (standards) including, (1) Eligibility of content/material, (2) Adequacy of presentation, (3) Adequacy of language, and (4) Graphical feasibility. These criteria have been listed in the components of the validation sheet which have been assessed by a team of experts. The criteria for good teaching materials are declared valid. The validity of books can be seen through validity tests with intervals obtained by $81\% \leq X \leq 100\%$ and $61\% \leq X \leq 80\%$ with very good and good criteria [23].

The student response questionnaire was filled out by students after using the book in the learning process which contained questions about students' opinions regarding the supplementary book that was developed. Data was obtained from the student response questionnaire that the Covid-19 supplement book could increase student scientific literacy, which was known from the student response to the 16th aspect of the questionnaire, which was 4 (very good). Students are also interested in the overall appearance of the developed scientific literacy-based books. It is known from the average student response in aspects 1 and 3 of the questionnaire which is 4 (very good). Students find it easy and happy to understand the material from the supplementary book that was developed because the book displays supporting illustrations [24].

The average percentage of students' classical completeness in the pretest questions obtained was 34% and the pretest score obtained a percentage of 75.6%. The percentage of classical completeness was obtained from students' scientific literacy tests before and after using books. Next to see the effectiveness of the media by using the N-Gain formula. From the average pre-test and post-test scores, a score of 0.63 was obtained. In line with research conducted by Suraida [25] which states that the development of teaching materials is effective if the level of completeness of the test results is greater than the results of the previous test. Afifah's research [26] also shows that the proper use of scientific literacy-based teaching materials has proven to be effective in increasing students' scientific literacy scores. In line with that, Juhji's

research [27] also conveys that scientific literacy-based books significantly increase students' scientific literacy scores.

4. CONCLUSION

Based on the formulation, objectives, results, and discussion of research and development regarding the scientific literacy-based Covid-19 supplement book for SMA/MA previously stated, it can be concluded as follows:

1. The feasibility of the Covid-19 Supplement book on class X virus material at SMAN 1 Hutabayuraja, Simalungun Regency based on material experts obtained a percentage of 90% with a very valid category.
2. The feasibility of the Covid-19 Supplement book on class X virus material at SMAN 1 Hutabayuraja, Simalungun Regency, based on linguists, obtained a percentage of 92% with a very valid category.
3. The feasibility of the Covid-19 Supplement book on class X virus material at SMAN 1 Hutabayuraja, Simalungun Regency, based on design experts, obtained a percentage of 83% in the valid category.
4. The Covid-19 Supplementary Book for class X SMA/MA was declared effective in increasing student learning outcomes with an average percentage of students' classical completeness on pretest questions obtaining 34% and pretest scores obtaining a percentage of 75.6% with an n-gain of 0. 63.

5. REFERENCES

[1] Tandra, H. 2020. Virus Corona Baru Covid-19: Kenali, cegah, Lindungi Diri Sendiri & Orang Lain. Yogyakarta: Rapha Publishing.

[2] Shihab, N. & Komunitas Guru Belajar. 2019. Literasi Menggerakkan Negeri. Tanggerang Selatan: Literati.

[3] Nuraini, Siti. 2018. Perbedaan Kadar Hemoglobin Sebelum Menstruasi dan Pasca Menstruasi. Jombang (ID) : STIKes Insan Sendekia Medika.

[4] Hasruddin, Harahap, F., & Mahmud, M. 2018. Efektivitas Penerapan Perangkat Perkuliahan Mikrobiologi Berbasis Kontekstual Terhadap Kemampuan Berpikir Tingkat Tinggi Mahasiswa Pendidikan Biologi Unimed. Bioedukasi: Jurnal Pendidikan Biologi, 11(1), 51-54.

[5] Harsono, T. 2016. Perbandingan Penggunaan Metode Peta Pikiran Dengan Peta Konsep Terhadap Belajar Siswa di kelas XI IPA SMA Negeri 19 Medan Tahun Pembelajaran 2015/2016. Jurnal Pelita Pendidikan, 4(1): 92-94.

[6] Kurniasari, D.A. D. 2014. Penembangan Buku Suplemen IPA Terpadu. Unnes Science Education Journal. 3(2) 455-463.

[7] LP3 Universitas Airlangga. 2016. Panduan Penulisan Buku Ajar atau Buku Teks Universitas Airlangga.

[8] Kurniasari, D. A. D., Rusilowati, A., & Subekti, N. 2014. Pengembangan Buku Suplemen IPA Terpadu. Unnes Science Education Journal, 3(2): 464-470.

[9] Shihab, N. 2019. Komunitas Guru Belajar: Literasi Menggerakkan Negeri. Tanggerang Selatan: Literati.

[10] Echols, J. M., & Shadily, H. 2005. Kamus inggris indonesia: an englishindonesian dictionary. Jakarta: Gramedia.

[11] Holbrook, J, dan Rannikmae, M. 2009. The Meaning of Science Literacy. International Journal of Environmental & Science Education. Vol. 4, No. 3: 275-288,

[12] Pudjiadi, S. 2005. Masalah Gizi Pada Remaja. Jakarta: FKM UI.

[13] National Research Councils. 1966. National Science Education Standards. Washington, DC: The National Academy Press.

[14] National Research Councils. 1966. National Science Education Standards. Washington, DC: The National Academy Press.

[15] OECD. 2003. The PISA: Assessment Framework-Mathematics, Reading, Science, and Problem-Solving Knowledge and Skills

[16] National Science Teacher Association INSTA. 1997

[17] Sudjana,Nana dan Ahmad Rivai. 2007. Teknologi Pengajaran. Bandung: Sinar Baru Algensindo.

[18] Sudjana,Nana dan Ahmad Rivai. 2007. Teknologi Pengajaran. Bandung: Sinar Baru Algensindo.

[19] Sothayapetch. P., Lavonen, J., & Juuti, K. 2013. An Analysis of Science Textbook. Eurasia Journal of Mathematics, Science & Technology Education. No. 9 Vol.1: 59-72.

[20] Permata, D.A., dan Sayuti, K. 2016. Pembuatan Minuman Serbuk Instan Dari Berbagai Bagian Tanaman Meniran (Phyllanthus niruri). Jurnal Teknologi Pertanian Andalas. 20(1): 44-49.

[21] Adhitama, Rizky.S. et,al. 2018. Kesadaran Metakognitif Siswa dalam Pembelajaran Berbasis Proyek pada Pokok Bahasan Pencemaran Lingkungan. Departemen Pendidikan Biologi FMIPA Universitas Pendidikan Indonesia. [Online] Tersedia: http://ejournal.upi.edu/index.php.asimilasi.

[22] Lepiyanti, A., Pratiwi, D. 2015. Pengembangan Bahan Ajar Berbasis Inkuiri Terintegrasi Nilai Karakter Peduli Lingkungan. BIOEDUKASI. 6(2): 143-147.

[23] Trianto. 2010. Pengantar Penelitian Pendidikan bagi Pengembangan Profesi Pendidikan dan Tenaga Kependidikan. Jakarta: Kentjana.

[24] Belawi. 2006. Pengembangan Bahan Ajar. Jakarta: Universitas Terbuka.

[25] Suraida, T. Susanti, dan R. Amriyanto. 2013. Keanekaragaman Tumbuhan Paku (Pteridophyta) di Taman Hutan Kenali Kota Jambi. Prosiding Semirata FMIPA Universitas Lampung.

[26] Afifah, V. A. and Sarwoko. 2020. “Faktor-faktor yang mempengaruhi Kualitas Hidup Pasien Kanker Payudara Yang Menjalani Kemoterapi,” Jurnal Komunikasi Kesehatan, XI(1), pp. 106–119.

[27] Juhji, Rachman, M. S., & Nurjaya. 2020. Media daring dan kuantitas pemberian tugas terhadap kepuasan belajar mahasiswa. Al-Tarbawi Al-Haditsah: Jurnal Pendidikan Islam, 5(2), 1–15.

International Journal of Computer Applications Technology and Research
Volume 12–Issue 03, 46-52, 2023, ISSN:-2319–8656
DOI:10.7753/IJCATR1203.1011

Cooperative Learning-Based E-LKPD Round Robin Type: English Reading Skills

Ovielia Putri Rahman
Education Technology
Postgraduate
Universitas Negeri Medan
Medan, West Sumatera
Indonesia

Abdul Hamid, K.
Education Technology
Postgraduate, Leacture
Universitas Negeri Medan
Medan, West Sumatera
Indonesia

Naeklan Simbolon
Education Technology
Postgraduate, Leacture
Universitas Negeri Medan
Medan, West Sumatera
Indonesia

Abstract: To find out the feasibility and to know the effectiveness of the E-LKPD (Student Worksheet) Based on the Round Robin Type Cooperative Learning Model in Class VII English Subjects at Private Middle School IT Permata Hati Tebing Tinggi. This research is a Borg & Gall product development research and is combined with the Dick & Carey model. Subjects included 2 material experts, 2 media experts, 3 students in the individual test, 9 students in the small group test, and 26 students in the limited field test. The results showed that the E-LKPD Based on Cooperative Learning Round Robin Type was feasible to use, based on the validation of learning material experts 98.59% were in very decent qualifications, media expert validation was 94.64% in the very feasible category, individual trials were 92.42% were in the very feasible category, 95.70% for small group trials were in the very feasible category and 91.87% for field trials were in the very feasible category. The results of submitting the hypothesis prove that the learning E-LKPD is feasible to use, and there is a significant difference between the learning outcomes of students who are given treatment using the E-LKPD and printed media. This is indicated by the results of data processing tcount = 5.63 at a significance level of α = 0.05 with df obtained t table = 50, so that tcount > ttable (5.63 > 1.63).

Keywords: student worksheets; cooperative learning; round robin type; results of learning english; reading skills

1. INTRODUCTION

As an international language that plays an important role in the era of globalization, English is expected to be mastered by everyone. Since then English has been declared as an International Language. According to Simbolon [1] English is the main subject that must be mastered by students to be able to adapt to the development of science and technology. Through teaching English in schools, it is hoped that students will be able to master language skills in accordance with the curriculum and achieve basic and core competencies in their respective schools.

Having good reading skills is very important for students. Regarding learning English at school, Mikulecky and Jeffries [2] state that reading is an important way to improve students' general language skills in English. Reading can also improve vocabulary, writing and speaking skills and also discover new ideas, facts and experiences. Furthermore, when students come to the next level of education, they must first pass an exam. This is done to see how well students learn at a certain level of education. Reading skills are usually used in exams. So, students must have good reading comprehension if they want to pass the exam.

In the learning process, supporting components are needed so that it runs well and is also able to change the quality of the learning itself. An educator plays an important role in preparing learning tools before the start of learning. Ibrahim in Trianto [2] that the learning tools prepared can be in the form of: syllabus, lesson plans, and worksheets. Dwi Kurnia [3] states that the presentation of LKPD is now more innovative, that is, LKPD is united with a learning model so that it is able to attract students' interest in learning. The learning model that can be combined with the LKPD in this study is the Cooperative Learning model.

The presentation of LKPD which is commonly known as printed media, now can be used with electronic or digital media, known as electronic LKPD (E-LKPD). To make this electronic LKPD requires supporting applications, one of which is the Flip PDF Corporate Edition application. Nurbayani [4] states that Flip PDF Corporate Edition is software for converting material in PDF file format into electronic worksheets (E-LKPD) which can be combined with attractive pictures or illustrations, animations and videos. The resulting output is in the form of a sheet of questions and this file can be shared with students in the form of a link. Users can run this application via smartphone, computer or laptop. E-LKPD can be an alternative learning tool for teachers and students that is more effective and efficient.

1.1 English Learning Outcomes

Hilgard and Maarquis in Sagala [5] argue that learning is a process that a person goes through at the stages of training and learning so that there is a change in the individual. Furthermore, according to Skinner in Dimyati [6] learning is a behavior which when the individual learns well, will get a better experience. Ihsana [7] says that learning is a process in which there is a shift in the process from not knowing to knowing, from ignorance to understanding, from the inability to get the best results. Slameto [8] reveals learning is an activity to achieve change, namely behavior as a result of experience gained from the environment.

Jenkins and Unwin in Kennedy [9] argue that learning outcomes are statements of what students are expected to be able to do as a result of a learning activity. Furthermore, Bingham in Kennedy [10] reveals that learning outcomes are an explicit description of what the learner wants to know and be able to do as a result of learning.

1.2 Reading Skills

Nunan [11] states that reading is a set of skills needed to understand and derive meaning from printed words. Then Anderson [12], reading involves the ability to decode printed words in the key to reading. Decoding activity has an impact on the reader's understanding. Reading also requires derived meaning. He added that reading is understanding the whole meaning of a sentence. More than that, Brown [13] mentions reading is a reading activity negotiating meaning by bringing to the test scheme to understand it, and finally understanding of the text is considered a product of negotiation. Spratt, et.al [4] defines reading as a process of responding to interpreting information, readers are connected to new knowledge obtained from texts on knowledge they already know.

There are two main categories of reading purposes: reading for pleasure and reading for information. Nunan [15] states that reading for pleasure is one of the goals of reading; For example reading bedtime stories. The point of reading bedtime stories is to have a pleasant reading experience. In addition, Grabe and Stoller [16] suggest the purpose of more reading, namely: (1) Simple Information Search and Quick Reading. In reading for information, the reader usually scans the text for a certain word, or certain information, or some representative phrase. In this reading purpose, the reader tries to get specific information in the text; (2) Reading to learn from the text. Reading to learn usually takes place in academic and professional contexts where a person needs to learn a large amount of information from a text. For example, a biology teacher who reads a book written in English entitled 'Amoeba' needs to study the detailed information in the book. He wanted to increase their knowledge on the topic; and (3) Reading To Integrate Information, Writing and Critical Texts. Reading to integrate information often occurs before an author writes a paper. In a paper, he needs to integrate a lot of information that will support his statement, idea, or someone's statement. Information is taken from many sources. Then, he decides what information to integrate and how to integrate it into his writing.

According to Penny McKay [17] reading assessment techniques can be carried out by reading and responding, (reading and retelling, reading and doing short answer assignments), reading and doing tasks that require long answers, and reading and answering questions. Furthermore, Brown [18] argues that assessment is divided into two types. The first type is an informal assessment. This is done by the teacher without planning the assessment first. This form of assessment is that the teacher can provide feedback or feedback to students such as giving praise: "Good job", "Good", and "Done". In addition, this kind of assessment can be done by commenting on student papers, and also correcting what students have done. The second type is a formal assessment. With this formal assessment, the teacher first prepares several exercises to assess student competence, for example: quizzes, assignments or exams. In teaching reading skills, teachers need to assess the ability of their students to find out whether students understand the reading.

1.3 E-LKPD (Electronic Student Worksheet)

Slameto [19] suggests that LKPD is helping student activities when studying. LKPD as a guide for educators in addition to the various types of learning devices. Two learning factors are influenced by internal factors related to students' initial abilities while external factors are related to the learning approach. The presentation of the material contained in the LKPD is by involving students to actively work on exercises, discussions and practice.

Meanwhile, according to Azhar Arsyad [20] that LKPD is a source of learning where the educator is a facilitator can develop it in learning activities. LKPD is packaged and adapted to the conditions and situations of the learning being carried out. LKPD as a learning tool, because it can be used in conjunction with other learning resources.

Prastowo in Laely [21] states that there are functions of LKPD, namely: (1) LKPD functions so that learning takes place based on student centered learning; (2) LKPD can be used by students to study and understand the material taught by the teacher; (3) LKPD is made concisely and concisely which is used as an exercise for students; (4) Its function makes it easier for educators to provide a summary of the material and questions for students.

Given the importance of creating good LKPD, Alan [22] states that in making LKPD it is important to follow the steps for making LKPD, namely: (1) The content of the material is guided by the curriculum; (2) Pay attention to the differences in students because in the independent curriculum it emphasizes competence and demands student abilities; (3) Activities in LKPD help students understand the subject matter; (4) Associating material with real activities and technology; (5) Having clear learning objectives; (6) Make the main material and details; (7) Compose simple, concise sentences that are easy to understand; (8) Systematic structure according to students' understanding; (9) Generating students to learn and carry out scientifically; (10) Materials must be in accordance with the time allotted; and (11) Implemented in the context of completing tasks and solving problems drawing conclusions

Smaldino [23] states that effective teaching is integrating and utilizing technology in learning. E-LKPD is a technology-based device equipped with attractive pictures, animations and videos so that participants are enthusiastic when participating in learning.

Anggraini [24] argues that E-LKPD is a presentation of teaching materials that are arranged sequentially into certain learning units and is formed in an electronic format and contains interesting videos so that it makes users more interactive. The E-LKPD tools accessed by students have different benefits and characteristics. In terms of benefits, this makes the learning process more interesting.

Based on several theories related to E-LKPD, it can be synthesized that E-LKPD is a learning tool that is designed using digital media, systematic and attractive in order to achieve what is desired. With technology, it is possible for activities to become easy and can also share knowledge and introduce educational technology to students. So far it has been implemented in schools using ICT-based media, such as PowerPoint media and so on, but it has not yet been integrated into a complex blend so it still takes time to access it.

Researchers developed E-LKPD using the Flip PDF Corporate website. This application is used as the main medium for developing LKPD with various kinds such as E-LKS and /E-LKPD. LKPD can be made by uploading LKPD in the prepared file (PDF), then LKPD can be edited using the

commands on the edit menu. Some of the directions on the sheet are drag and drop, match, and so on.

1.4 Cooperative Learning Models

Cooperative Learning is one application of constructivist theory. Cooperative learning departs from the concept that students are able to get and understand a difficult concept when students discuss it with their classmates. Students regularly work in groups and then help solve complex statements. Trianto in Slavin [25] states that social nature in groups is the main aspect of cooperative learning. The idea of cooperative learning is that students work together to learn actively, are obliged to improve the learning process of their group members; Cooperative learning here is more focused on achieving goals and group success.

In addition, Sanjaya [26] also defines cooperative learning as a teaching method with a group or small group system. backgrounds of heterogeneous academic abilities, ethnicity and gender. This kind of method has 2 main components, the cooperative task component and the cooperative incentive structure. Cooperative tasks are related to things that make members work together in groups to complete tasks. The incentive structure is something that motivates a person to work. together for the same goal.

Meanwhile, Johnson, Johnson, and Holubec in Jacobs [27] define cooperative learning as learning that uses groups so that students work together to optimize their own learning with one another.

Ibrahim [28] states that cooperative learning steps are divided into several phases, namely:

Table 1. Cooperative Learning Steps

No	Phase	Teacher Activity
1.	Present goals and set	Convey what goals must be achieved in reading material related to the topic of the text and motivate students to be enthusiastic about learning during learning.
2.	Present Information	Presenting information to students through reading.
3.	Organize student into learning teams	Explain to students how to form study groups using the Cooperative Learning Model steps.
4.	Assist team work and Study	Monitor each teacher when students work on assignments.
5.	Test on the material	Analyzing learning outcomes on the material studied or each group presenting work results.
6.	Provide the materials	Give awards for learning outcomes to groups or per person.

Based on the table 1 above, it can be concluded that there are 6 steps that must be taken in cooperative learning, namely conveying what goals are to be achieved and motivating students, presenting reading material, organizing students, guiding groups in assignments, evaluating learning outcomes and giving awards.

1.5 The essence of Round Robin

Round Robin was developed by Spencer Kagan [29] as part of the cooperative learning model. Kagan said that implementing the Round Robin strategy can improve students' social skills that there is a spectrum of social skills needed to be a good team member. Team members must know how to help when help is asked for. But they also don't want to be a know-it-all. They need to know how to be a good leader. But they don't want to be too bossy. They can't be too shy to participate, but they can't be too loud or assertive to get their teammates into trouble.

In addition, Kohonen [30] also stated that in groups that are good at cooperative learning, there are heterogeneous groups consisting of four members including high achievers, one or two average achievers, and low achievers. This statement is supported by Jacobs [31] which explains the benefits of placing students in groups. He stated that larger groups (more than two) have advantages due to more complex tasks, where more people and perhaps cooperative learning have a wider range of skills.

Jacobs, Lee, & Bell [32] explain that this strategy is called Round Robin, because they rotate in a circle with everyone getting a chance to speak as the Robins sing. Groups use the Round Robin cooperative technique to discuss their own beliefs about learning.

Based on the expert opinion above, it is synthesized that Round Robin is a cooperative learning strategy in which each group member will rotate to present their work. With Round Robin, learners should know how to motivate their teammates when they are down. They should listen to their teammates to understand their perspective. They must know how to take rejection well when their ideas are not voted on. They should know how to take turns, politely disagree, resolve conflicts, and reach a consensus. These are just a few of the many skills required to be a good teammate. In general, it is also an essential life skill for success at work, for family life, and for positive social relationships.

Based on the formulated problems are: (1) Is the development of the E-LKPD based on the Round Robin Type Cooperative Learning Model being developed suitable for use in English subjects; and (2) Can the development of E-LKPD based on the Round Robin Type Cooperative Learning Model that is developed effectively improve student learning outcomes in English subjects?

2. METHOD

This study uses research & development methods. This research method is to produce products, test the feasibility and test the effectiveness of these products. The product developed is the development of an E-LKPD based on the Round Robin Type Cooperative Learning Model in English Subjects in Class VII. Borg and Gall [33] state that research and development is a step to develop and validate products. The purpose of research and development is not just to develop a product, but also to gain new knowledge or to answer specific questions about practical problems. The Borg and Gall development model is shown in Figure 1:

International Journal of Computer Applications Technology and Research
Volume 12–Issue 03, 46-52, 2023, ISSN:-2319–8656
DOI:10.7753/IJCATR1203.1011

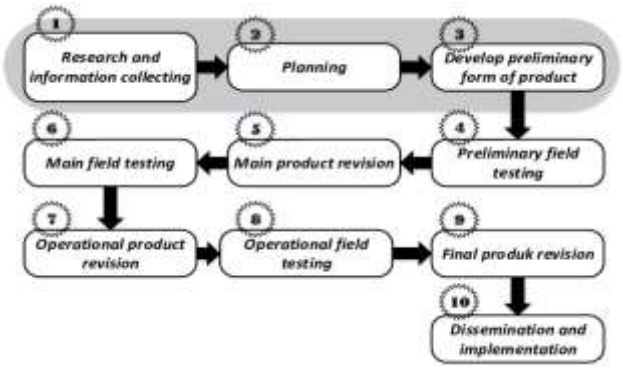

Figure 1. The Borg & Gall Development Model

The location of the research implementation was carried out at Private Middle School IT Permata Hati Tebing Tinggi which is located at Jl. Abd. Rahim Lubis, Rambung, Tebing Tinggi Deli, City of Tebing Tinggi, North Sumatra. the subjects were class VII-A and class VII-B Private Middle School IT Permata Hati Tebing Tinggi. Class VII-A, namely the experimental class as a whole, has 26 students. And class VII-B as the control class which as a whole numbered 26 students.

Product feasibility tests were carried out in order to obtain information about the appropriateness of the learning device products being developed, through the results of questionnaire assessments which were disseminated to learning experts (materials and media), individual trial evaluations, small group and field evaluations. The answers to each statement item were then measured using a Likert scale. The results of the validation from experts as well as the acceptance of E-LKPD users determine the level of eligibility for the revision of the E-LKPD using the qualification criteria in the table 2 below:

Table 2. Qualification Criteria for Assessment Qualification Questionnaires Validation of Experts, and Instruments for Student Responses to Student Worksheets Based on the Cooperative Learning Model Round Robin Type Assisted with Flip PDF Corporate Edition

Achievement Rate Percentage	Appropriatenes s	Information
81,26% ≤ X < 100%	Very good	No need for revision
62,6% ≤ X < 81,25%	Good	No need for revision
43,76% ≤ X < 62,25%	Less	Revision
25% ≤ X < 39 %	Very Less	Revision

Source: Akbar [34]

Based on the quantitative data from the results of the validator by material experts, media experts and student response questionnaires, the next step is to analyze the data and calculate the percentage level of achievement based on the formula:

$$P = \frac{\sum x}{\sum xi} \times 100\ \%$$

Information:
x : The answer score from the validator
x_i : Score the highest answer
P : Presentation of eligibility leve

Product Effectiveness Test Data Analysis Techniques
The effectiveness test aims to obtain information about whether or not the product development being tested is effective in the learning process.

Based on the formulation of the first problem, namely whether the Round Robin Type Cooperative Learning-based E-LKPD developed is suitable for use in class VII IT Private Middle School Permata Hati Tebing Tinggi. E-LKPD can be said to be feasible to use based on the results obtained from expert validation regarding suggestions and improvements related to the developed E-LKPD. The next step is to carry out individual trials of 3 students, small group tests of 9 students to find out the response to the developed E-LKPD. Then a field trial was carried out with 26 students to find out the responses to the E-LKPD that was made.

Based on the formulation of the next problem, namely whether the developed E-LKPD is effective in improving the English learning outcomes of class VII students of IT Permata Hati Tebing Tinggi Private Middle School. Learning is said to be effective if there are significant differences in learning outcomes between classes that are given treatment and classes that are not given treatment. The hypothesis uses the mean difference test or t-test. The t-test is the average difference to find out whether there is a significant difference at the 0.05 significance level with Microsoft Excel 19.

The hypothesis formulated is
Ho: μ1 = μ2 (there is no mean difference between the treated and untreated classes).
Ha : μ1 ≠ μ2 (there is an average difference between the treated and untreated classes).
Decision making Ho is accepted if the significance is greater than 0.05. The following is the calculation using the 2 difference test on the population average according to Sudjana [35]:

$$t = \frac{\bar{X}1 - \bar{X}2}{s\sqrt{\frac{1}{n1} - \frac{1}{n2}}}$$

Where:
$\bar{X}1$ = total average score of the experimental class sample.
$\bar{X}2$ = total average score of the control class sample.
s = standard deviation

3. RESULTS AND DISCUSSION

3.1 Results

The results of the assessment by media experts, material experts, individual trials, small group trials and limited field trials for all aspects of the assessment are determined by the average score. The results of the assessment were then analyzed and determined whether or not it was appropriate to develop a Round Robin Cooperative Learning Type E-LKPD on the material This is My Beautiful Family. The average percentage of the results of the assessment of media experts, material experts, individual trials, small group trials and field trials as follows:

Table 3. The Average Percentage of Assessment Results on E-LKPD Based Cooperative Learning Round Robin Type on This is My Beautiful Family Material

No	Categorization	Percentage of average score	Criteria
1.	Media Expert Validation	94,64%	very worth it
2.	Material Expert Validation	98,59%	very worth it
3.	Individual Trial	92,42%	very worth it
4.	Small Group Trial	95,70%	very worth it
5.	Field Tria	91,87%	very worth it
Average		94,64%	very worth it

E-LKPD Based Cooperative Learning Type Round Robin on the material This is My Beautiful Family from the validation of experts and trials shows a percentage of 94.64% in media validation, 98.59% in material validation, 92.42% in individual trials, 95.70% in small group trials, 91.87% in field trials. Overall, the average percentage is included in the "Very Eligible" category, which means that the use of E-LKPD based on the Round Robin Type Cooperative Learning Model meets the needs of students.

Based on research that has been done on learning outcomes, it can be seen that the E-LKPD learning outcomes score based on the Round Robin Type Cooperative Learning Model obtained the lowest score of 70 and the highest score of 96, the average score X = 83.15, standard deviation (SD) = 6.28. An overview of the learning outcomes of E-LKPD based on the Round Robin Type Cooperative Learning Model can be seen in Table 4 below:

Table 4. Learning Outcomes Learning Outcomes of English Using E-LKPD Based Cooperative Learning Round Robin Type on This is My Beautiful Family Material

Class	Class Intervals	F. Absolute	F. Relative %
1	70-74	2	7,69
2	75-78	3	11,53
3	79-83	7	26,81
4	84-88	3	11,53
5	89-92	1	3,84
6	93-96	10	38,46
	Amount	26	100

Based on research on the results of learning English, it is known that the score of learning outcomes using printed worksheets obtained the lowest score of 60 and the highest score of 93, the average score of X = 73.25, standard deviation (SD) = 7.98.

To see student scores using class intervals, namely scores between absolute frequencies, namely the number of students from learning achievement scores, and the relative frequency of the number of percent of learning achievement scores. Student learning outcomes using printed worksheets can be seen in Table 5 below:

Table 5. Student Learning Outcomes Using Printable LKPD

Class	Class Intervals	F. Absolute	F. Relative %
1	60–66	10	38,46
2	67–73	8	30,76
3	74-80	1	3,84
4	81–86	1	3,84
5	87-93	4	15,40
6	94–100	2	7,69
Amount		26	100

The analysis requirements test performed is the normality and homogeneity tests. Testing was carried out using the Liliefors test. A summary of the normality of the two samples can be seen in Table 6 below:

Table 6. Summary of Data Normality Test with Liliefors

No.	Data	Class	L count	L table	Conclusion
1	Pre-test	Experiment	0,125	0,154	Normal
2		Control	0,058	0,157	Normal
3	Post-test	Experiment	0,138	0,154	Normal
4		Control	0,052	0,157	Normal

Thus the pre-test values for the experimental class and the control class Lcount < Ltable, while the post-test values for the experimental class and control class Lcount <Ltable, it is synthesized that the two sample group data are normally distributed.

Homogeneity test analysis using the F test is to prove the largest variance and the smallest variance with the formula:

$$F = \frac{Varian\ terbesar}{Varian\ terkecil} = \frac{S_1^2}{S_2^2}$$

A summary of the homogeneity of the two samples is seen in Table 7 below:

Table 7. Summary of Data Homogeneity Test

No	Data	Class	F_{count}	F_{table}	Conclusion
1	Pre-test	Experiment	1,02	1,86	homogeneous
2		Control			
3	Post-test	Experiment	1,61	1,86	homogeneous
4		Control			

So it can be seen that Fcount <Ftable at the significant level α = 5% states that the data of the two samples have a homogeneous variance and it can be concluded that the research data meets the requirements for hypothesis testing.

Hypothesis testing uses the t-test with the formula, namely:

$$t = \frac{\bar{x}1 - \bar{x}2}{s\sqrt{\frac{1}{n1} + \frac{2}{n2}}}$$

The following is the formulation of this statistical hypothesis, namely:
Ho : μA1 ≤ μA2
Ha : μA1 > μA2

Information:
μA1 : average student learning outcomes taught using the E-LKPD based on the Round Robin Type Cooperative Learning Model
μA2 : average learning outcomes of students taught with printed worksheets

The t-test is used as a hypothesis testing tool because the research data is normally distributed and homogeneous. The hypothesis in the research is:

Ho: E-LKPD based on the Round Robin Type Cooperative Learning Model that was developed is not effective for improving English learning outcomes.
Ha: E-LKPD based on the Round Robin Type Cooperative Learning Model which was developed effectively to improve English learning outcomes

The calculation results obtained tcount. 5.63 > t table = 1.63 price t table dk = 63 with a significant level of 0.05 through interpolation t table 1.63. The price obtained is tcount > ttable, then Ho is rejected and Ha is accepted. Therefore, the research hypothesis concluded that the E-LKPD based on the Round Robin Type Cooperative Learning Model that was developed was effectively used and verified.

3.2 Discussion

The E-LKPD learning device based on the Round Robin Type Cooperative Learning Model is feasible to use. This is in line with the average rating at all stages showing very good results. Based on observations and studies during the research, this E-LKPD learning tool increases the attractiveness of students studying English subjects. It can be seen in the enthusiasm of students when using the E-LKPD and learning outcomes have increased compared to before.

Some of the uses and benefits of using the E-LKPD based on the Round Robin Type Cooperative Learning Model are: (1) learning becomes more enjoyable due to the availability of varied video sources (2) each group contributes to having a sense of responsibility in completing assigned tasks. there are (3) student-centered learning-centered teaching patterns and the teacher is a facilitator, (4) materials and questions are available so that it makes it easier for students to understand the topic of learning English.

Based on the results of the validation and testing, the E-LKPD is very suitable for use in the learning process. As stated by Rita Erlina [36] that with these learning tools, the learning process is carried out effectively. So, the researcher concluded that the use of E-LKPD based on the Round Robin Type Cooperative Learning Model is very appropriate for students to use in English subjects.

Learning devices are categorized as feasible after there are satisfactory results in achieving a goal. In this case, product trials were carried out in the learning process. The effectiveness of a learning device is obtained from student learning outcomes. E-LKPD learning based on Round Robin Type Cooperative Learning is also able to increase effectiveness in learning. In processing the data it was shown that there was an average result at the time of the posttest in the experimental class, which was 86.79. While the results of the control class were not treated using the E-LKPD but only used printed worksheets, which was 74. Thus, the E-LKPD learning tools in the field trial fulfilled the very good and effective category for use in learning English in class VII Permata Hati Private Middle School Tebing Tinggi.

E-LKPD which is easy to use and flexible in nature. Making it easier to carry and can be used anytime and anywhere is one of the reasons that E-LKPD is easy to accept. Erina Dwi Susanti [37] with her research to improve the achievement of students' mathematical knowledge competencies, where it is stated that the results of material validation show 93.4% (very good). Media expert validation results show 95.6% (very good). This causes increased learning effectiveness.

According to Handoko [38] effectiveness is the capacity to choose the right goals or tools to realize the goals that have been set. Effectiveness can be meaningful as the success of what is achieved with certain efforts in accordance with certain goals. According to Trianto [39] that the result of teaching and learning activities is the effectiveness of learning. According to him, learning is considered effective if it fulfills several key criteria, including: (1) a high percentage of student study time allocated for teaching and learning activities; (2) Students generally behave well in terms of completing assignments, (3) the contents of learning materials are accurately related to students' abilities (learning success orientation), (4) a warm and supportive learning environment is created.

Students can use this E-LKPD media to study in the classroom or at home. E-LKPD is run by students themselves, and they have the freedom to choose the order of learning activities and set their own learning pace. As explained by Heinichi Molenda, Smaldino [40] claims that one advantage of using the E-LKPD is that it displays the information needed by its users and helps students who have slow learning speeds. In other words, it can encourage effective learning activities for students who are slow to respond, but can also stimulate learning activities for students who are fast responding.

4. CONCLUSION

Based on the results of the research and discussion, research on the development of E-LKPD based on the Round Robin Type Cooperative Learning model on the topic This Is My Beautiful Family on the material Simple Present Tense, Family Members, and Possessive Adjective/Possessive Pronouns, the following conclusions are obtained:

The product in the form of an E-LKPD based on the Round Robin Type Cooperative Learning model is very feasible to be the final product that can be disseminated and implemented to users. This is done in several stages, namely validation to media experts, material experts, individual trials, small group trials, field trials. The results of the assessment obtained from this stage get a total score of 94.64% in the "Very Eligible" category.

The average learning outcomes of students using the E-LKPD based on the Round Robin Cooperative Learning model with the learning outcomes of students using printed (conventional) LKPD show that students using the E-LKPD based on the Round Robin Cooperative Learning model are "more effective" than students using conventional LKPD. This is shown by the results of the t test at a significant level $\alpha = 0.05$, the results of testing the hypothesis on learning outcomes between two classes, after being given treatment, the value of t count > t table is 5.63 > 1.63, meaning that it is concluded that Ho rejected and accepted Ha, the research hypothesis stated that there was an increase in English learning outcomes using the E-LKPD based on the Round Robin Type Cooperative Learning model compared to using printed worksheet media.

5. REFERENCES

[1] Simbolon, N. 2012. The Effect of Instructional Approach and Verbal Reasoning on Students' English Speaking Competence, SMA Negeri 14 dan 21 Medan. Journal PGSD FIP Unimed. Vol.1(1), 73-83
[2] Trianto. 2011. Mendesain Model Pembelajaran Inovatif-Progresif. Jakarta: Kencana Prenada Media Group, 201.

[3] Hayati, Dwi. Kurnia.,dkk. 2020. Pengembangan LKPD Berbasis Cooperative Learning Materi Sintesis Protein Untuk Siswa Kelas XII SMA. Al Jahiz: Journal of Biology Education Research. Vol.1 (1), 44-51
[4] Nurbayani, A., Rahmawati, E., Nurfaujiah, I. I., Putriyanti, N. D., Safira, Y., & Ruswan, A. 2021. Sosialisasi Penggunaan Aplikasi Liveworksheets sebagai LKPD Interaktif Bagi Guru-guru SD Negeri 1 Tegalmunjul Purwakarta. Indonesian Journal of Community Services in Engineering & Education (IJOCSEE), Vol.1. No.(2), 126-133.
[5] Syaiful,Sagala. 2012. Supervisi Pembelajaran. Bandung:Alfabeta, 13.
[6] Dimyati dan Mudjiono. 2015. Belajar dan Pembelajaran. Jakarta: Rineka Cipta, 10.
[7] Ihsana. 2017. Belajar dan Pembelajaran.Yogyakarta: Pustaka Pelajar, 4.
[8] Slameto. 2015. Belajar dan Faktor-faktor yang Memengaruhinya. Jakarta: Rineka Cipta, 2.
[9] Kennedy, D. 2006. Writing And Using Learning Outcomes: A Practical Guide, Cork, University College Cork, 20.
[10] Kennedy, D. 2006. Writing And Using Learning Outcomes: A Practical Guide, Cork, University College Cork. 20.
[11] Nunan, David. 1999. Second Language Teaching and Learning. Boston: Heinle &Heinle Publisher, 249.
[12] Alderson, J.C.2000. Assessing Reading. New York: Cambridge University Press, 3.
[13] Brown,H. Doughlas. 2004. Language Assessment: Principle and Classroom Practices. New York:Pearson Education.
[14] Spratt, Mary., Alan Dulverness, and Melanie Williams. 2005. The Teaching Knowledge Test (TKT). Cambridge: Cambridge University Press, 21.
[15] Nunan, David. 1999. Second Language Teaching and Learning. Boston: Heinle &Heinle Publisher, 251.
[16] Grabe, William and Fredericka L. Stoller. 2011. Teaching and Researching Reading. New York: Pearson Education Limited, 6-10.
[17] Mckay, Penny. 2006. Assesing Young Language Learners. New York: Cambridge University Press, 237.
[18] Brown,H. Doughlas. 2001. Teaching by Principles an Interactive Approach to Language Pedagogy Second Edition NewYork: Pearson Education Company, 5.
[19] Slameto. 2015. Belajar dan Faktor-faktor yang Memengaruhinya. Jakarta: Rineka Cipta, 45.
[20] Arsyad, Azhar. 2010. Media Pembelajaran. Jakarta: Raja Grafindo Persada, 29.
[21] Laely. 2021. Pengembangan LKPD Elektronik Berbasis Problem Based Learning (PBL) Bermuatan EtnoSains Pada Materi Reaksi Redoks Kelas X di MAN 1 Cirebon. Semarang: UIN Walisongo Semarang, 14.
[22] Alan. 2012. Lembar Kerja Peserta Didik yang Mudah Digunakan. Jakarta: Gramedia, 32.
[23] Smaldino, Sharon. E., Lowther, Deboran. L., Russel, James.D. 2011. Teknologi Pembelajaran dan Media untuk Belajar. Jakarta: KENCANA, 110.
[24] Anggraini, Eka. 2019. Mengatasi Kecanduan Gadget pada Anak. Serayu Publishing, 18.
[25] Slavin, R. E. 2006. Educational Psychology Theory and Practice (8th ed.). Boston: Pearson, 56-57.
[26] Sanjaya, W. 2009. Strategi Pembelajaran Berorientasi Standar Proses Pendidikan. Jakarta: Kencana Prenada Media, 240-241.
[27] Jacobs, Lee and Bell. 2006. Issues in implementing cooperative learning and Second Language Teaching. USA: Cambridge University Press, 3.
[28] Muslimin,Ibrahim. 2000. Pembelajaran Kooperatif. Surabaya: University Press, 10.
[29] Kagan, Spencer. 2009. Cooperative Learning. Kagan Publishing, 117.
[30] Kohonen, V. 2003. Experential Language Learning. In Nunan,D (Ed.), Collaborative Language Learning and Teaching. New York:Cambridge University Press, 36.
[31] Jacobs, Lee and Bell. 2006. Issues in implementing cooperative learning and Second Language Teaching. USA: Cambridge University Press, 31-32.
[32] Jacob, Lee,and Bell. 1997.Cooperative Learning. Singapore: SEAMEO Regional Language Centre,28.
[33] Borg,W.R and Galll,MD. 2003. Educational Research: An Introduction 4th edition. London: Longman Inc, 569.
[34] Akbar, S. 2016. Instrumen Perangkat Pembelajaran. Bandung: Remaja Rosda Karya.
[35] Sudjana, Nana. 2009. Penilain Hasil Proses Belajar Mengajar, Bandung: Remaja Rosda karya.
[36] Erlina Rita,dkk. 2022. Development of E-Module Elasticity Materials and Hooke's Law Using Flip PDF Corporate Edition to Improve Critical Thinking Ability of High School Students Finger: “Jurnal Pendidikan Teknologi Informasi dan Komunikasi” Vol.1(1),16-25
[37] Susanti, E. D., & Sholihah, U. 2021. Pengembangan E-Modul Berbasis Flip Pdf Corporate Pada Materi Luas Dan Volume Bola. Jurnal Pendidikan Matematika, 3(1), 37-46.
[38] Handoko, T. Hani dan Reksohadiprodjo. 2003. Manajemen Sumber Daya Manusia dan Perusahaan. Edisi Kedua. BPFE: Yogyakarta, 7.
[39] Trianto. 2013. Mendesain Model Pembelajaran Inovatif-Progresif. Jakarta: Kencana Prenada Media Group, 20.
[40] Heinich, Molenda, Russel,Smaldino. 1996. Instructional Media and Technologies for Learning. New Jersey: Printice-Hall, Inc. A Simon & Schuster Company.

International Journal of Computer Applications Technology and Research
Volume 12–Issue 03, 53-55, 2023, ISSN:-2319–8656
DOI:10.7753/IJCATR1203.1012

The Analysis of Inulin From Yam Tubers using FTIR (FOURIER TRANSFORM INFRA RED)

Irving Josafat Alexander
Physics Education Program
HKBP Nommensen University
Medan, Indonesia

Rumondang Bulan
Chemistry Department
University of North Sumatera
Medan, Indonesia

Emma Zaidar
Chemistry Department
University of North Sumatera
Medan, Indonesia

Ramlan Silaban
Department of Chemisitry
State University of Medan
Medan, Indonesia

Timotius Agung Soripada
Artha Medica Hospital
Binjai, Indonesia

Gloria Sirait
Biology Education Program
HKBP Nommensen University
PematangSiantar, Indonesia

Abstract: Research on inulin which was isolated from yam tubers (Pachyrhizuserorus).This research is a experimental laboratory research. The Qualitative Analysis of Inulin is Reduction Sugar make a Bennedictand The Quantitative Analysis Inulin was isolated from yam tubers is characterized by using Forrier Transform Infra Red (FTIR).

Keywords: inulin, yam tubers, reduction sugar, benedict, forrier transform infra red

1. INTRODUCTION

In recent years, probiotic functional foods have gained quite a popularity and become a preferred choice among consumers, due to their positive effects on the gut microbiota and overall health. However, it is imperative for a probiotic strain to remain live and active at the time of consumption in high enough population density, in order to provide such health benefits [3].

Inulin as a prebiotic provides important benefits in the body because it can bind air from several important polysaccharides in maintaining air in the stomach. Given its various health benefits, it is unsurprising that researchers have already begun investigating the potential uses of inulin in food products. Inulin has been used a successful fat substitute and as a dietary fibre in breakfast cereals, yoghurts, cheeses, and even chocolate. Some countries already have rules regarding the standard amount of prebiotics consumed mainly inulin. Inulin is a type of prebiotic that is widely used in food products so it needs to be added to the appropriate level for processed food products such as fermented milk. The level of administration of inulin is very important to know to get the optimal amount of inulin which is beneficial for the health of the body[5]. The beneficial physiological functions of this inulin-type prebiotic also included management of diabetes mellitus and obesity as well as improvement of serum lipids concentrations and mineral absorption [1]

As concept introduced by Gibson & Roberfroid (1995), prebiotics are nondigestible food ingredients that beneficially influence the host by stimulating the growth and/or activity of a limited number of bacteria species resident in the colon, and thus improve host health. This definition has been revised along the time, but the main features have mostly been retained. The great interest in the development of prebiotics is aimed at nondigestible oligosaccharides. Some of the prebiotics are the inulin-type fructans, because they provided evidence of their ability to change the gut flora composition after a short feeding period based on results from in vitro studies and human subjects. Inulinis a versatile fructooligosaccharide generally extracted from chicory that is applied in the stabilization of proteins and modified drug delivery. Another interesting carbohydrate for encapsulation is inulin, a polysaccharide composed of fructose units linked by-(2,1) bonds and containing a glucose unit. Inulin can be commercially obtained from chicory and has prebiotic effects, dietary fiber actions ,among other health related benefits [4]. Although inulin has several applications in diverse areas, including in the food area for decades, the use of inulin as wall material in the food field is a few exploited. Wall materials commonly used in the en-capsulation of bioactive compounds are gums, modified starches,whey proteins and dextrins [2]. However, such substances do not present functional activities as inulin does. Looking for the substitution of gums, maltodextrinor starches by prebiotic materials, some researchers are studying the use of inulin. Recently, Fernandes, Borges, & Botrel (2014a) evaluated theeffects of the partial or total replacement of gum Arabic by inulin onthe characteristics of rosemary essential oil microencapsulated by spray-drying. Saénz, Tapia, Chávez, & Robert (2009) also reported theability of inulin for microencapsulation of bioactive compounds from cactus pear fruit. Thus, the use of inulin can favor the application oforegano extract in functional [7]

2. METHOD

2.1 Tools and Materials

The materials that needed in this study were yam tuber.

2.2 Preparation of yam bulbs extract

The first step that carried out in this study was the extraction process of the yam. About ±1000 grams of yam tuber sample that has been cut, then peeled and washed thoroughly.

International Journal of Computer Applications Technology and Research
Volume 12–Issue 03, 53-55, 2023, ISSN:-2319–8656
DOI:10.7753/IJCATR1203.1012

2.3 Isolation inulin of a yam tubers extract

The next step is yam tuber mixed with 1:2 (b:v) water. Then, it is heated to a water bath at a temperature of 80ºC for ± 30 minutes. After being cold, the filtrate is taken and filtered. The filtrate is then dissolved in 30% ethanol by 40% of the filtrate volume. The solute is stored at 0ºC for ±18 hours. The solute is left at temperatures' room for 2 hours or allowed to stand until come such of sediment. The precipitate that obtained is wet inulin 1 which is then reconstituted with water, with a ratio of 1:2 (b:v). Furthermore, the next process is same as above to obtain wet inulin II. In the final stage, wet inulin II was dried at 50ºC for 6-7 hours and been smoothed to become inulin powder.

2.4 Analysis of Inluin with Bennedict (Qualitative)

1 gram of inulin is dissolved in 10 mL aqquades and then taken as 5 drops and added to 5 mL of Benedict's solution then heated in a water bath for 5 minutes. Brownish-red precipitate shows a positive test for reducing sugars

2.5 Analysis of Inulin Function with FT-IR Spectroscopy

Inulin has been prepared in the form of mull. The slurry is examined in a thin filet placed between flat salt plates. The test is done by clamping the mixed film on the sample site. Then, the film is placed on the plate in a way of infrared light. The result is then recorded to a paper in the form of a curve wave 4000-200cm^{-4} to the intensity. Insulin that has been produced from yams is characterized by a functional group using a forrie transform infra red (FTIR) device at 4000-500cm^{-1} wave number.

3. RESULTS AND DISCUSSION

3.1 Results of Inulin Isolation from Yam Bulbs

The results of inulin isolation from yam tubers as much as 1059 grams obtained 23,298 grams of pure inulin (2.23% of the initial mass of yam tuber samples that used in this study). Inulin isolation included the extraction process using aquadest solvent and dissolved with 30% ethanol solvent in the sample. This isolation process produces pure white inulin. The results of inulin isolation that obtained from the study can be seen in the following figure.

Figure 1. Inulin was isolated from yam bulbs

3.2 Results of Inulin Analysis with Bennedict Solution

The results of a qualitative test of reducing sugars using Benedict reagents produce a brownish-red precipitate after heating for 5 minutes on a water bath indicating the presence of inulin.

The results of inulin isolation from yam tuber as much as 1059 grams obtained 23,298 grams of pure inulin (2.23% of the initial mass of yam tuber samples used in this study). Yam tubers (Pachyrhizus erosus) is one of the tubers which contains inulin. This yam tuber (Pachyrhizus erosus) contains hypoglycemic substances niacin, inulin, fiber, calcium and vitamin C which can reduce blood glucose levels and can increase the weight of patients with hyperglycemia.

3.3 Results of Inulin Analysis with FTIR (Forrier Transform Infra Red)

The results of the functional group analysis of inulin from tubers of dahlia and inulin tubers using the *Fourier Transform Infra Red Spectroscopy* (FTIR) can be seen in the Figure 2, and inulin wave numbers of dahlia tubers and inulin tubers can be seen in Table 1 below.

Table 1. Wavenumber of Yam Tuber Inulin and Commercial Inulin

Number	Wavenumber (cm^{-1})		Fuctional Groups
	Commercial Inulin	Yam Tuber Inulin	
1	3371.57	3402.43	O-H
2	2931.80	2924.09	C-H
3	1126.43	1157.29	C-O
4	1026.13	1018.41	C-O

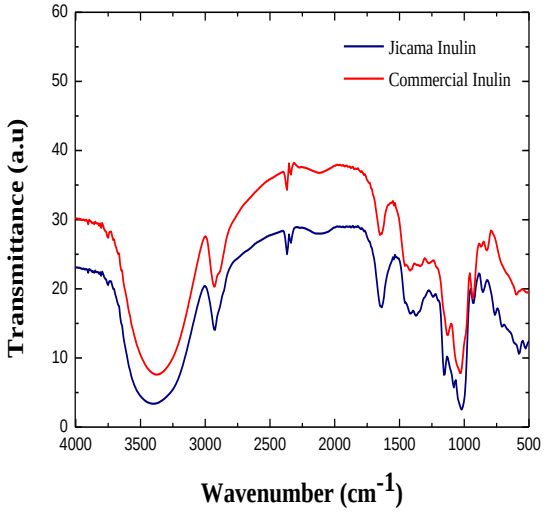

Figure 2. The FTIR Spectra of inulin from yam tubers

In the analysis of functional groups using FTIR for both inulin spectra of yam tuber and commercial inulin showed that there was no significant difference between inulin bands of commercial yam tuber and inulin. This is because the two types are both inulin. The results of the analysis of both inulin samples using FTIR spectroscopy showed that the presence of a widening band in the absorption area of 3371.57 cm^{-1} in commercial inulin and 3402.43 cm^{-1} in inulin from yam tuber which showed the presence of O-H strain vibrations from the alcohol structure. In the molecule followed from the vibration of the C-H strain of the alkane chain in the absorption area of 2931.80 cm^{-1} in commercial inulin and 2924.09 cm^{-1} in inulin from yam tuber. The peak of vibration was also seen in the absorption areas 1126.43 and 1026.13 cm^{-1} in commercial inulin and 1157.29 and 1018.41 in inulin from yam tuber which showed strain (C- O) in this FTIR spectrum from yam tuber.

FTIR spectroscopy may be an option very good among other techniques where This technique is very efficient because it is easy to use, fast and cheap. The spectrum generated from FTIR is data a very complex depiction of the character and identity of a natural substance as a whole based on its composition. that difference exist in the spectral pattern, the position of the absorption peak and its intensity in the FTIR spectrum describes there is a difference in chemical composition natural ingredients. Therefore, the FTIR spectrum can be used to distinguish one substance with the others [6].

4. CONCLUSION

1. The results of inulin isolation from yam tuber as much as 1059 grams obtained 23,298 grams of pure inulin (2.23% of the initial mass of yam tuber samples used in this study). Yam tuber (Pachyrhizus erosus) is one of the tubers which contains inulin.
2. In the analysis of functional groups using FTIR for both inulin spectra of yam tuber and commercial inulin showed that there was no significant difference between inulin bands of commercial yam tuber and inulin.

5. REFERENCES

[1] Dominguez AL , Rodrigues LR , Lima NM, Teixeira JA. 2014. An overview of the recent developments on fructo oligosaccharide production and applications. *Food Bioprocess Technol, 7 (2014), pp. 324-337*

[2] Chranioti C, Nikoloudaki A, Tzia C. 2015. Saffron and beetroot extracts encapsulate dinmaltodextrin, gum Arabic, modified starch and chitosan: Incorporation in achewing gum system. *Carbohydrate Polymers,127,252–263*

[3] Karimi R, Azizi MH, Ghasemlouc M, Vaziri M. 2015. Application of inulin in cheese as prebiotic, fat replacer and texturizer: A review. *Carbohydrate Polymers, 119, 85–100*

[4] Lacerdaa ECQ, Caladob VMA, Monteiroc M, Finotellid PV, Torresa AG, Perrone D. 2016. Starch, inulin and maltodextrinas encapsulating agents affect the quality and stability of jussara pulp microparticles. *Carbohydrate Polymers 151(2016) 500–51*

[5] Majeed M., Majeed S, Nagabushanam K, Arumugam S, Beede K, Ali F. 2019. Evaluation of probiotic Bacillus coagulans MTCC 5856 viability after tea and coffee brewing and its growth in GT hostile environment. *Food Research International 121 (2019) 497-505*

[6] Triawan Deni Agus., Ghufira Ghufira., Adfa Morina ., Rafi Mohamad. 2022. Pencirian Kopi Robusta Bengkulu dari Kemungkinan Bahan Pencampur Menggunakan Kombinasi Spektroskopi FTIR dan Kemometrik. agriTECH, 42 (4) 2022, 321-328

[7] Zabota GL., Silva EK, Azevedob VM, Meireles AA. 2016. Replacing modified starch by inulin as prebiotic encapsulant matrix oflipophilic bioactive compounds. *Food Research International 85 (2016) 26-35*